Mechanisms of neurodegeneration and potential rescue effects with respect to synaptic plasticity

Von der Fakultät für Lebenswissenschaften

der Technischen Universität Carolo-Wilhelmina zu Braunschweig

zur Erlangung des Grades

einer Doktorin der Naturwissenschaften

(Dr. rer. nat.)

genehmigte

D i s s e r t a t i o n

von Leonie Rahel Salzburger

aus Salzgitter

1. Referent: Professor Dr. Martin Korte

2. Referent: Professor Dr. Reinhard Köster

eingereicht am: 11.11.2019

mündliche Prüfung (Disputation) am: 03.02.2020

Druckjahr 2020

Vorveröffentlichungen der Dissertation

Teilergebnisse aus dieser Arbeit wurden mit Genehmigung der Fakultät für Lebenswissenschaften, vertreten durch den Mentor der Arbeit, in folgenden Beiträgen vorab veröffentlicht:

Publikationen:

Richter MC, Ludewig S, Winschel A, Abel T, Bold C, **Salzburger LR**, Klein S, Han K, Weyer SW, Fritz AK, Laube B, Wolfer DP, Buchholz CJ, Korte M, Müller UC (2018). Distinct in vivo roles of secreted APP ectodomain variants APPsα and APPsβ in regulation of spine density, synaptic plasticity, and cognition. EMBO Journal 37:11.

„Das, was du heute denkst, wirst du morgen sein...“

“What you think today you will be tomorrow...“

-Buddha (560 - 480 v. Chr.)-

Diese Arbeit widme ich meiner wundervollen Familie!

Table of Contents

Abstract

Synaptic plasticity and stability are the most important mechanisms in the brain for establishing memory processes. Neural networks are constantly changing to transform newly learned knowledge into synaptic connections and strengthen existing connections. Especially the hippocampus is the region for memory consolidation. Thus, a high-frequency activation of CA1 neurons in the hippocampus lead to an amplification of existing synaptic contacts, also known as long-term potentiation (LTP), whereas low frequency stimulation leads to weakening of synaptic contacts, long-term depression (LTD). Synaptic processes are particularly vulnerable with age to various internal molecules as well as environmental factors. Many of these molecules are already well researched but the mechanisms behind are still unclear. For example, an application of APPsα a cleavage product of the amyloidogenic precursor protein (APP) leads to a physiological LTP in mouse models of Alzheimer's disease (Hick et al., 2015), but the receptor remains unknown. In this study, I was able to identify a potential receptor. Another important role in terms of altered synaptic plasticity during age play inflammatory processes. They have remained unexplored for a long time but over the last few decades they gained more importance. As the age limit in today's society is steadily increasing and inflammatory processes occur especially with age, there must be more effort towards inflammatory research. In this study, I was able to show a positive age- and gender-dependent role of the knockout (KO) of the NALP3 inflammasome, localized in microglia cells, the macrophages of the brain. Aged female NLRP3 KO animals show an increased LTP compared to age-matched males and wildtype animals. In addition, experiments on human autoimmune antibodies (AAB) were also conducted in this thesis. I was able to show that the long-term application of human AAB leads to reduced LTP and lower spine density in the hippocampus. These results are epitope specific, as different patients suffering from different autoimmune diseases show different results.

Zusammenfassung

Synaptische Plastizität und Stabilität sind die wichtigsten Mechanismen im Gehirn für die Etablierung von Gedächtnisprozessen. Neuronale Netzwerke befinden sich im ständigen Wandel, um neu erlernte Kenntnisse in synaptische Verknüpfungen umzuwandeln und bestehende Verknüpfungen zu verstärken. Vor allem der Hippokampus ist die Region für Gedächtnis-Konsolidierung. So führt eine hochfrequente Aktivierung von CA1 Neuronen im Hippokampus zu einer Verstärkung von bestehenden synaptischen Kontakten, auch bekannt als Langzeitpotenzierung (LTP), wohingegen eine niederfrequente Stimulation zur Abschwächung der synaptischen Kontakte führt, auch Langzeitdepression (LTD) genannt. Synaptische Prozesse sind vor allem mit dem Alter angreifbar gegenüber verschiedensten körpereigenen Molekülen sowie Umweltfaktoren. Viele dieser Moleküle sind bereits gut erforscht doch die Wirkungsmechanismen sind immer noch unklar. So führt eine Zugabe von APPsα, einem Spaltprodukt des amyloidogenen Vorläuferproteins (APP) zu einem physiologischen LTP in Mausmodellen der Alzheimer Krankheit (Hick et al., 2015), doch der Rezeptor bleibt unbekannt. In dieser Arbeit konnte ich einen Rezeptor identifizieren. Eine weitere wichtige Bedeutung in Bezug auf veränderte synaptische Plastizität während des Alters kommt den inflammatorischen Prozessen zu. Diese sind im Laufe der letzten Jahrzehnte immer mehr in den Vordergrund gerückt und blieben lange Zeit unerforscht. Da die Altershöchstgrenze in der heutigen Gesellschaft stetig steigt und inflammatorische Prozesse vor allem mit dem Alter auftreten muss ihnen mehr Bedeutung zugestanden werden. In dieser Studie konnte ich eine positive alters- und geschlechtsabhängige Rolle des *knockouts* (KO) des NALP3 Inflammasomes, lokalisiert in Mikrogliazellen, den Makrophagen des Gehirns, zeigen. Gealterte, weibliche NLRP3 KO Tiere zeigen ein gesteigertes LTP gegenüber altersgleichen Männchen und Wildtyp-Tieren. Zudem wurden in dieser Arbeit auch Experimente bezüglich humaner Autoimmunantikörper (AAK) durchgeführt. Ich konnte zeigen, dass die Langzeitzugabe von humanen AAKs zu einer verringerten Langzeitpotenzierung und zu einer geringeren Dichte von Dornfortsätzen, den postsynaptischen Endigungen im Hippokampus, führt. Dieses Ergebnis ist zudem Epitop-abhängig, da die verschiedenen Patienten, die an verschiedenen Autoimmunerkrankungen leiden, verschiedene Resultate zeigten.

"As long as our brain is a mystery, the universe, the reflection of the structure of the brain will also be a mystery."

- Santiago Ramón y Cajal -

1. Introduction

The brain is a very complex organ with millions of neurons, dendrites and synapses that form contacts to spread information through the brain. It is in constant balance between stability and plasticity to create new synapses and strengthen existing neuronal connections. These activity-dependent functional and structural changes at synapses are called synaptic plasticity and are fundamentally important for learning and memory formation occurring especially in the hippocampus. The ability to learn and store memory can be influenced by mental disorders like Alzheimer's disease where the balance of stability and plasticity is shifted to one or another direction. Systemic innate immune activation has been identified as risk factor for Alzheimer´s disease in humans as a kind of inflammation. Inflammatory processes occur on the one hand with age and on the other hand through external influences and can differ between sexes. Especially autoinflammatory processes have gained in importance in research in the last decades as they can lead as well to a balance shift in the brain and therefore to cognitive diseases.

This thesis focuses on the connection between cognitive impairments like Alzheimer's disease and autoinflammatory pathways in terms of synaptic plasticity in the hippocampus. Another part focuses on sex dependent differences in an inflammatory pathway during age.

1.1 Synaptic plasticity

It is very impressive, that neuronal cells in the mammalian brain can change their connectivity, structure and functionality in response to activity. This process is called synaptic plasticity. The neuroanatomist Santiago Ramon y Cajal was hypothesizing that plasticity in the brain can be described as the generation of new contacts between cortical neurons which is essential for the persistence of memory (Cajal, 1894). The plasticity occurs on a structural level (structural plasticity) and is defined by the number and strength of synaptic contacts, as well as on the molecular level, when it alters the efficiency of synaptic transmission (functional plasticity). The psychologists Donald O. Hebb postulates how neurons respond to neighboring neuronal activity and change during activity:

"When an axon of cell A is near enough to excite a cell B and repeatedly or persistently takes part in firing it, some growth process or metabolic change takes place in one or both cells such that A's efficiency, as one of the cells firing B, is increased '' (Hebb, 1949)

The so-called firing is described as an electrically evoked signal, which spreads throughout an axon of one cell and is able to evoke a signal in the neighboring cell. As Santiago Ramon y Cajal described the neurons are separated but contiguous entities, the electrical signal of the axon of the one cell needs to be modulated to get a chemically signal, which is able to get through the synaptic cleft, the part between two neurons, to evoke another electrically signal in the postsynaptic cell. This is the mechanism of the signal spreading from one to another neuron. The long-lasting activity change of neurons is called long-term potentiation and is the process behind the postulate of Hebb. It was first described by Bliss and Lømo (1973) who showed long-lasting strengthening of synaptic connections through high electrical frequency stimulation. The experiments of Bliss and Lømo took place in the hippocampus, a brain region which is nowadays highly intensive studied in terms of memory formation and activity dependent synaptic plasticity.

1.1.1 The Hippocampus

The hippocampus is a main part of the limbic system and the location of memory consolidation, the transfer of short-term into long-term memory. Indeed, hippocampal lesion studies like the famous H.M case could show that the hippocampus is not only the main area for the formation of memory, but furthermore for the recall of consolidated memory (O'Keefe and Nadel, 1978). H.M, a patient suffering from epilepsy underwent a surgery where the hippocampus was bilaterally dissected. H.M. was relieved by epilepsy and displayed an intact short-, long-term and working memory whereas the acquisition of new declarative memories was no longer possible (Scoville and Milner, 1957). The study also proofed that the hippocampus is not the region of memory storage. The hippocampus is able to embed the incoming information coming from the entorhinal cortex into context-specific depictions which are then stored in the cortex. With its highly organized structure including the dentate gyrus (DG) and the ammon's horn (CA, lat. *cornu ammonis*), the hippocampus is a suitable model for studies in mammalian brains. The CA region can be divided into CA1, CA2 and CA3 and is forming a highly precise trisynaptic circuit. (Andersen, 1975) (Figure 1).

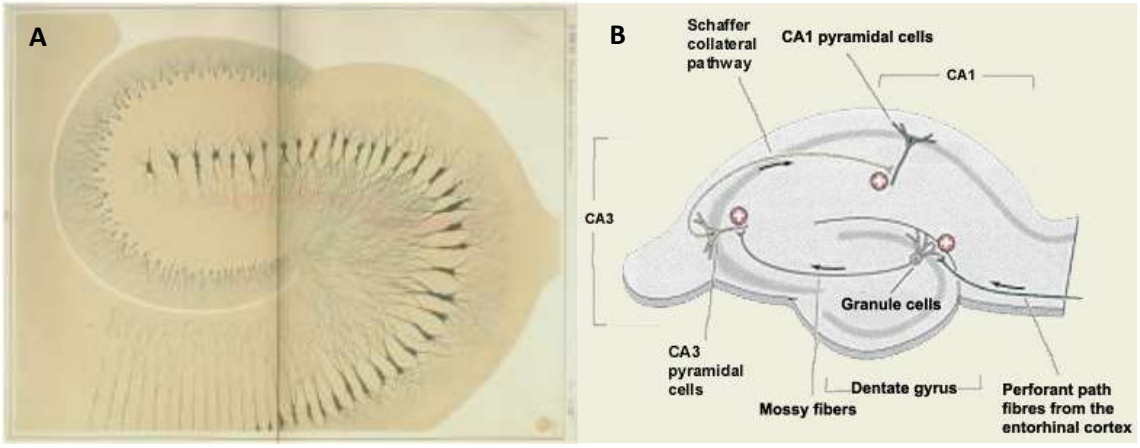

Figure 1: Hippocampal organization. A hippocampal transversal section labeled via Golgi method (adapted from hippocampus book). *B* Neurons of the enthorinal cortex layer II project to granule cells of hippocampal Dentate Gyrus and CA3 field via perforant pathway. Mossy fiber projections from granule cells project to CA3 pyramidal cells. Schaffer collaterals of CA3 project to CA1 pyramidal cells in the hippocampus (Patten, 2015).

The entorhinal cortex (EC) spreads information via the perforant path to dentate gyrus granule cells. Axons of dentate gyrus granule cells end up in mossy fibers, which itself are connected to CA3 pyramidal cells. Dentate gyrus also projects to CA2 area, which itself innervates neurons of the CA1 region (Kohara et al., 2014). Schaffer collaterals, axons of CA3 pyramidal cells, project to CA1 pyramidal cells. The CA1 pyramidal neurons are connected to the subiculum, which then closes the loop and projects to deep layers of the EC (Andersen et al., 2006). Inhibitory interneurons exist in all regions of the hippocampus that mediate feed-back and feed-forward inhibition to assure the synchronization of the hippocampal network (Freund et al., 1996). With its compact but highly defined structure, the hippocampus is the perfect model system to study synaptic activity. Additionally, preparations of hippocampal transversal slices keep these neuronal projections mostly intact (Korte and Schmitz, 2016), so it is not only an interesting model for *in vivo*, but also for *in vitro* studies. In this dissertation I investigated synaptic basal activity, as well as activity-dependent modifications at Schaffer-collateral pathway in murine hippocampal transversal slices.

1.1.2 Long-term potentiation and long-term depression

The mammalian brain is able to change (strengthen and loosen) synaptic connections during activity generated by experiences. Hebb postulates in 1949, that upon distinct stimuli, a second neuron can increase its firing rate evoked by stimulation of a first neuron. This process, where a distinct high frequent stimulus leads to a persistent increase in synaptic strength over one hour or more is called long-term potentiation (LTP) (Bliss and Lømo T, 1973; Bliss and Collingridge 1993), whereas on the opposite site, a low frequent stimulus can lead to a persistent synaptic

weakening called long-term depression (LTD) (Ho et al., 2011). Long-term plasticity is bidirectionally modifiable (Dudek and Bear, 1993) and interestingly the same synapse can induce LTP and LTD dependent on the stimulus it receives but the mechanism underlying LTP and LTD is not equal in all brain regions. At the mossy fiber pathway, LTP is independent from the N-methyl-D-aspartate receptor (NMDAR) but most studies focus on NMDA receptor dependent LTP (Lynch, 2004), like at hippocampal CA3-CA1 pathway as well as I did in this thesis. The NMDAR is an ionotropic receptor which is permeable for calcium (Ca^{2+}) and sodium (Na^{+}). The ligands for NMDAR are glutamate and the co-agonist glycine or D-serine (Henneberger et al., 2013). Under resting membrane conditions (-70 mV), NMDAR is blocked by a magnesium ion (Mg^{2+}) and therefore Ca^{2+} and Na^{+} are unable to enter the cell via this receptor. Basal synaptic transmission is mainly mediated via another receptor called the α-amino-3-hydroxy-5-methyl-4-isoxazole propionic acid receptor (AMPAR), which is permeable for Na+ and potassium (K+) ions in response to glutamate binding (Citri and Malenka, 2007). Upon entering of positive ions and therefore depolarization of the membrane the Mg^{2+} block in NMDAR can be released and it becomes permeable for Ca^{2+} and Na^{+} ions when glutamate binding occurs at the same time (Herron et al., 1986). This Ca^{2+} influx via NMDAR leads to the activation of downstream protein kinases, e.g. calcium/calmodulin-dependent kinase II (CaMKII) which in turn are responsible for AMPAR stabilization within the post-synaptic density (PSD) (Citri and Malenka, 2007, Korte and Schmitz, 2016, Barria et al., 1997). Being only conductive when pre- and post-synapse are co-active characterizes the NMDAR as a coincidence detector. These finding defines moreover the first of three key features of LTP (Bliss and Collingridge, 1993):

1) Input-specificity restricts the activation of synapses only to specific postsynaptic parts, at the spine head.

2) Cooperativity means, multiple synapses need to be activated at the same time to generate a sufficient postsynaptic depolarization

3) Associativity means that in a pairing protocol a weak and a strong synaptic input induce LTP at both synapses.

Characteristically for NMDAR dependent LTP (and LTD) is to sustain the connection between the presynapse and the postsynaptic compartment. The shape of the spine head can give rise to the connection strength to the presynaptic part (Holtmaat and Svoboda, 2009). A lower spine head volume is related to a lower number of receptors for neurotransmitter and thus reflects a lower synaptic strength (Holtmaat und Svoboda, 2009). At basal conditions a low number of AMPAR are internalized into the postsynaptic membrane generating excitatory postsynaptic potentials

(EPSPs) upon stimulus. When an action potential reaches the presynaptic part, voltage gated Ca^{2+} channels (VGCCs) are activated and allow the influx of Ca^{2+}, which leads to fusion of vesicles with neurotransmitters with the presynaptic membrane and the release of neurotransmitters into the synaptic cleft. These neurotransmitters like glutamate are binding to AMPAR allowing Na^{+} and Ca^{2+} influx into the postsynaptic compartment. The depolarization of the postsynaptic membrane leads to the release of the Mg^{2+}-block from the NMDAR, which makes them permeable to $Ca^{2+}$and Na^{+}. The influx of Ca^{2+} via NMDARs activates Ca^{2+}-dependent enzymes like protein-kinase C (PKA) and CamKII relief AMPAR trafficking by phosphorylation of specific receptor subunits. Additionally, auto-phosphorylation of the CamKII initiates downstream signaling cascades for example the synthesis of new proteins (Fukunaga et al., 1995). This late phase of LTP (L-LTP) and also of LTD (L-LTD) that lasts for hours or even days is dependent on *de novo* protein synthesis (Manahan-Vaughan et al., 2000) whereas the early phase of LTP (E-LTP), lasting from one to three hours is independent of protein synthesis. Not only the lasting time of LTP is crucial, but also the frequency of stimulus is decisive. LTP can only be induced via repetitive or tetanic stimulation of synapses with prolonged trains at high frequencies (Bliss and Lømo, 1973). In contrast, short bursts result in plasticity lasting only for milliseconds to minutes and are called short-term synaptic plasticity (Zucker and Regehr, 2002).

1.1.3 Short-term and long-term synaptic plasticity

Different forms of synaptic plasticity are widely discussed and are mainly distinguished by their duration. Unlike long-term plasticity that can last for hours or even days, preceding short-term plasticity (STP) only lasts for milliseconds to minutes and is thought to be involved in short-term memory formation as well as temporary changes in behavior due to sensory input adaption (Citri and Malenka, 2007). STP is a presynaptic phenomenon as Ca^{2+} gets transiently accumulated in the presynaptic terminals following short bursts of activity and therefore neurotransmitter release is enhanced due to biochemical processes that lead to vesicle exocytosis (Zucker and Regehr, 2002). By applying two stimuli within a short interval, presynaptic properties can be easily measured. The second stimulus can be either enhanced compared to the first one (Paired-pulse facilitation, PPF) or depressed (Paired-pulse depression, PPD) (Katz and Miledi, 1968). Longer inter stimulus intervals (ISIs) lead in most synapses to PPF whereas ISIs of 20 ms or less lead to PPD. In case of PPD the ready releasable pool (RRP) of vesicles in the presynapse is still depleted due to the first stimulation, leading to less transmitter release in response to the second stimulus. In case of ISIs from 20 ms up to 500 ms residual Ca^{2+} in the presynapse, left over from first stimulus, increases the release of synaptic vesicles to the second stimulus and

lead to PPF (Zucker and Regehr, 2002). Additional mechanisms are thought to be involved as well, like activation of protein kinases regulating the activity of presynaptic proteins like the phosphoprotein synapsin (Rosahl et al., 1993). Interestingly, the same synapse can be more prone to PPF or PPD depending on their history. A synapse with low probability of transmitter release will show a depression due to the second stimulus, whereas a synapse with high transmitter release probability will show facilitation due to second stimulus applied (Dobrunz et al., 1997). In addition to the briefly lasting forms of STP, high frequent stimuli leading to persistent forms that can last for several seconds up to minutes, called post tetanic potentiation (PTP) and augmentations, lasting five to ten seconds (Citri and Malenka, 2007; Regehr, 2012). In both cases, high amounts of Ca^{2+} and biochemically alterations of proteins in the presynapse lead to a higher probability of synaptic vesicle release and therefore to high amount of neurotransmitter release (Zengel and Magleby, 1982). PTP is characterized by a large enhancement of synaptic efficacy after high frequency stimulation and displays the very first phase of LTP followed by STP which displays the early LTP (E-LTP) phase up to hours. E-LTP describes the very first phase of LTP and lasts less than one hour whereas late LTP (L-LTP) lasts for hours (*in vitro*) up to weeks or even months (*in vivo*) (Citri and Malenka, 2007). Taken together STP is acting like a processing filter between neurons, whereas LTP and LTD display learning and memory formation at a cellular level. The understanding of their mechanisms on a cellular level is very important with respect to neurodegenerative diseases.

1.2 Alzheimer's disease

One of the most commonly studied neurodegenerative disease besides Parkinson's and epilepsy is Alzheimer's disease (AD). AD is the most common cause of dementia with 60 to 80 percent of the cases. In 1901 Alois Alzheimer described the first case of AD on his 51-year-old patient Auguste Deter who suffered from various symptoms like depression, disorientation and progressive memory loss and finally died at the age of 55. After her death the brain underwent an autopsy and Alois Alzheimer himself described his finding as follows:

> *''Finally, the nucleus and the cell itself disintegrate and only a tangle of fibrils indicates the place where a neuron was previously located.''* (Alzheimer, 1907)

These findings display the typical biochemical symptoms of AD, on the one hand a progressive extracellular accumulation of the amyloid-β (Aβ) protein resulting in so called amyloid plaques and on the other hand the formation of intracellular neurofibrillary tangles (NFTs) resulting finally in neuronal death. Plaques as well as NFTs can be observed in brain regions that are

mainly involved in learning and memory as well as emotional behavior like hippocampus, entorhinal cortex and amygdala. NFTs are resulting from aggregation of biochemically changed microtubule associated protein tau, leading nearby neurons to reduced numbers of synapses as wells as neuronal death (Goedert et al., 1988). In the healthy brain the microtubule binding protein tau is essential for the stabilization of microtubules and present in all neurons and glia cells. However, its hyperphosphorylation leads to self-aggregation into plaques and as a result into neuronal and glial death. Worldwide about 30 million people suffer from Alzheimer's disease but only little is known about the factors influencing progression from mild cognitive impairment to AD. In 2050 the Alzheimer cases will be three times higher than now (Hebert et al., 2013) therefore it is important to know the mechanisms. So far known there are two hypothesis of AD to occur: on the one hand the familiar case of AD (FAD) in which dominant mutations cause early-onset AD occur either in the protease presinilin1 or presinilin2 (PS1 or PS2) or in the amyloid precursor protein (APP) leading mainly to an overproduction of Aβ (Selkoe and Hardy, 2016). On the other hand, the non-dominant case of AD resulting from a failing of Aβ clearance resulting in a constant increase of Aβ in the brain. The deposition of Aβ oligomers, mediating toxic effects (Schaeffer et al., 2011), activate microglia and astrocytes and cause inflammatory responses for example the activation of the NALP3 inflammasome.

1.3 Amyloid Precursor Protein Family Members

The amyloid precursor protein (APP) is a type I integral membrane protein and localized at the chromosome 21 in humans. There are three major isoforms of APP: APP_{695}, APP_{751} and APP_{770}, differ in size respectively and are generated by alternative splicing and posttranslational modifications (Yoshikai et al., 1990). The protein family also includes amyloid precursor-like protein 1 and 2 (APLP1 and 2) in mammals. Both, APP_{695} as well as APLP1 are mainly found in neurons whereas the two longer isoforms of APP and APLP2 can also be found in other tissues. Because of its extensive post-translational processing resulting in a variety of cleavage products it is very hard to figure out the exact function of APP. Investigations so far could show various functions of APP in development, where it is spread nearly throughout the whole body and had additionally multiple functions also in the adult CNS (Aydin et al., 2012).

1.3.1 APP processing pathways

Members of the APP protein family undergo a complex but comparable processing pathway due to a high degree of sequence homology (Figure 2).

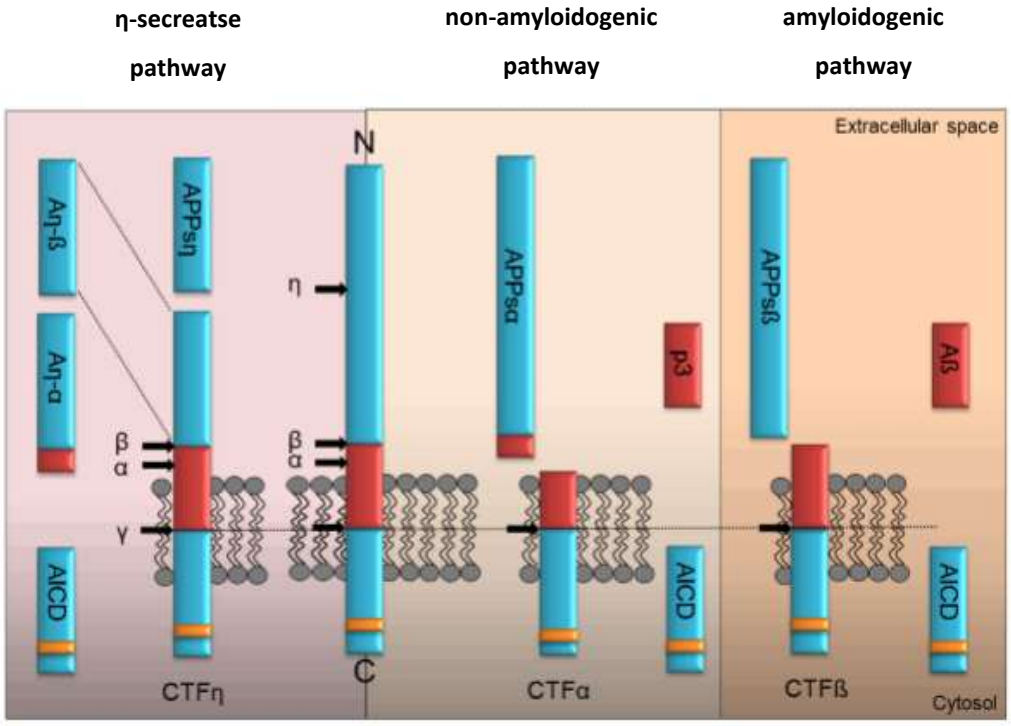

Figure 2: Processing pathways of APP. APP can be processed via α-, β-, η-, and γ-secretases. A-secretase cleavage belongs to the non-amyloidogenic pathway, shown in the middle figure sector. This processing pathway leads to the formation and release of APPsα into the extracellular. Subsequently cleavage of membrane anchored CTFα by γ-secretase leads to the formation of extracellular p3 peptide and cytoplasmic AICD containing the highly conserved interaction motif YENPTY (yellow stripe). Cleavage of the ms APP by β-secretase generates extracellular APPsβ and the membrane attached CTFβ. Further cleavage of CTFβ by γ-secretase generates cytosolic AICD and the very short peptide Aβ. The third processing pathway of APP is via the η-secretase, generating membrane bound CTFη and APPsη in the extracellular space. Further cleavage of CTFη by γ-secretase leads to cytosolic AICD. Cleavage of CTFη via β-secretase generates the extracellular Aη-β, whereas cleavage via α-secretase generates the longer Aηα peptide (reproduced from Ludewig and Korte, 2017).

The full-length Protein APP can be cleaved via three pathways depending on the kind of secretase in the non-amyloidogenic, amyloidogenic or as a new study have shown via the η-secretase pathway (Willem et al., 2015). Cleavage of APP with the α-secretase, in neurons mainly ADAM-10 (α-disintegrin and metalloproteinase), is leading to APPsα and the membrane attached CTFα (Jorissen et al., 2010; Kuhn et al., 2010). Further cleavage by the γ-secretase generates the extracellular p3 fragment and AICD (APP intracellular domain) in the cytoplasm. BACE-1 (β-site APP cleaving enzyme) is the most common protein for β-secretase cleavage leading to extracellular APPsβ and membrane anchored ACID (Cao and Sudhof, 2001. γ-secretase cleavage generates the extracellular Aβ fragment and again the cytosolic ACID. As APP is present in dendrites as well as in axons it can be released from both (DeBoer et al., 2014). In the healthy organism APP is cleaved in 90% of the cases in the non-amyloidogenic pathway and

thus preventing the secretion of Aβ. A recent study of Willem et al. (2015) could show a new cleavage pathway besides the amyloidogenic and non-amyloidogenic pathway via the η-secretase. In this pathway a cleavage site in extracellular domain of APP lead to a short extracellular APPsη ectodomain. There are some studies about the function of Aηα and one hypothesis is an impairment of hippocampal LTP. Previous studies with acute application of synthetic Aηα on hippocampal slices lead to a decreased and unstable LTP (Willem et al., 2015). Cleavage of the membrane anchored CTFη via α- or β-secretase is generating two peptides, on the one hand processing via α-secretase releasing Aηα and on the other Aηβ is generated, when cleaved via β-secreatse (Willem et al., 2015). Depending on the site of release, the generated fragments could interact with receptors or intracellular by activating signaling cascades.

1.3.2 Function of APP and its cleavage products

During the last decades, research focusses on the function of APP and its cleavage products as they have multiple functions in regulating biological processes in the body and the nervous system (Aydin et al., 2012). Depending on their processing, they can act as a receptor on the cell surface or as a ligand in case of Aβ binding to the full-length protein (Lorenzo et al., 2000). Cell-cell interacting has been described for APP localized at the cell surface (Soba et al., 2005), which is essential to form synaptic contacts and is therefore crucial for synaptic plasticity. A recent study (Mayer et al., 2016) identified APLP1 as a protein mediating neuronal adhesion in a dynamic way, whereas APP and APLP2 are processing basal adhesive functions. These distinct functions of the APP family members allow the brain to act on synaptic plasticity very precisely and modulate synaptic function in a certain manner. The soluble APPsα fragment is well studied and involved in many neuronal processes like synaptic plasticity and memory enhancement as well as in neuroprotection (Turner et al., 2003; Copanaki et al., 2010). Aβ peptide in contrast seems to have only negative effects on synaptic plasticity via formation of oligomers, as it is the main player in AD it is investigated in an extensive way (Walsh and Selkoe, 2007; Reinhard et al., 2005). Nevertheless Abramov et al. showed in 2009 that Aβ could have a positive influence: a positive endogenous regulation of the release probability at synapses in the hippocampus. In small amounts Aβ is acting positively on LTP as well as STP and can enhance PPF (Abramov et al., 2009; Wang et al., 2012; Puzzo et al., 2008). Even the shortest part of APP the intracellular domain (AICD) can interact with its YENPTY motif and might regulate transcription via the interaction with several proteins like Fe65 or mint proteins (Cao and Sudhof, 2001; Borg et al., 1996). Mice lacking the YENPTY motif show impaired induction as well as maintenance of LTP and altered hippocampal dependent behavioral functions (Klevanski et al., 2014). APPsß as well

as APPsα are shown to be involved in inflammatory events, activating microglia cells. In the presence of APPsß, APPsα increases activation markers in microglia and enhance their production of neurotoxins but in the absence of APPsβ, APPsα is acting in a neuroprotective manner (Barger and Harmon, 1997). Various studies could proof a positive effect of APPsα on LTP. Ishida et al., could show in 1977 that the extracellular domain of APP is able to facilitate LTP induction in hippocampal slices. Additionally, the rescue of the LTP deficits in APP/APLP2 cDKO mice through the acute application of the recombinant peptide *in vitro* (Hick et al., 2015) show a rapid rescue effect. Moreover, a recent study showed that recAPPsα is able to rescue age dependent LTP deficits (Moreno et al., 2015). Also, on morphological level APPsα has an essential role on structural plasticity in the brain. It is responsible for spine density regulation as well as spine dynamics (Tyan et al., 2012; Weyer et al., 2011). Reverse experiments by knocking out the major α-secretase, ADAM-10, responsible for APPsα processing, resulted in strongly impaired LTP (Prox et al., 2013). Besides all the knowledge about supporting LTP it is still unclear how and on which receptor APPsα is acting. There might be some hints towards acting directly at the presynaptic part by influencing the NMDAR function (Taylor et al., 2008).

1.4 Inflammatory processes

Even in the healthy brain inflammatory processes occur all the time. Small neuronal damages as they occur in the daily life for example due to aging processes or small injuries, lead to an instant activation of the immune system of the brain. Therefore, especially microglia cells, macrophages of the brain, are essential. Microglia contain small inflammatory machineries to recognize potential risk factors (Andreasson et al., 2016). On the other hand, consistent activation of microglia cells occurring within age or neurodegenerative diseases lead to chronic inflammation and neuronal damage (Streit at al., 2014; Heneka et al., 2014). In this study especially the NALP3 inflammasome was investigated.

1.4.1 NALP3 inflammasome and microglial cells

Microglial cells, a special form of glial cells in the brain, reflect a large part of the inflammatory system in the central nervous system (CNS). In the healthy brain, they form a dense network around neurons and are responsible for example for synapse formation and the release of neurotrophic factors (Figure 3) (Heneka et al., 2014). They act as special macrophages in the central nervous system and react quickly to pathogenic infections or other messengers like Aβ in AD. The immune response let the microglia change its phenotype to an activated form. Due

to the release of proinflammatory mediators, such as cytokines (interleukin 1 beta or interleukin 10 (Norden et al., 2016))or reactive oxygen species, neurodegenerative diseases can be triggered (Saijo und Glass, 2011). Therefore, it is important not only to see neurons and the immune system as individual components, but to look at them together to find out whether hyper- or hypo-activation of the immune system with age can lead to damage to the brain (Lucin and Wyss-Coray, 2009). The activated form of microglia shows phenotypical markers as they have thicker, less branched microglial spouts (Cunningham, 2013). The activation occurs via pattern recognition receptors (PRR) or other surface receptors like the toll-like receptors (TLR) (Andreasson et al., 2016). Activation can take place via pathogenic associated molecules or via cell internal molecules (Saresella et al., 2016). These internal molecules can be oxidized mitochondrial DNA, which can be released for example under stress (Latz et al., 2013). The spectrum of activation results in either an M1 or M2 phenotypes. The M2 phenotype is characterized by an increased release of neurotrophic factors such as brain-derived neurotrophic factor (BDNF) or parallel phagocytosis of damaged neurons (Heneka et al., 2014). On the other hand, however, activation can result in a microglia M1 phenotype. In this case, the secretion of neurotrophic factors is downregulated. Instead, there is a release of proinflammatory cytokines, which can cause significant damage to the neurons leading to chronic inflammation and structural damage to neurons (Heneka et al., 2014).

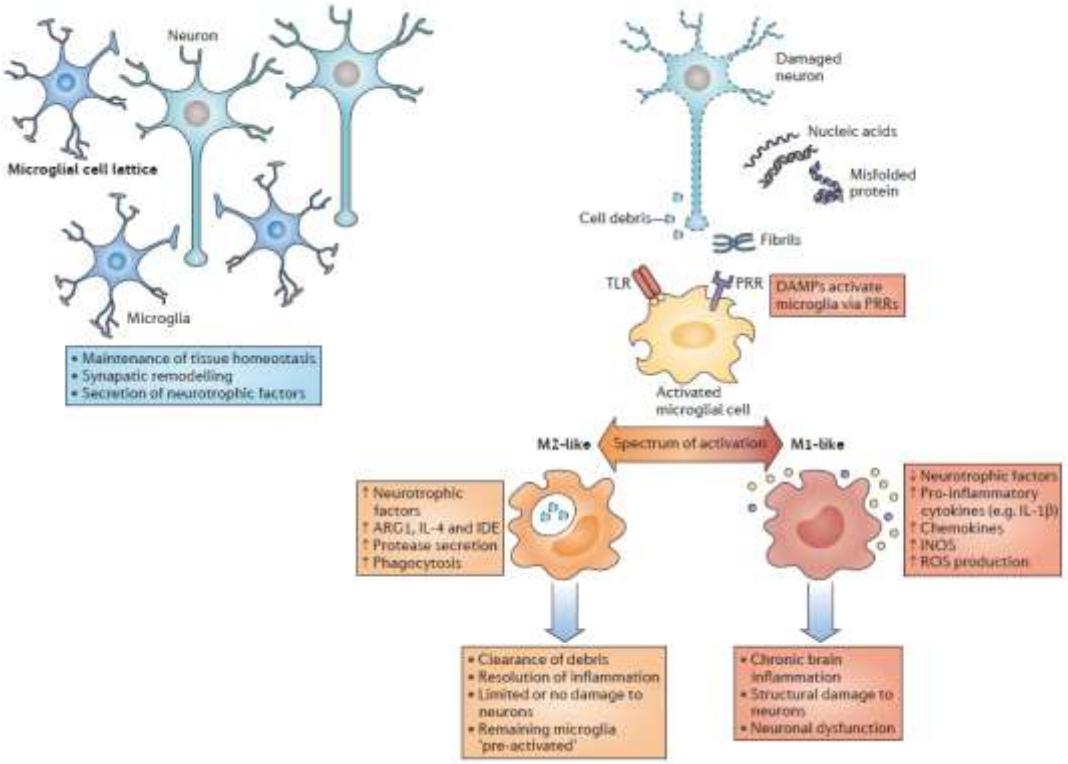

Figure 3 Activation of microglia cells. In the healthy brain, microglia form a dense network. They are responsible for eliminating inactive synapses or emitting neurotrophic factors to ensure the growth and stability of neurons. Through

surface receptors, such as TLRs, DAMPs are detected and lead to activation of the microglia. This activation can result in either the M1 or M2 phenotypes. While the M2 phenotype uses neurotrophic factors or phagocytosis of inactive synapses to rid the brain of harmful substances and reduces damage to neurons, the M2 phenotype leads to chronic Inflammation. TLR = "toll-like" receptor, PRR = "pattern recognition" receptor, DAMP = "damage-associated molecular pattern," ARG = arginase, IL = interleukin, IDE = "insulin-degrading" enzyme, iNOS = "inducible nitric synthase," ROS = "reactive oxygen species" (Heneka et al., 2014).

The NALP3 domain of the NALP3 Inflammasome is localized in microglia cells and contains three different domains: nucleotide-binding oligomerization domain (NOD), leucin rich repeat (LRR) and pyrin domain-containing 3 (PYD). NALP3 itself is part of the NALP3 inflammasome, which is made up of three different subtypes: NALP3 (also known as NLRP3), ASC (apoptosis-associated speck-like protein, which contains a CAR (caspase recruitment domain) and pro-caspase 1 (Saijo and Glass, 2011, Strowig et al., 2012). The inflammasome thus represents a multiprotein complex (Jin et al., 2010). In addition to the NALP3 inflammasome, there are other inflammasomes, localized in different regions and cell types. One of these is the NALP1 inflammasome, which is mainly found in neurons or pyramid cells and oligodendrocytes (Kummer et al., 2007) and is one of the mainly anti-microbial inflammasomes (Coll et al., 2015). However, this work deals exclusively with the NALP3 inflammasome. The NALP3 inflammasome activation takes place in two steps. The first step involves activating nuclear factor ' kappa-light-chain-enhancer ' activated B-cells (NFκB), a transcription factor that in turn is responsible for the expression of the inactive form of NALP3 (Bauernfeind et al., 2009). The second step is the activation of NALP3. NALP3 and ASC contain a pyrine domain, which binds together and thus activates the NALP3 inflammasome, followed by an oligomerization, which means that CAPS1 binds to the CARD domain of ASC (Rathinam et al., 2012). The active inflammasome now processes and secretes IL-1β, which is previously present as an inactive form (Abderrazak et al., 2015). Due to the missing of a signal peptide, the pro-shape of IL-1β is inactive. Accordingly, it is present within the cell and cannot cause any damage to the brain (Dinarello, 1998). Active IL-1β, on the other hand, is the main player in infections and leads to chronic brain inflammation (Martinon et al., 2002). Persistently high levels of IL-1β lead to deficiencies in spatial learning (Moore et al., 2009), altered eating and drinking behavior, limited social contact and altered exploratory behavior (Goshen and Yirmiya, 2009)

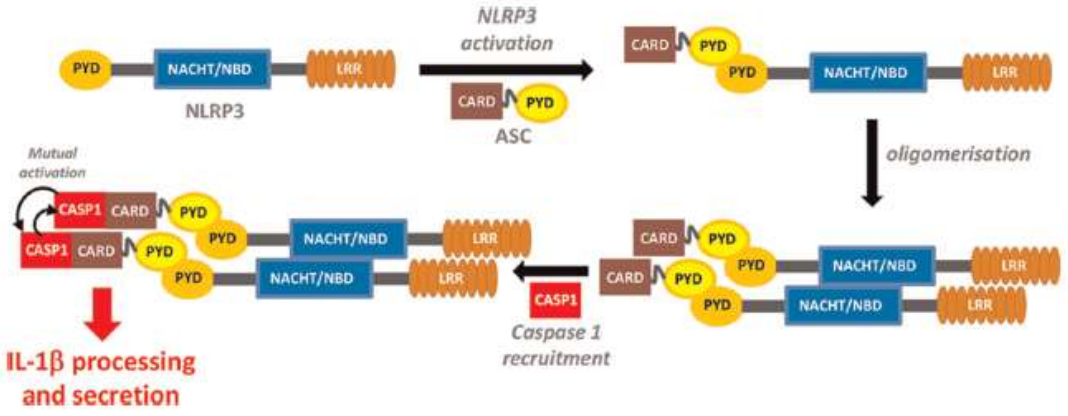

Figure 4 Activation of NALP3 inflammasome. The NALP3 inflammasome consists of NALP3, which binds via the pyridine domain ASC and is thus activated. It then oligomerizes and recruits IL-1β using the CARD domain Caspase-1. The now active NALP3 inflammasome. CARD = "caspase recruitment" domain; LRR = "leucine-rich repeat"; NIGHT NBD = nucleotide binding domain; PYD = Pyrin domain; CAP1 = Caspase-1, IL-1β = interleukin 1 beta (Abderrazak et al., 2015).

1.4.2 Inflammation in physiological aging

Changes of microglial cells towards its active form are also found in the aging brain (Streit et al., 2014). Internal molecules like oxidized, mitochondrial DNA, which can be released for example under stress, are elevated with age (Latz et al., 2013). Previous studies (Heneka et al., 2013), could show specific markers for the M2 phenotype of microglia found after deletion of NLRP3 in 16 months old mice. This means that the KO of NLRP3 in older animals can have a positive effect on the microglial cells in the brain. Another study from Youm et al. (2013), which shows that the IL-1β concentration in 23 months old NLRP3 KO mice is decreased and instead the concentration of BDNF is increased. If microglia change their phenotypes to an M2 phenotype, the neurotrophic factor BDNF is increased, the IL-1β secreted by NALP3 and processed is reduced and age-related damage to neurons is not as pronounced (Heneka et al., 2014; Norden et al., 2016; Saijo und Glass 2011). A study by Lamason et al., in 2006, in the murine spleen of 24-28 weeks old mice shows that female mice have an increased expression of genes of the adaptive immune response, while males show an increased expression of genes of the innate immune response. This may suggest that the effects of the NLRP3 KO have a greater impact on females. Furthermore, it has been shown that the activation of the NALP3 inflammasome can promote estrogen-mediated anxiety and depression (Xu et al., 2015). The inverse conclusion would be that female mice with a knockout in NALP3 inflammasome would have a beneficial phenotype compared to male mice in terms of anxiety behavior and depression. In general, human aging is characterized by a chronic and low-grade inflammation (Franceschi and Campisi, 2014). As most age-related diseases share an inflammatory pathogenesis, inflammation is a highly significant risk factor for both morbidity and mortality in the elderly people (Franceschi et al., 2006).

Another source of inflammation during age might be represented by harmful products produced by the microbial constituents of the human body, such as gut microbiota, which can leak into surrounding tissues as well as circulation (Biagi et al., 2011). Therefore, the ability of the gut to secrete these microbes and/or their products declines with age, leading to chronic low-grade inflammation. Another possibility is that the gut microbiota itself change with age so that the microbes present in the aged gut elicit an inflammatory response. Taken together, the host–pathogen balance is very important (Biagi et al., 2011).

1.5 Autoimmune antibodies

Not only during age, but also in young people, some molecules like body-own antibodies can lead to chronic inflammation. The second most frequent form of Autoimmune-mediated encephalitis (AE) is associated with autoimmune antibodies (AAB) against leucin-rich glioma-inactivated protein 1 (LGI1) (Van Sonderen et al., 2016; Arino et al., 2016). LGI1 is a secreted protein and consists of two major motifs: a leucin-rich repeat (LRR) section for LGI1/LGI1 interaction and an epitempin (EPTP) section mediating the interaction of LGI1 and the α-disintegrin and metalloproteinase (ADAM22) receptor , following the formation of a tetramer (Fukata et al., 2006; Yamagata et al., 2018). This tetramer is crucial for synaptic transmission by interaction with presynaptic Kv1 channels and postsynaptic AMPA receptor (Fukata et al., 2006, 2017; Seagar et al., 2017). Application of AAB from LGI1 AE patients on hippocampal slices interrupted the LGI1-ADAM22 interaction and lead to a decrease in AMPAR density and therefore a decreased synaptic transmission level (Ohkawa et al., 2013). This finding of Ohkawa was strengthened by Petit-Pedrol and colleagues in 2018 using chronic infusion of LGI1-AABs enriched CSF resulting in a decrease of AMPA receptors and Kv1 channels. Patients suffering from AE usually have initially facial brachial dystonic seizures (FBDS) a form of epilepsy, which is characterized by frequent, brief seizures affecting arm and face. Immunosuppressive therapy of LGI1 AAB-associated encephalitis in this early stage of the disease is efficient (Irani et al., 2013; Thompson et al., 2018). At the stage of FBDS a magnetic resonance imaging (MRI) displays a predominantly physiological phenotype (Navarro et al., 2016; Miller et al., 2017; Thompson et al., 2018) whereas patients with limbic encephalitis develop a hippocampal atrophy (Heine et al., 2018). Unaltered MRI results in the early stage of AE make it hard to determine the disease. Subsequently, the clinical phenotype changes to epilepsy and cognitive decline (Van Sonderen et al., 2016; Irani et al., 2012, 2013) and therefore AABs are involved in neurodegenerative processes leading to dementia-like-symptoms (Dalmau et al., 2008: Doss et al., 2014).

1.6 Sex dependent differences in health and disease

It is well known that various diseases show a sexual prevalence. Just to mention some examples: women are nearly twice as likely diagnosed with depression compared to men (Krishnan and Nestler, 2010) and many disorders linked to autoimmune etiologies, for example multiple sclerosis are predominantly female specific (Whitacre, 2001; Werling and Geschwind, 2013). Males are more likely to suffer from autism spectrum disorder (ASD) additionally neurodevelopmental disorders, like attention deficit hyperactivity disorder and language impairment show a male bias (Viding et al., 2004; Szatmari et al., 1989). However it is not entirely clarified about the biochemically mechanisms behind the sexual addiction of some diseases, the study of Sarubin and colleague in 2017 supports the notion of an association between variants of glucocorticoid receptor (GR) related genes in women and the pathophysiology of depression: females suffering from major depressive disorder showed a more than three times higher frequency of the Thymin/Cytosin polymorphism compared to controls, which thus seems to be one reason for sexual differences in depression associated diseases. This result correlates with the fact that also in AD woman are predominantly affected (Seshadri et al., 2006).

1.6.1 Differences in immune associated molecules in male and female brain

New research could show that microglia are not only essential for neuroinflammatory processes like clearing of debris and neuroprotection but are also active players in many basic processes in the healthy brain including brain development and sexual differentiation in the brain (Schwarz and Bilbo, 2012). For example, in processes like cell proliferation, synaptic connectivity and physiology microglia cells are main players (Lenz and McCarthy, 2014). In the developing rodent brain males have more microglia cells than females across the neonatal period. Currently it is not known whether there are more microglia progenitor cells recruited into the male brain in early life, whether more cells survive in males than females or whether there is enhanced proliferation in the male brain (Lenz and McCarthy, 2014). Additionally, microglia are involved in regulating synaptic patterning selectively in males versus females thus influencing neighboring neurons and astrocytes. Steroid hormone signaling initiated in neurons leading to microglial release of prostaglandins as an essential contributor to the induction and maintenance of dendritic spine excitatory synapses in the developing male brain (Lenz and McCarthy, 2014). Therefore, not only in diseases, but also in the physiological development of the male and female brain differences occur which are leading to altered functions of the immune system in the brain between sex. The sex dependent differences in the mammalian

brain during inflammatory processes are still few investigated. Therefore, I analyzed the NALP3 Inflammasome in terms of sex dependent differences within age.

1.7 Scope of this Study

AD is one of the most common neurodegenerative disorders with increasing numbers of patients every year. Some studies indicate that the full-length APP as well as some other APP cleavage products act in a neuroprotective way, but Aβ is the main player acting in the process of progressive decline of synapses occurring due to its oligomerization finally resulting in cell death. This mainly occurs in the hippocampus, the brain region responsible for memory formation. Recent studies could also indicate that autoimmune antibodies involved in neurodegenerative processes in the hippocampus lead to dementia-like-symptoms. With its binding to LGI1 the interaction of LGI1/ADAM22 gets interrupted, which is crucial for synaptic transmission by interaction with presynaptic Kv1 channels and postsynaptic AMPAR. This is resulting in a decrease in AMPAR density further to a decreased synaptic transmission level and finally synaptic death. Cell death therefore is responsible for activation inflammatory signal processes spreading for example debris, which in turn causes the activation of inflammatory processes. One major inflammasome in the mammalian brain is the NALP3 inflammasome mainly located in microglial cells. Activation of it through surface receptors acting on inflammatory signals, leading to clearance of damaged neurons in turn resulting in fewer synaptic connections. The KO of the NALP3 inflammasome is leading to sex dependent outcomes in electrophysiological measurements during aging.

In this study, I will make a possible connection via inflammation between common diseases like AD, autoimmune antibodies and inflammasomes. I analyzed the function of APPsα, a cleavage product of the APP family, in terms of LTP and get rise to a potential receptor of APPsα. Additionally, I analyzed the electrophysiological as well as morphological function of human autoimmune antibodies on murine hippocampal slices. Moreover, I included a sex dependent view on the involvement of inflammasomes on synaptic degeneration during age.

2. Materials and Methods

2.1 Mice strains and Patient samples

2.1.1 Mice stains

2.1.1.1 NLRP3 KO mice

To investigate the role of the NALP3 inflammasome complex on physiological aging of mice a knockout mice strain was created. Briefly, the generation of NLRP3$^{-/-}$ mice was performed as follows: The NLRP3 KO animals are based on a homozygous knockout of an intracellular sensor of the NALP3 inflammasome. This sensor is activated by molecular structures resulting from cell damage or pathogens. The mice have no inferior phenotype compared to the WT. In old age, KO animals have an advantageous phenotype in many areas (motor function, bone density, etc.). They were generated in Bonn in the group of clinical neurosciences under Prof. Eicke Latz and were kindly provided for this work (Heneka, 2013).

2.1.1.2 Htau.P301S mice

For the Alzheimer's disease studies a mouse line was used that express, under the control of the murine Thy1.2 promoter, the 383 amino acid-long alzheimer-associated human tau isoform with mutations at position P301S. This htau.P301S mouse line displays a progressive tau pathology that starts at the age of 2 months and is characterized by tau hyperphosphorylation. At the age of 2.5 months, brain tauopathology is accompanied by a reduction of excitatory postsynapses, so called spines, in the hippocampus. This is associated with impairment of spatial memory. At the age of about 4 months, mature tau aggregates and tangles develop, as they are also found in AD patients (Figure 5). This line also shows tau expression in motor neurons of the lumbar spinal cord and thereby degeneration of motor neurons. This leads to progressive impairments of motor coordination and locomotion, increased weight loss, a neurological phenotype with "hind feet clasping" and finally a progressive paralysis of the hind legs, which requires euthanasia of the mice (Allan et al., 2002; Schindowski et al., 2006).

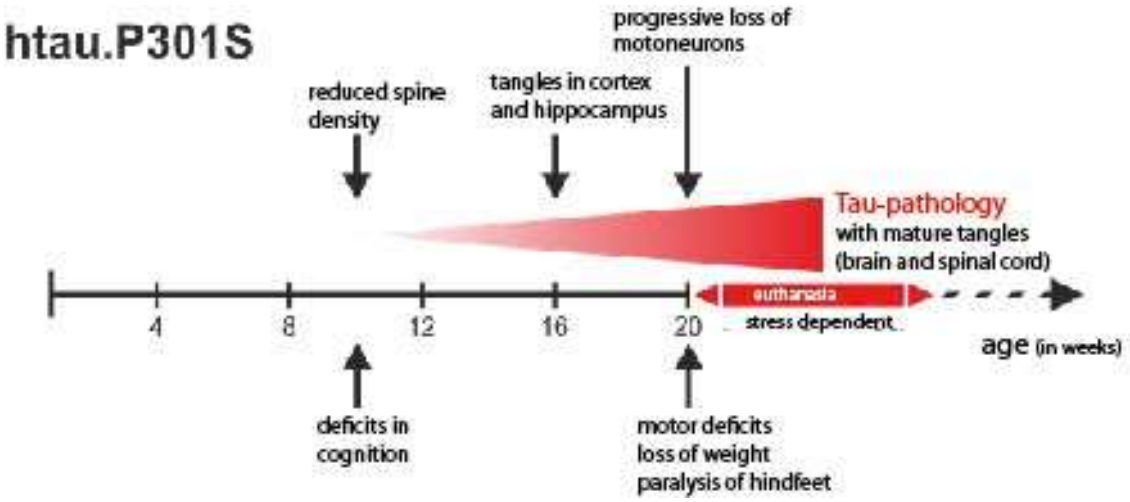

Figure 5: Phenotype of the htau.P301S mouse line. This mouse line expresses the 383 amino acid-long Alzheimer-associated human tau isoform with mutations at position P301S under the control of the Thy1.2 promotor. Cognitive deficits and reduced spine density at the age of 2.5months with tangles in cortex and hippocampus at the age of 4 months are the consequences. Progressive loss of motor neurons and therefore deficits in locomotion and motor coordination as well as weight loss and finally paralysis of the hind feet leads to euthanasia of the mice (adapted from U. Müller, unpublished).

2.1.1.3 NexCre cDKO APP mice

To circumvent lethality of APP/APLP2 double KO mice and to elucidate the role of APP and APLP2 in the adult CNS Hick et al., generated animals with a conditional CNS specific APP/APLP2 double knockout (cDKO). They crossed $APP^{flox/flox}$/APLP2-KO mice to NexCre mice leading to APP gene deletion selectively in excitatory forebrain neurons of the cortex and hippocampus. Generation of NexCre cDKO mice was done by crossbred of three mice strains: APPflox (Mallm et al., 2010), APLP2-KO (von Koch et al., 1997) and NexCre (Goebbels et al., 2006). Final mating were $APP^{flox/flox}/APLP2^{-/-}$ × $APP^{flox/flox}/APLP2^{-/-}/NexCre^{+/T}$ expressing Cre prenatally (from about E11.5 onwards) in postmitotic neuronal progenitor cells as confirmed by crosses to Cre reporter mice (Hick et al., 2015).

2.1.1.4 Aηα injection

Viral Aηα injection was performed in Heidelberg in the lab of U. Müller. WtR6 littermate control (LM) animals were injected with a vector only containing Venus (pAAVss-Syn-lckVenus (1x10e9)) whereas Aηα injection was performed with two different titer pAAVss-Syn-lckVenus-T2A-Aη-α (1*10e9) and pAAVss-Syn-lckVenus-T2A-Aη-α (1*10e10). Three weeks after injection the pyramidal cell layer of CA1-CA3 hippocampal neurons was intact. Injection took place four weeks

before starting electrophysiological experiments. Fluorescent signal in the CA1-CA3 and DG hippocampal region was tested right before measurements to be sure of vector expression.

2.1.2 Patients samples

This part of the study is approved by the ethics committee of the university hospital Magdeburg and every patient gave written and informed consent. LGI1 Patient1 was admitted with a limbic encephalitis (LE) after a series of four grand mal seizures on one day and MRI-FLAIR intense lesion in the hippocampus. Investigation on previous symptoms revealed no signs of FBDS, no cognitive decline and no complex partial seizure before admission. Immunosuppressive therapy was initiated in Patient1 and Patient2 including plasma exchange, methylprednisolone (MP) and long-term immunosuppression with Rituximab. Patient3 returned to normal after recurrent MP. Patient1 returned almost back to normal with only subjective attentional and amnestic deficits. Patient2 and Patient3 had a normal performance in recurrent CERAD plus test (Consortium to Establish A Registry for Alzheimer's Disease). CERAD is a collection of different dementia tests to assess the severity of dementia.

2.2 Acute hippocampal slices

2.2.1 ACSF'S

ACSF is used to obtain best conditions for the slices during preparation, cutting and measurements. To achieve these properties, the ACSF needs to contain all important ions and glucose for optimal neuronal function (see Table 1). To supply the tissue with an adequate amount of oxygen and to reach a physiological pH of 7.3 the ACSF was constantly carbogenated (95% O2, 5% CO2). In this study for preparation and electrophysiological recordings two different ACSFs were used depending on LTP or LTD measurements. Both ACSFs contained a high Mg^{2+} concentration of 2 mM to prevent a prematurely release of the Mg^{2+} block from the NMDA receptor which would result in a pre-potentiation in the acute slices due to stress resulting from the preparation steps.

2.2.2 Preparation of acute hippocampal slices

For the preparation of acute transversal hippocampal slices, mice were briefly anesthetized with Isoflurane and rapidly decapitated. The skull was opened, and the brain was removed. It was immediately transferred into ice-cold, carbogenated (95 % O2 and 5 % CO2) artificial cerebral

spinal fluid (ASCF) for three minutes. All following steps were also performed in ice-cold ACSF to prevent oxidative stress.

For preparation of the hippocampi the cerebellum and a part of the forebrain containing the olfactory bulb was removed via a razor blade. In the next step the two hemispheres were separated by a razor blade as well. To uncover the hippocampus, the hemisphere was placed with the cerebellum to the top and the striatum was removed with two rounded spatulas from the medial side. The first spatula was placed directly under the *fimbria hippocampi* to loosen the hippocampus and the second spatula dissecting it from the subiculum. Afterwards the hippocampus could be easily folded out of the remaining cortical tissue.

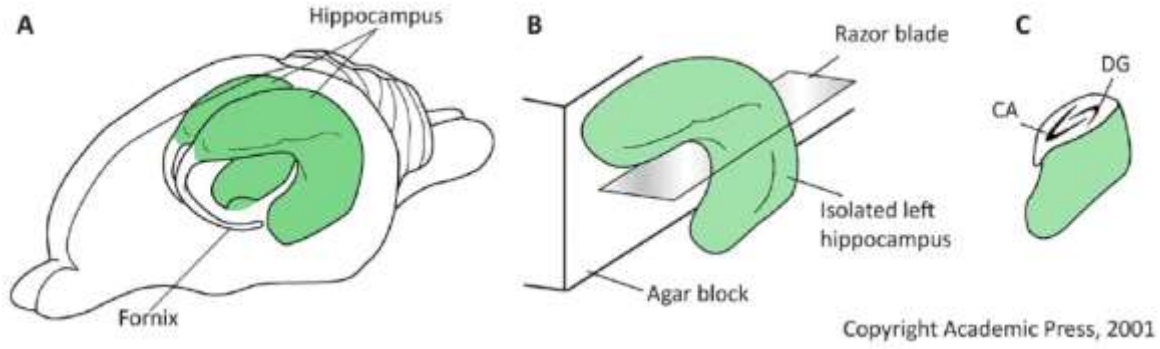

Figure 6: Location of the hippocampus in the rat brain. *A* Schematic illustration of the location of both hippocampi in the rat brain. *B* Alignment of the hippocampus to the agar block and preparation of 400µm sections with the vibrating microtome blade. *C* View of the transversely cut, intact hippocampus. A = Cornu ammonis, DG = dentate gyrus (Hammond, 2001).

To receive 400 µm thick transversal slices, the hippocampus was glued with the ventral part down on a specimen plate while leaning on an agar block with the dentate gyrus facing it (Figure 6). The specimen plate was quickly placed into ice-cold ACSF and with the VT1200S vibrating microtome (Leica Microsystems, Germany) the hippocampus was cut along its longitudinal axis in a slow and gentle, tissue protecting manner. After cutting the slices were transferred into a custom-made submerged chamber to rest for 90 min in ACSF at room temperature (RT). All these steps together not should not exceed a time of 20 minutes.

Table 1: Composition of ACSFs. All Chemicals obtained from Applichem (Konnerth et al, 1984).

Substance	LTP ACSF Molarity[mM]	LTD ACSF Molarity[mM]
$NaHCO_3$	26,0	26,0
$NaH_2PO_4*H_2O$	1,25	1,25
NaCl	125,0	125,0
$MgCl_2*6H_2O$	2,0	2,0
KCl	2,5	3
D(+)-Glucose	25,0	10,0
$CaCl_2*H_2O$	2,0	2,5

2.3 Electrophysiology

2.3.1 Extracellular field recording

For electrophysiological measurements two nearly identical setups were used. Blinded to phenotype, control as well as altered slices were measured alternating on both setups to create similar conditions. Additionally, flow rate, temperature and filter setting were kept customizable to achieve comparable results. With the help of a pre-programmed stimulus pattern in the Master trigger (Master 8 A.M.P.I., Israel), an impulse could be applied to the slices via the stimulus isolator (A360 or A365, WPI, USA). The signal was visualized using oscilloscope (HM507, HAMEG Instruments). To minimize signal interference, upstream of the recording electrode an amplifier was positioned (HS-2A, Axon Instruments), which strengthen the mediated signal by a factor of ten. In addition, the chamber and the micromanipulators were attached to a vibration-steamed table to avoid interference in the signal. To achieve a consistent temperature, the chambers were placed on an aluminum heating base (PH-1, Warner Instruments). Upstream of the chambers an additional preheating element (in-line solution heater SC-20, Warner Instruments) was installed and both heating elements were connected to an adjustable Dual Channel Heater Controller (TC-334B, Warner Instruments). A constant temperature of 23 °C (RT) for fiber volley measurements and 32 ± 0.2 °C for basal recordings as well as LTP and LTD measurements was adjusted. To adjust flow rate peristaltic pumps (Ismatech, Switzerland or Abimed, Germany) were used. ACSF was led through PVC tubings (TYGONE, Ismatec) for standard recording whereas silicon tubings (PharMed® Ismaprene, Ismatec) were used for autoimmune antibody experiments and for experiments were inhibitors or peptides were

applied in order to prevent sticking to the tubing walls. After approximately 1.5 h of recovery time from preparation, slices were placed in recording chambers (RC-22, Warner Instruments, Conneticut, USA or custom-made, MPI Martinsried) with a continuous flow rate of 1.5 ml/min of ACSF using a stereo microscope (SMZ 654, Nikon, Japan or Heerbrugg at Leica Microsystems). Slicers were aligned with the CA3 region on the side of the mechanically adjustable stimulus electrode (Leitz) and with the CA1 region parallel to the electrically adjustable recording electrode (Wetzler and Nano stepper). Glass microelectrodes filled bubble-free with 3 M NaCl were used to record electrically evoked field excitatory postsynaptic potentials (*f*EPSP) in the CA1 hippocampal region. Borosilicate glass capillaries (0.58 x 1.00 x 100 mm, Biomedical Instruments, Germany) used as recording electrodes were pulled with a Flaming Micropipette Puller (P-97, Sutter Instruments, USA) generating tips of approximately 1 to 3 MΩ resistance and placed in CA3 Schaffer collaterals at a depth of 120-150 µm (Figure 7).

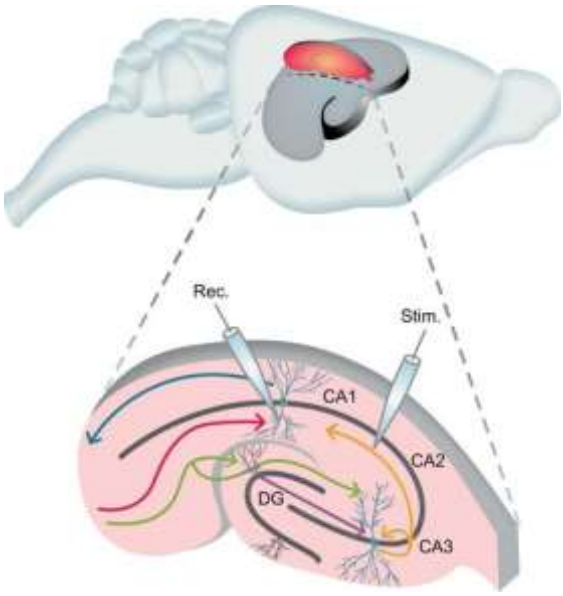

Figure 7: Orientation of the hippocampus within the rodent brain and placement of the stimulating and recording electrode in transversal hippocampal slices. *Upper image section:* localization of the hippocampus (dark grey) in the rodent brain. Transversal hippocampal slice in displayed (red) and enlarged. *lower panel:* anatomy of the hippocampus, Entorhinal cortex (EC) display starting point of signal transduction via perforant path (green) to the dentate gyrus (DG) granule cells or CA3 pyramidal cells or to CA1 region (red). Mossy fiber cells of DG (violet) transfer signals to CA3 pyramidal cells, were they are transferred via schaffer collaterals (yellow) to CA1. CA1 pyramidal cells deliver the Signal back to the EC (blue). For electrophysiological measurements stimulating electrode (Stim.) was placed in CA3 schaffer collaterals and Signal was recorded via recording electrode (Rec.) in CA1 dendrites (Korte and Schmitz, 2017).

2.3.2 Stimulating protocols

To investigate basal synaptic activity Input/ Output measurements were performed. Fiber volley measurements that reflect the presynaptic part of *f*EPSP, or in more detail the summation of action potentials of stimulated axons, were performed at RT to avoid overlapping of FV and

*f*EPSP Signal. Therefore, stimulus intensity was adjusted to fiber volley amplitudes from 0.1 to 0.8 mV and correlated stimulus strength of *f*EPSP response was measured. The second method to investigate basal synaptic activity is the measurement of the *f*EPSP signal (Figure 8) in relation to defined current values (25-250 µA) at a temperature of 32 °C.

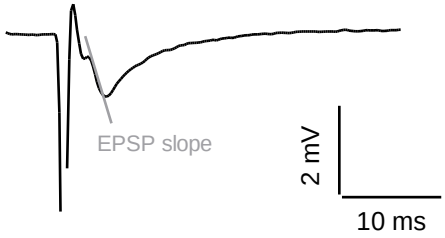

Figure 8: *f*EPSP Signal. Example of excitatory postsynaptic signal at 32 ± 0.2 ° C with initial stimulating artefact. Light grey line = negative increase in signal measured before and after LTP.

Presynaptic function was investigated by Paired-pulse facilitation (PPF) measurements. These measurements are based on the probability of neurotransmitter release of the presynapse (see 1.1.3). Through an incoming action potential at the presynapse, vesicles filled with neurotransmitters merge with the membrane, at the so-called active zone. By shortening the interstimulus intervals of the incoming signals, the neurotransmitter release occurs at even shorter intervals (up to 10 ms) until the presynaptic cell is no longer able to recycle the vesicles before the next stimulus arrives (Zucker and Regehr, 2002). Due to the remaining calcium of the first signal, the second signal is amplified. This type of plasticity is also called short-term plasticity and can take place within milliseconds (Regehr, 2015). The measurements were taken at 40% of the maximum rise of the signal, in which a population spike occurs, which means that not only the area of interest, but also nearby dendrites were stimulated. Three values were recorded for each interstimulus interval of 160, 80, 40, 20 and 10 ms (Figure 9).

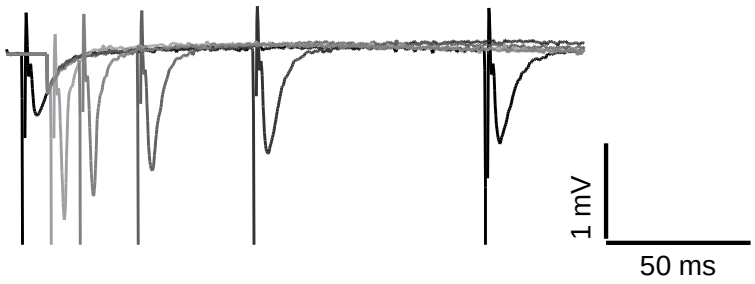

Figure 9: Paired pulse facilitation. Various interstimulus intervals (ISI) shown. Black line left = first signal, light grey/white line = ISI 10 ms, light gray line = ISI 20 ms; Gray line = ISI 40 ms; Dark grey line = ISI 80 ms; Black line on the right = ISI 160 ms.

To investigate long-term synaptic changes, LTP was induced. These measurements as well as LTD measurements took place at 32 °C. Initially and similar to PPF measurements, 40% of maximum *f*EPSP increase was defined. After 20 minutes baseline recording at 0.1 Hz, TBS stimulating protocol was applied (10 trains of 4 pulses at 100 Hz in an 200 ms interval, repeated 3 times)(Figure 10).

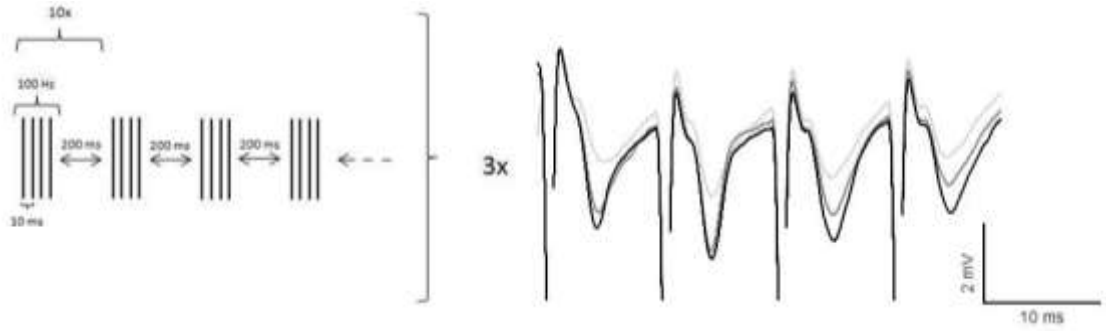

Figure 10: stimulating protocol. CA3 schaffer collaterals stimulation to induce LTP. 3 repetitions of a high frequency pulse were given at a distance of 10 s. This consists of 10 stimuli with a frequency of 5 Hz. Each stimulus consists of four pulses with a distance of 10 ms and an interstimulus interval of 200 ms. Light grey line = 1st repetition; Grey line = 2nd repetition; Dark grey line = 3rd repetition.

2.3.3 Peptides and Proteins

2.3.3.1 Autoimmune antibodies

For electrophysiological autoimmune antibodies (AAB) experiments slices of adult (4 to 9 months old) C57BL/J6 or Thy-1 mEGFP (on a C57BL/6J-SV129 background) mice were used. In a volume of 30 ml, which has turned out to be enough to circulate through the whole system during an experiment, slices were continuously incubated with either purified autoimmune

antibodies of three different patients or of healthy controls in a final concentration of 4 µg/ml. Acute hippocampal slices were pre-incubated for 1 hour or 6 hours in 10 ml gently carbogenated ACSF containing autoimmune antibodies of the three different patients or healthy controls.

2.3.3.2 APPsα and BTX

For investigations on the NexCre cDKO APP mouse line, recAPPsα and α-Bungarotoxin was applied to the acute hippocampal slices during the experiments. In a volume of 30 ml, recAPPsα or recAPPsα together with α-Bungarotoxin (BTX, Merck Millipore, Germany) has been solved in a final concentration of 10 nM based on previous acute peptide recordings with recAPPsα (Hick et al., 2015). Acute slices were pre-incubated with 10 nM recAPPsα alone or 10 nM recAPPsα + 10 nM BTX for 1 hour or treated with 10 nM BTX acutely for 10 minutes before baseline recording. After 1.5 h resting time, after preparation, slices were transferred to a submerged recording chamber where *f*EPSP recording was performed at the CA3-CA1 pathway. ACSF with 10 nM recAPPsα or recAPPsα + 10 nM α-BTX circulated continuously throughout LTP recording. To further avoid osmolality changes caused by evaporation, moisturized carbogen was directed in the 30 ml recording solution which was additionally covered with Parafilm® (Bemis, USA).

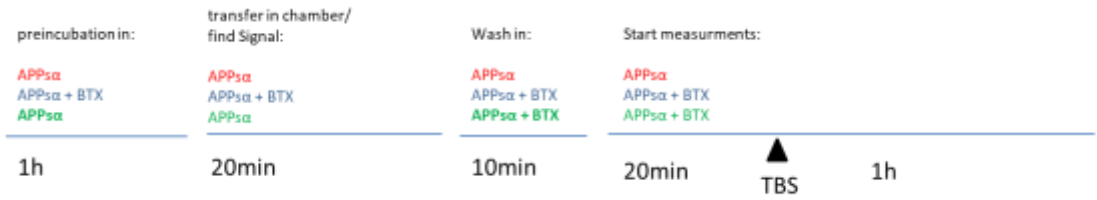

Figure 11: Experimental setup for recAPPsα, BTX measurements on NexCre cDKO APP mouse line. Acute slices of NexCre DKO mice were pre-incubated with 10 nM recAPPsα alone (red) or 10 nM recAPPsα + 10 nM BTX (blue) for 1 hour or treated with 10nM BTX acutely 10 minutes before baseline recording (green). After 1.5h resting time (including pre-incubation), after preparation, slices were transferred to a submerged recording chamber where fEPSP recording was performed at the CA3-CA1 pathway. ACSF with 10 nM recAPPsα or recAPPsα + 10 nM α-BTX circulated continuously throughout LTP recording.

2.3.4 Data analysis

Electrophysiological recording data were analyzed using custom made programs (ANA-DAP version 4.755 or ANA-PPF version 4.2) (M. Korte and V. Staiger) generating Microsoft Excel files (Microsoft, USA). A manually defined window made it possible to precisely measure the negative *f*EPSP slope of fiber volley, LTP and EPSP measurements. For PPF analysis the negative *f*EPSP slope of the second signal was divided by the first using an equation $(\frac{slope fEPSP2}{slope fEPSP1})$*100. Generated Excel files containing one single value for the *f*EPSP slope every 10 seconds for LTP

measurements were further analyzed by generating the mean value for 1 minute out of 6 single values. The LTP data were plotted as a relative increase compared to baseline measurements and calculated as follows: $(\frac{slope fEPSP}{slope fEPSP baseline})$*100. Only experiments with variance of baseline under 10% were included as well as physiological LTP curves without seizures or extensive population spikes. Baseline synaptic transmission experiments like FV, EPSP or PPF were plotted as the average of three values per measured condition.

2.4 Spine analysis

2.4.1 Golgi Cox staining

In case of NLRP3 only one hemisphere was used for electrophysiological experiment whereas the other one was used for morphological analysis via Golgi Cox Method. Golgi staining was performed as described in manufactures instructions in the GolgiStain™ Kit (FD NeuroTechnologies, Inc., USA). During acute hippocampal slice preparation for electrophysiological experiments one hemisphere remained untouched after separating the two hemispheres. This hemisphere was stored for two weeks at RT in equal amounts of Solution A and B. The mixture of solution A and B was prepared at least 24 hours before experiment and changed after 24 h. After two weeks, the hemisphere was transferred into solution C for two up to seven days and stored at 4 °C. After 24 h solution C was renewed. Brain was embedded in 2% Agar in 0.1 M PB and cutting of 200 µm sections took place with a vibrating microtome (Leica, VT1200S, Germany). Coronal brain sections were mounted on a gelatin coated slide (1 % gelatin/0.1 % Chromalaun) and stained as described in manufacturer's instructions (exception: Xylene was replaced by Appiclear). In the last step, slices were cover-slipped with Permount (Fisher Scientific, Germany).

Imaging was performed using an Axioplan 2 Microscope (Zeiss, Germany). CA1 and CA3 apical hippocampal dendrites (2nd or 3rd order branches) were imaged using a 63x oil objective with a stack thickness of 0.5 µm. In total 100 µm dendritic length was taken and divided by the number of spines analyzed using ImageJ (1.48v, National Instruments of Health, USA). Blinded to genotype two animals per genotype and five neurons per animal were at minimum analyzed. Using GraphPad Prism (Version, 5.01) software, data were finally analyzed.

2.4.2 Spine analysis in Thy-1 GFP expressing animals

In case of AAB experiments, spine analysis was done on acute slices of Thy-1 GFP mice, expressing GFP in neurons under the Thy-1 promotor. Therefore, images of 30 µm thick slices treated long or acute with certain ABB were cut with a freezing microtome (2.5.1 Cryosections) and imaged with a digital camera (AxiocamMR, Zeiss, Germany) at the Axioplan2 microscope (Zeiss, Germany) using the 63x oil objectives. Further processing was performed with ImageJ (1.48v, National Instruments of Health, USA). At least 100 µm of DG, CA1 and CA3 apical hippocampal dendritic length (2^{nd} or 3^{rd} order branches) were measured and divided by the number of spines. Blinded to genotype and treatment three animals per genotype and five neurons per animal were at minimum analyzed. Using GraphPad Prism (Version, 5.01) software, data were finally analyzed.

2.5 Immunohistochemistry

2.5.1 Cryosections

To determine the penetration depth of the AABs into the acute hippocampal slices during electrophysiological measurements, the slices were fixed in ice cold paraformaldehyde (Applichem, 4% w/v in 0.1 M phosphate buffer) for 1 h. Afterwards the slices were transformed in 30% sucrose solution (Applichem, 30% w/v in 0.1 M phosphate buffer) at least overnight. 30 µm thick slices were cut with a freezing microtome and mounted on gelatin coated slides, dried for 1 h at RT and stored at 4 °C. Secondary antibody treatment could be performed immediately, because slices were already treated with first antibody during electrophysiological experiments. Therefore, slices were washed with 1xPBS and incubated 2 h with the secondary antibody dilution 1:500 in PBS (Cy3-AffiniPure Rabbit Anti-Human IgG (H+L), Dianova). Afterwards slices were washed 5-6 times over 30 minutes with 1xPBS and DAPI (4'6-di-amidino-2-phenylindol) staining, diluted 1:1000 in PBS was performed for 5 minutes. Following 5-6 times washing with PBS, slices were mounted in Fluoro-Gel®. For analyzing the sections, they were imaged with a digital camera (AxiocamMR, Zeiss, Germany) at the Axioplan2 microscope (Zeiss, Germany) using the 10x and 20x objectives. Further processing was performed with ImageJ (Wayne Rasband) and Adobe Photoshop CS (Adobe, USA).

2.5.2 Solutions and Antibodies

4% Paraformaldehyde (in 0.1 M phosphate buffer, pH 7.4)

40 g PFA in 500 ml warm dH_2O, cool down and filtrate

add 500 ml of 0.2 M phosphate buffer

0.1M PB

0.78 g NaH_2PO_4

3.45 g Na_2HPO_4

in 500 ml MilliQ water

10x Phosphatebuffered saline (1 M PBS, pH 7.4)

11.5 g $Na_2HPO \times H_2O$

2.0 g KH_2PO_4

80.0 g NaCl

2.0 g KCl

in approx. 900 ml MilliQ water (pH to 7.4) fill up to 1 L final volume with MilliQ water

Table 2: List of first and secondary Antibodies used for immunohistochemistry/immunocytochemistry.

Antibody	manufacturer	species	dilution
DAPI	Applichem		1:1000
Anti-Human IgG (H+L) Cy3	Dianova	rabbit	1:500

2.6 statistical analysis

The statistical analysis was performed using Microsoft Excel or GraphPad Prism. To compare two different experimental conditions or genotypes an unpaired two-tailed Student's t-test was used. Data including more than 2 different groups were analyzed using a One-Way ANOVA followed by a post-hoc Bonferroni´s Test. Values of $p \leq 0.05$ were considered significant and plotted as follows *$p < 0.05$; **$p < 0.01$; ***$p < 0.001$. All data shown were generated with GraphPad Prism with mean values ± standard error of the mean (SEM).

3. Results

3.1 The role of Amyloid precursor protein in synaptic plasticity

Previous studies have shown positive functions of APP and some of its cleavage products in synaptic plasticity (1.3.2 Function of APP and its cleavage products). Additionally, a short incubation of slices with recAPPsα is enough to largely rescue the LTP deficits of NexCre cDKO mice (Hick et al, 2015). As Aβ is acting negatively on neurons in neurodegenerative diseases like Alzheimer's disease, APPsα was shown to have a positive effect (Fol et al., 2016), but it was not clear on which receptor APPsα is binding to act on synaptic plasticity. In this part of the study investigations on the α7-achetylcholinreceptor (α7-nAChR) and its antagonist BTX with respect to binding of recAPPsα took place.

3.1.1 Inhibition of α7-nAChR by BTX blocks positive effects of recAPPsα on LTP

Previous studies showed that α7-nAChR seems to be a target receptor to rescue deficits in hippocampal LTP in Aβ infused rats (Chen et al., 2006). Therefore, investigations on the role of recAPPsα in context with the α7-nAChR were done. In this part of my thesis I investigated the role of recAPPsα and αBTX on the α7-nACh receptor in case of electrophysiological LTP recordings.

Acute slices of NexCre cDKO mice treated with recAPPsα (green) or recAPPsα with wash in of BTX 10 minutes before starting baseline recording (dark orange) displayed an indistinguishable LTP curve in induction and maintenance (Figure 12A). The application of BTX together with recAPPsα (light orange) on the other hand lead to a reduction of LTP induction and maintenance. This result is also shown in a bar graph, which shows significant differences in induction (t20-25; p=0.041) and maintenance (t75-80; p= 0.017) of LTP tested via ANOVA and Post-hoc Bonferroni test (Figure 12B). Overall these results indicate that α7-nAChR is a potential receptor for recAPPsα.

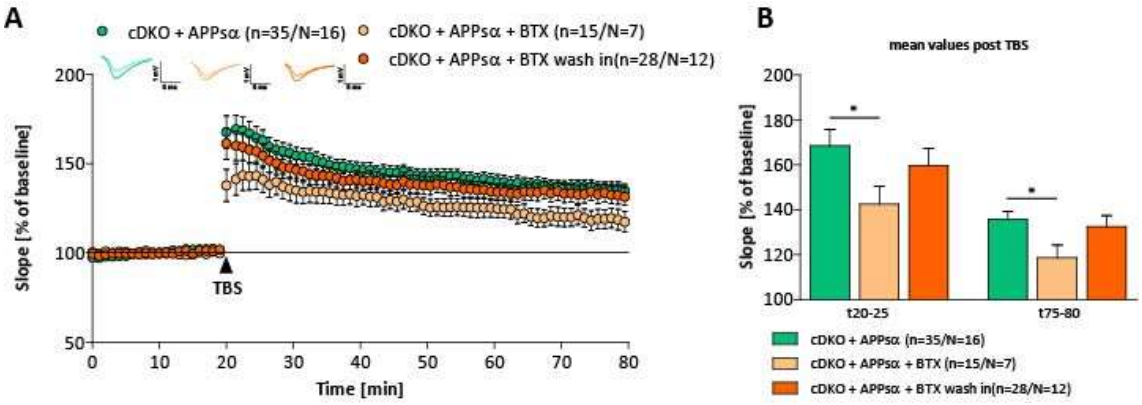

Figure 12 Reduced LTP in cDKO mice treated with recAPPsα and BTX. Field excitatory postsynaptic potentials (fEPSPs) of acute hippocampal slices of NexCre cDKO mice treated with 10 nM recAPPsα (green circles), 10 nM recAPPsα + 10 nM BTX 1 h preincubation (light orange circles) or with 10 nM recAPPsα + 10 nM BTX acute treatment 10 minutes before Baseline recordings (dark orange circles) were recorded in CA1 region by stimulating Schaffer collateral axons of area CA3 at a frequency of 0.1 Hz. **(A)** LTP was induced by application of TBS after 20 min baseline stimulation (arrowhead) in slices pretreated for 1 hour with recAPPsα, recAPPsα + BTX or acute treatment of BTX 10 minutes before baseline measurements in slices pretreated for 1 h with recAPPsα. The LTP induction rate is shown as percentage % of mean baseline slope. During LTP measurement slices were continuously perfused with either recAPPsα or recAPPsα + BTX. RecAPPsα treated cDKO slices revealed a trend of a higher induction as well as maintenance of LTP compared to recAPPsα + BTX 1 h preincubation treatment. This trend is quantified in a bar graph **(B)**, which shows the first (induction) and last five minutes (maintenance) of LTP. cDKO slices treated only with recAPPsα (168.49±7.20) and cDKO slices treated with recAPPsα + acute BTX (159.65±7.65) show a higher induction compared to slices co-treated with recAPPsα and BTX for 1 h before measurements (142.57±7.75). The same trend could be seen also in maintenance of LTP (recAPPsα= 135.59±3.81; recAPPsα+acute BTX=132.43±4.87; recAPPsα+BTX=118.58±5.51). Statistics: one-way ANOVA with post hoc Bonferroni test.

3.1.2 Young htauP301S mice

Tau is a microtubule-associated protein normally found in the axons of neurons and is thought to promote microtubule assembly and stabilization (Polydoro et al., 2009). In young htau.P301S mice, mutation of tau on position 301 is leading to an AD phenotype represented by tau tangles in the cortex and hippocampus. Electrophysiological investigations on 10-13 weeks old htau.P301S mice with a mild phenotype (Figure 5) reflected by initial spine loss displayed a reduced induction phase of LTP compared to BL6 littermates (LM) (Figure 13A). Bar graph of the first five minutes after LTP induction support these findings. The mean potential value of littermate controls with 166.71±6.15% is significantly increased compared to young htau.P301S with only 142.86±6.27% (p=0.014) (Figure 13B). Maintenance of LTP in turn was indistinguishable between both phenotypes. The bar graph of the last five minutes of LTP shows quantitative results where littermate controls show a potential level of 142.89±4.86% and htau.P301S show 136.94±4.86% (Figure 13C).

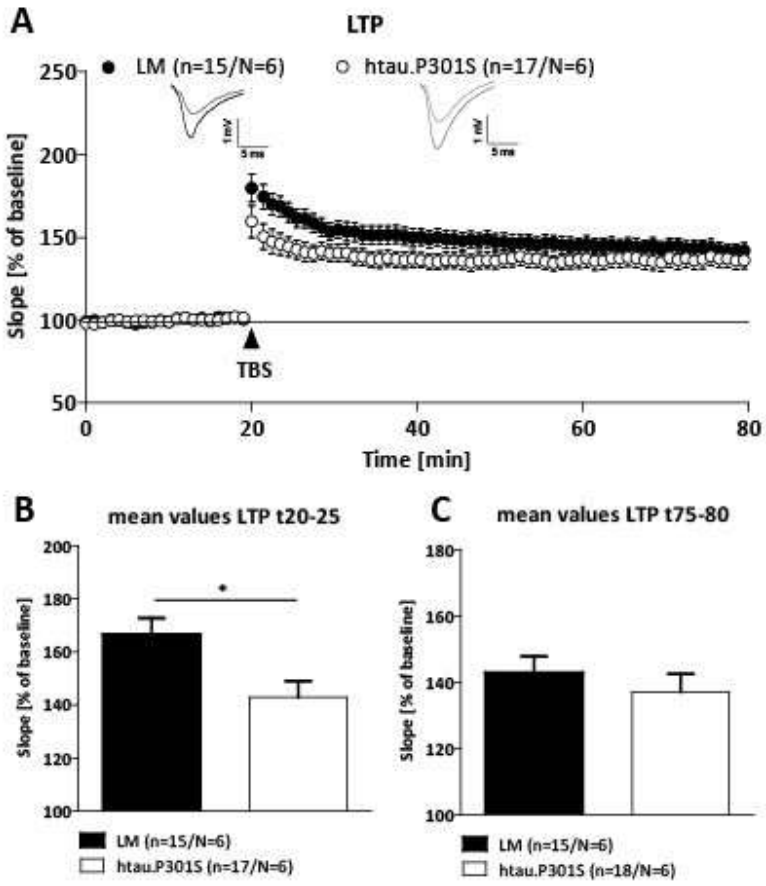

Figure 13 LTP measurements on acute hippocampal slices of 10-13 weeks old htau.P301S mice. Activity-dependent synaptic plasticity was investigated on acute hippocampal slices of 10-13 weeks old littermate control (LM, black circles) and htau.P301S mice (open circles). Field excitatory postsynaptic potentials (fEPSPs) were recorded in CA1 region by stimulating Schaffer collateral axons of area CA3 at a frequency of 0.1 Hz. The LTP induction rate is shown as percentage % of mean baseline slope. Data points were averaged over 6 time points and error bars indicating SEM, n= number of recorded slices/N= number of animals. Data were analyzed by Student´s t-test. (A) After 20 min baseline recording, LTP was induced by application of Theta burst stimulation (TBS, arrowhead). Acute slices of htau.P301S mice displayed a LTP curve that is significant lower in induction compared to littermate controls. (B) Bar graph of the first five minutes after TBS show a significant higher induction of LTP in littermate controls (166.71±6.15) compared to htau.P301S (142.86±6.27) (p=0.014). (C) In comparison analysis of last five minutes of LTP is statistical indistinguishable in both genotypes (LM: 142.89±4.86; htau.P301S: 136.94±4.86).

Investigation of LTP, LTD as well as basal synaptic transmission via EPSP as well as PPF measurements in young htau.P301S mice were done and compared to age-matched littermate controls. LTD curves are indistinguishable between both phenotypes at the age of 10-13 weeks (Figure 14A). The quantification of the potentiation of the last five minutes of LTD recording mirrors these findings. Acute hippocampal slices of htau.P301S mice display potentiation levels of -1.08±4.22% and littermate controls -8.26±3.35% shown in a bar graph (Figure 14B). Same is true for the induction phase where LM control displays values of: -26.00±1.87% compared to those of htau.P301S with -27.67±2.07% (Figure 14C). Basal synaptic transmission reveal overlapping EPSP curves and PPF paradigm comparing htau.P301S and age-matched littermate controls (Figure 14D, E).

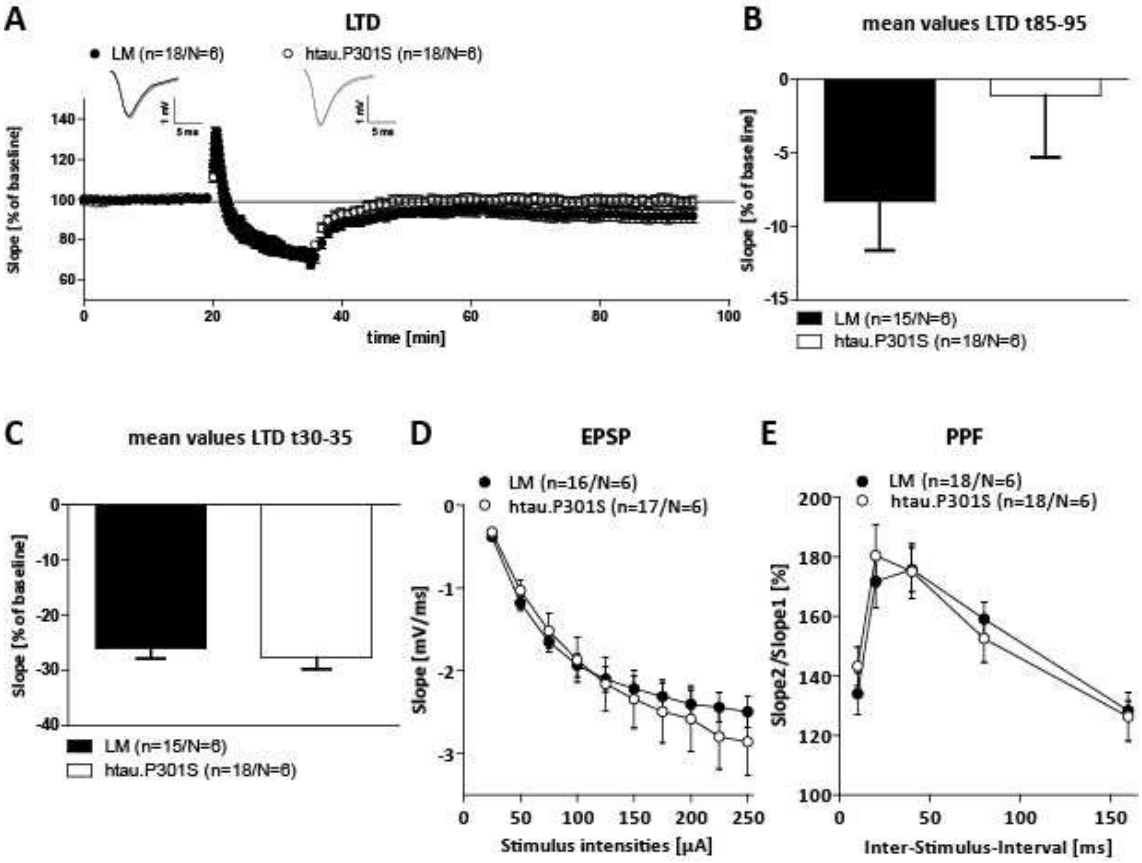

Figure 14 LTD, EPSP and PPF measurements on acute hippocampal slices of 10-13 weeks old acute hippocampal slices of htau.P301S mice. Activity-dependent synaptic plasticity was investigated on acute hippocampal slices of 10-13 weeks old littermate control (LM, black circles) and htau.P301S mice (open circles). Field excitatory postsynaptic potentials (fEPSPs) were recorded in CA1 region by stimulating Schaffer collateral axons of area CA3 at a frequency of 1 Hz. The LTD induction rate is shown as percentage % of mean baseline slope. Data points were averaged over 6 time points and error bars indicating SEM, n= number of recorded slices/N= number of animals. Data were analyzed by Student´s t-test. After 20 min baseline recording, LTD was induced by application of low frequency stimulus for 15 minutes. (A) Acute slices of htau.P301S mice displayed an LTD curve that is statistical indistinguishable maintenance to that of littermate controls. (B) Bar graph of the last five minutes of LTD show no significance between genotypes but a slight trend of an decreased LTD in htau.P301S mice (LM: -8.26±3.35; htau.P301S: -1.08±4.22). (C) Bar graph of the last five minutes of induction show no significance between groups (LM: -26.00±1.87; htau.P301S: -27.67±2.07). (D) Neuronal excitability was comparable at all stimulus intensities (25-250 µA) between genotypes. (E) PPF was not altered at all ISI between littermates and htau.P301S mice.

3.1.2.1 Increased LTP of aged htau mice rescued via application of recAPPsα

I investigated the role of recAPPsα on LTP curve of aged htau.P301S mice and their age-matched littermate controls. The phenotype of the mice at this aging time point is characterized by cognitive decline resulting from tau tangles in hippocampus and cortex (Figure 5). Acute slices of htau.P301S mice (open circles) display a LTP curve that shows a trend of higher LTP at induction phase which is significant at maintenance compared to littermate controls (black circles). This increased LTP can be rescued to LM control level via application of recAPPsα for one hour preincubation and during measurements (grey circles, Figure 15A). These findings are reflected in the bar graph, showing the averaged potential levels of the first (Figure 15B) and last five minutes (Figure 15C). Bar graph of the first five minutes after TBS shows no significant differences in induction of LTP between littermate controls with 161.93±7.41% and the other groups. Potential levels of htau.P301S with 177.04±9.45% show no differences compared to LM and htau.P301S + recAPPsα with 162.32±6.62%. Potential levels of the last five minutes of LTP show significant increased ($p=0.004$) values for htau.P301S with 153.29±5.13% compared to LM with 127.59±5.13%. Application of recAPPsα rescues the significantly enhanced LTP back to LM control level with 135.64±4.31% ($p=0.044$).

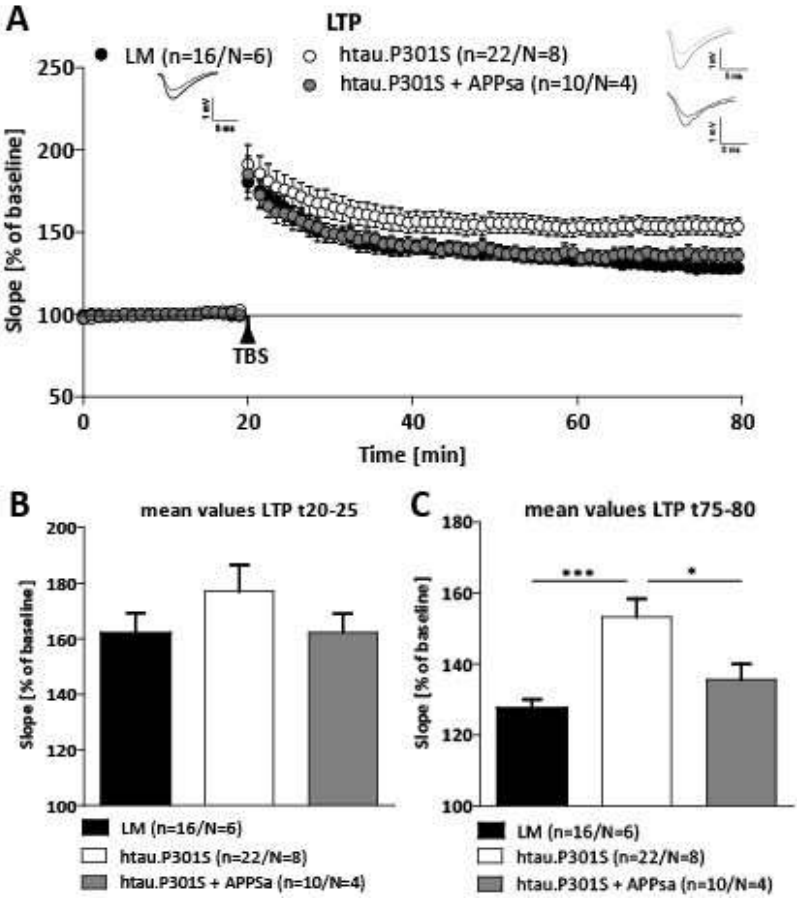

Figure 15 LTP measurements on acute hippocampal slices of 16-18 weeks old htauP301S mice. Activity-dependent synaptic plasticity was investigated on acute hippocampal slices of 16-18 weeks old littermate control (LM, black circles), htau.P301S mice (open circles) and htau.P301mice with recAPPsα application during measurement (grey circles). Field excitatory postsynaptic potentials (fEPSPs) were recorded in CA1 region by stimulating Schaffer collateral axons of area CA3 at a frequency of 0.1 Hz. The LTP induction rate is shown as percentage % of mean baseline slope. Data points were averaged over 6 time points and error bars indicating SEM, n= number of recorded slices/N= number of animals. Data were analyzed by one-way ANOVA with Bonferroni´s post-hoc test. (A) After 20 min baseline recording, LTP was induced by application of Theta burst stimulation (TBS, arrowhead). Acute slices of htau.P301S mice displayed a LTP curve that is significant higher in maintenance compared to littermate controls and htau.P301S mice treated with recAPPsα. (B) Bar graph of the first five minutes after TBS show no significant differences in induction of LTP between groups, but a slight trend of an increase in htau.P301S mice (LM: 161.93±7.41; htau.P301S: 177.04±9.45; htau.P103S+recAPPsα: 162.32±6.62). (C) The analysis of last five minutes of LTP revealed significantly higher potentiation levels for htau.P301S mice (153.29±5.13) compared to the both other groups (LM: p=0.0004; htauP301S+recAPPsα: p=0.044). Application of recAPPsα (135.64±4.31) rescued the effect of enhanced LTP in htau.P301S mice towards littermate control level (127.59±5.13).

Acute slices of htau.P301S mice displayed a LTD curve that is statistical indistinguishable maintained to the other groups. Interestingly, the LTD induction is strongly enhanced upon recAPPsα treatment, but not as stable as in LM or htau.P301S mice during 60 minutes of LTD recording (Figure 16A). Quantification of the last five minutes of LTD shows no significant differences between the three groups with: htau.P301S mice -6.53±3.88%, htau.P301S + recAPPsα -3.25±3.19% and littermate controls with -10.30±3.92% (Figure 16B). Potential levels of the first five minutes of LTD show no significance between groups with LM -20.46±3.52% and htau.P301S with -20.24±3.52% but a slight trend of an increase when recAPPsα is added -30.64±4.55% (p=0.06 compared to htauP.301S, p=0.1 compared to LM)(Figure 16C). Basal

synaptic transmission was measured via EPSP and PPF paradigm. The neuronal excitability was comparable at all stimulus intensities (25-250 µA) between LMs and htau.P301S + recAPPsα, but impaired in htau.P301S mice compared to littermate controls reaching significance at a stimulus intensity of 175 µA (p=0.047). PPF was statistically not altered at all ISI between all groups. Interestingly, recAPPsα treatment leads to the highest PPF curve within that paradigm. Therefore, lower EPSP values in htau.P301S mice compared to LM could be rescued whereas physiological PPF paradigm gets enhanced.

Taken together the results suggest an altered homeostasis in aged htau.P301S mice that could be restored under recAPPsα treatment.

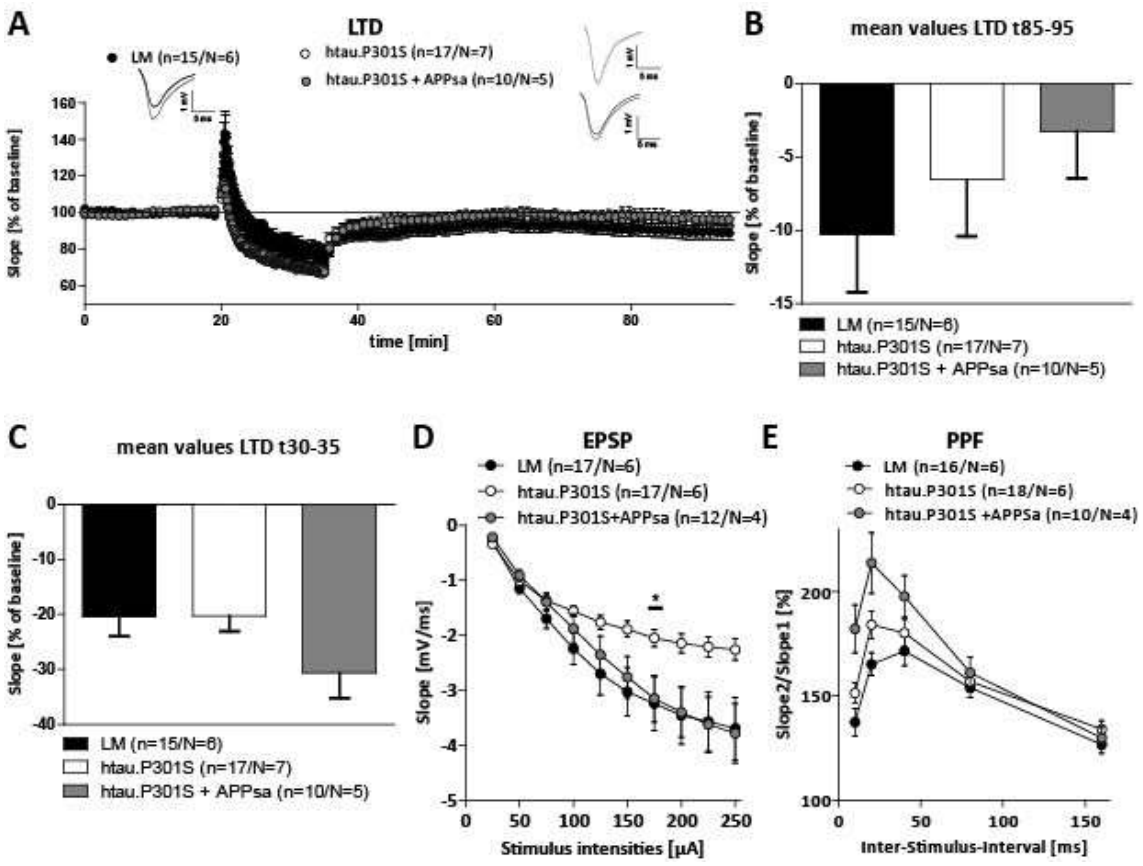

Figure 16 LTD, EPSP and PPF measurements on acute hippocampal slices of htau.P301S mice. Activity-dependent synaptic plasticity was investigated on acute hippocampal slices of 16-18 weeks old littermate control (LM, black circles), htau.P301S mice (open circles) and htau.P301mice with recAPPsα application during measurement (grey circles). Field excitatory postsynaptic potentials (fEPSPs) were recorded in CA1 region by stimulating Schaffer collateral axons of area CA3 at a frequency of 1 Hz. The LTD induction rate is shown as percentage % of mean baseline slope. Data points were averaged over 6 time points and error bars indicating SEM, n= number of recorded slices/N= number of animals. Data were analyzed by one-way ANOVA with Bonferroni´s post-hoc test. After 20 min baseline recording, LTD was induced by application of low frequency stimulus for 15 minutes. (A) Acute slices of htau.P301S mice displayed an LTD curve that is statistical indistinguishable maintenance to the other groups. Interestingly, the LTD induction is strongly enhanced upon recAPPsα treatment, but not as reduced as in LM or htau.P301S mice during

60 minutes of LTD recording. (B) Bar graph of the last five minutes of LTD show no significant differences between groups, but a slight trend of an decreased LTD in htau.P301S mice (-6.53±3.88) and an even higher effect in htau.P301S+recAPPsα (-3.25±3.19) compared to littermate controls (-10.30±3.92). (C) Bar graph of the LTD induction show no significance between groups (LM: -20.46±3.52; htau.P301S: -20.24±3.52) but a slight trend of an increase when recAPPsα is added (-30.64±4.55). (D) Neuronal excitability was comparable at all stimulus intensities (25-250 µA) between littermate controls and htau.P301S + recAPPsα, but impaired in htau.P301S mice compared to littermate controls reaching significance at a stimulus intensity of 175µA (p=0.047). (E) PPF was statistically not altered at all ISI between all groups. Interestingly, recAPPsα treatment lead to the highest PPF curve within that paradigm.

3.1.3 Injection of Aηα show no effect on hippocampal synaptic plasticity

Various cleavage products of APP are well studied at this time point. There are two physiological pathways that either prevent or promote Aβ generation from its precursor protein (APP), in a competitive manner. Here, I investigate cleavage products of a new physiological APP processing pathway by the η-secretase (Willem et al., 2015, Figure 2). One hypothesis is an impairment of hippocampal LTP due to Aηα. Previous studies with acute application of synthetic Aηα on hippocampal slices lead to a decreased and unstable LTP (Willem et al., 2015). Injection of mice took place four weeks before measurements.

Acute slices of pAAVss-Syn-lckVenus-T2A-Aη-α (1*10e9) (open circles) and pAAVss-Syn-lckVenus-T2A-Aη-α (1*10e10) (grey circles) injected mice display a LTP curve that is indistinguishable to littermate control injected pAAVss-Syn-lckVenus (1*10e9) (LM, black circles) (Figure 17A). Quantifications of the results are shown in a bar graph for the last five minutes of LTP that shows no differences between littermate control with 130.4±2.9% and Aηα injected mice with both titers 1*10e9 with 126.4±3.2 and 1*10e10 with 131.2±4.5% (Figure 17B). Neuronal excitability is comparable at all stimulus intensities (25-250 µA) (Figure 17C) and fiber volley amplitudes (0.1-0.8 mV) between groups (Figure 17D). PPF is not altered at all ISI (10 ms-160 ms) (Figure 17E).

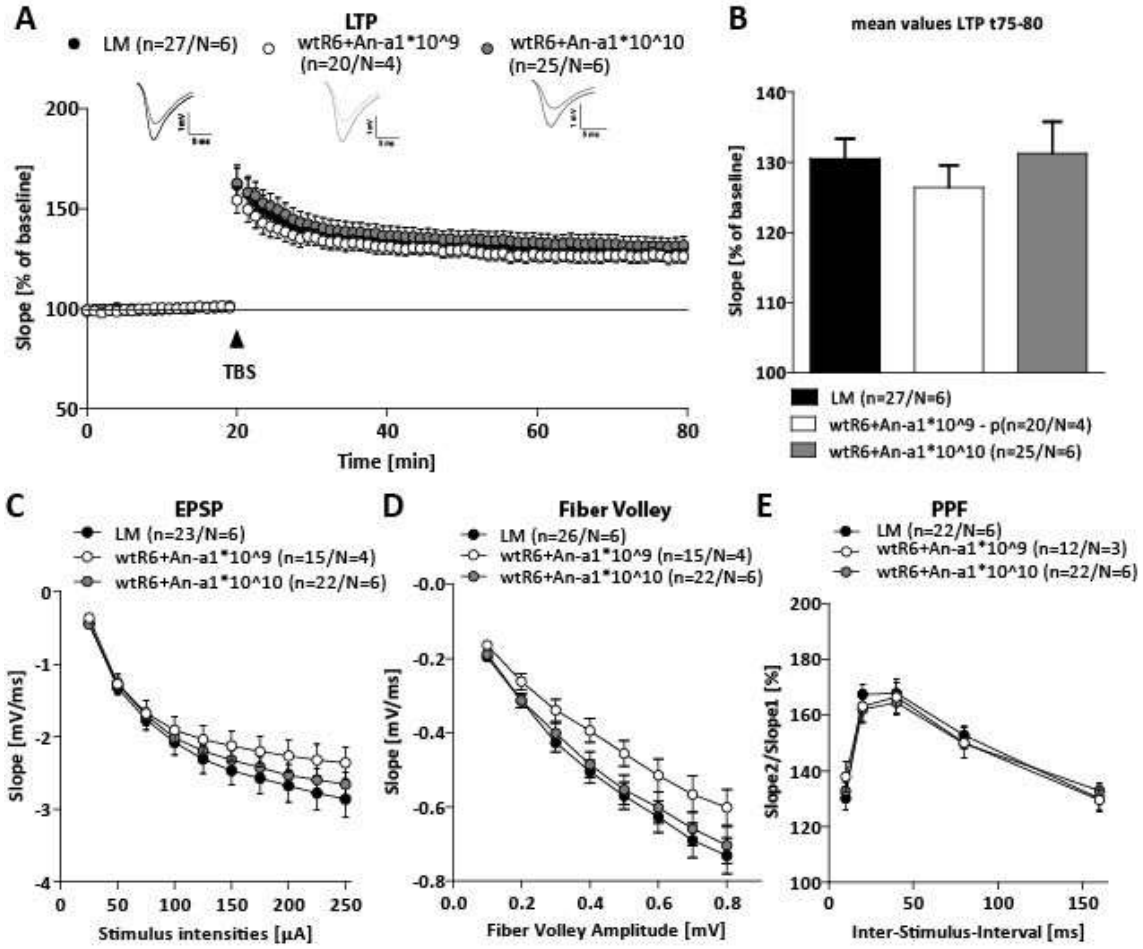

Figure 17 Electrophysiological measurements on Aηα injected mice. Activity-dependent synaptic plasticity was investigated on acute hippocampal slices of 10-15 weeks old littermate control pAAVss-Syn-lckVenus (1*10e9) (LM, black circles) and Aηα injected mice: pAAVss-Syn-lckVenus-T2A-Aη-α(1*10e9) (open circles) and pAAVss-Syn-lckVenus-T2A-Aη-α(1*10e10) (grey circles). Field excitatory postsynaptic potentials (fEPSPs) were recorded in CA1 region by stimulating Schaffer collateral axons of area CA3 at a frequency of 0.1 Hz. The LTP induction rate is shown as percentage % of mean baseline slope. Data points were averaged over 6 time points and error bars indicating SEM, n= number of recorded slices/N= number of animals. Data were analyzed by one-way ANOVA with Bonferroni´s post-hoc test. (A) After 20 min baseline recording LTP was induced by application of Theta burst stimulation (TBS, arrowhead). Acute slices of pAAVss-Syn-lckVenus-T2A-Aη-α (1*10e9) (open circles) and pAAVss-Syn-lckVenus-T2A-Aη-α (1*10e10) (grey circles) injected mice displayed a LTP curve that is indistinguishable to littermate control pAAVss-Syn-lckVenus (1*10e9) (LM, black circles). Example traces before TBS (light line) and after TBS (strong line) are shown for all groups. (B) Bar graph of the last five minutes of LTP shows no differences between littermate control (130,4±2,9) and Aηα injected mice with both titers (1*10e9=126,4±3,2; 1*10e10=131,2±4,5).(C) Neuronal excitability was comparable at all stimulus intensities (25-250 µA) and fiber volley amplitudes (D) Fiber volley was comparable (0.1-0.8 mV) between groups. (E) PPF was not altered at all ISI (10 ms-160 ms). Injection of mice took place 4-7 weeks before measurements.

3.2 NLRP3 in physiological aging

The study of Heneka and colleagues 2013 suggests a potential rescue effect of the NALP3 inflammasome deficit on spine density reduction in APP/PS1 mice. They suggest that KO of NLRP3 has a putative positive effect on the spine loss in physiological aging as well. Therefore, I started measurements on NLRP3 KO mice at different ages. Extensive results on earlier time points are present in my Master thesis. Here, I present the results of electrophysiological and morphological experiments of the 24 months old NLRP3 KO mice and will compare sex dependent differences at all other time points.

LTP curve of NLRP3 KO mice is indistinguishable to littermate controls in induction as well as maintenance (Figure 18A). Quantification of the last five minutes of LTP showed no differences between littermate control with 143.9±4.2% and NLRP3 KO mice with 143.2±5.3% (Figure 18B). Neuronal excitability was comparable at all stimulus intensities (25-250 µA) and fiber volley amplitudes (0.1-0.8 mV) tested (Figure 18C, D). Additionally, the presynaptic function was intact. PPF paradigm was not altered at all ISI between littermates and NLRP3 KO mice (Figure 18D).

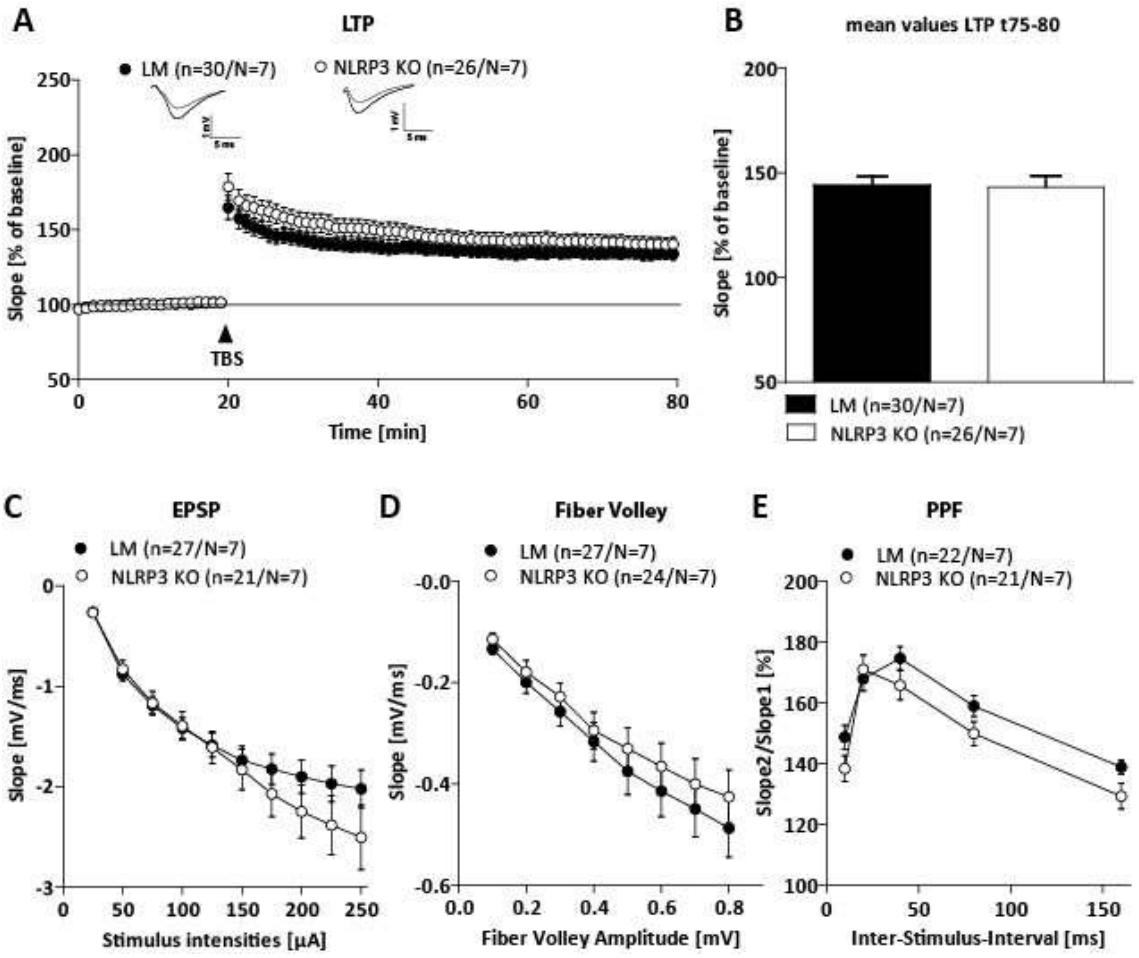

Figure 18 Electrophysiological measurements of 24 months old NLRP3 KO mice. Activity-dependent synaptic plasticity was investigated on acute hippocampal slices of 24 months old littermate control (LM, black circles) and NLRP3 KO mice (open circles). Field excitatory postsynaptic potentials (fEPSPs) were recorded in CA1 region by

stimulating Schaffer collateral axons of area CA3 at a frequency of 0.1 Hz. The LTP induction rate is shown as percentage % of mean baseline slope. Data points were averaged over 6 time points and error bars indicating SEM, n= number of recorded slices/N= number of animals. Data were analyzed by Student´s t-test. (A) After 20 min baseline recording LTP was induced by application of Theta burst stimulation (TBS, arrowhead). Acute slices of NLRP3 KO mice displayed a LTP curve that is indistinguishable to littermate controls. (B) Bar graph of the last five minutes of LTP showed no differences between littermate control (143.9±4.2) and NLRP3 KO mice (143.2±5.3). (C) Neuronal excitability was comparable at all stimulus intensities (25-250 µA) and fiber volley amplitudes (0.1-0.8 mV) tested. (E) PPF was not altered at all ISI between littermates and NLRP3 KO mice.

As there are hints towards gender differences during aging in literature (1.4.2 Inflammation in physiological aging) I additionally analyzed spine density as well as for electrophysiological measurements divided by sexes.

3.2.1 Sex dependent differences occur during aging

As I suspect sexual differences in LTP rate between sexes in very old mice. I decided to analyze electrophysiological and morphological measurements at different aging time points of 3, 6, 9, 12 and 24 months to see at which time point exactly the sex dependent differences occur. Therefore, I performed electrophysiological measurements on LTP as well as basal synaptic properties via EPSP, FV and PPF paradigm. Additionally, I analyzed the CA1 apical spine density in the murine hippocampus.

3.2.1.1 Electrophysiological analysis of 3-12 months old NLRP3 KO mice

As the number of animals per group (N of 2 to 3) is too low at the aging time points of 3, 6, 9 and 12 months one could only have a look at a trend. At a very early lifetime point of 3 months the LTP rate is nearly identically between male and female NLRP3 KO mice. Bar graph of the last five minutes of LTP shows no differences between female with 144.78±5.4% and males with 138.69±5.07% NLRP3 KO mice (Figure 19A). The quantification of the last five minutes of LTP between female littermate controls with 144.78±5.41% and male mice with 158.41±6.6% seems to display a higher LTP for male mice (Figure 19A'). Quantification of the last five minutes of LTP at 6 months old mice shows a trend of female NLRP3 KO mice to have a higher LTP with 171.43±8.53% compared to males with 145.01±4.92% (Figure 19B), but still no statistics possible due to low N. Bar graph of the last five minutes of LTP between female littermates with 166.02±6.58% and male littermate mice with 149.3±7.3% (Figure 19B') show a slight trend of decreased LTP in male mice. Bar graph of the last five minutes of LTP at the aging time point of 9 months shows a trend of male NLRP3 KO mice to have a higher LTP with 136.16± 5.57% compared to females with 127.83±2.02% (C). Bar graph of the last five minutes of LTP between female and male littermate and mice shows a very slight trend of female LM mice to have a

higher LTP 140.11±7.42% compared to male mice with 132.4±4.9% (Figure 19C`). Quantification of the last five minutes of LTP in 12 months old NLRP KO mice show a trend of female NLRP3 KO mice to have a trend towards a lower LTP with 135.79±3.93% compared to males with 160.28±9.24% but still no statistic possible due to low N (Figure 19D). Bar graph of the last five minutes of LTP between LM females with 147.30±7.37% and LM male with 143.1±6.9% show no differences (Figure 19D'). These findings indicate a fluctuation in LTP rate of NLRP3 KO mice as well as littermates when divided by sex.

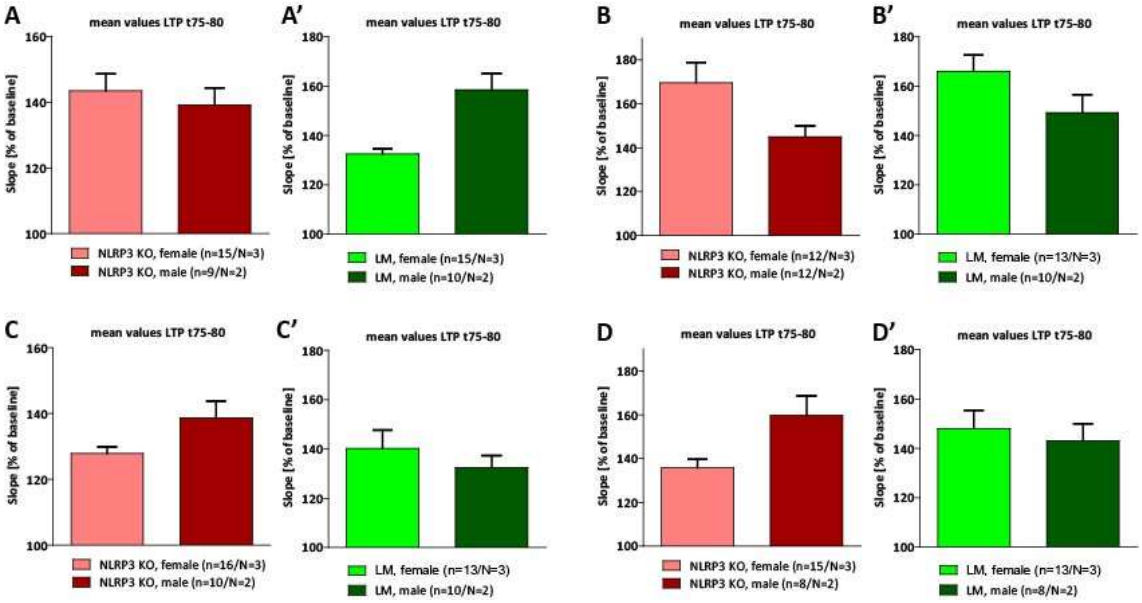

Figure 19 Bar graph quantification of the last five minutes of LTP of 3 to 12 months old NLRP3 KO mice. Activity-dependent synaptic plasticity was investigated on acute hippocampal slices of 3-12months old littermate control female (LM female, light green circles), NLRP3 KO female mice (light red circles) and NLRP3 KO male mice (dark red circles) and quantified via analysis of the last 10 minutes of LTP. Field excitatory postsynaptic potentials (fEPSPs) were recorded in CA1 region by stimulating Schaffer collateral axons of area CA3 at a frequency of 0.1 Hz. The LTP induction rate is shown as percentage % of mean baseline slope. Data points were averaged over 6 time points and error bars indicating SEM, n= number of recorded slices/N= number of animals. Data were analyzed by Student´s t-test. (A) Bar graph of the last five minutes of LTP show no differences between female with 144.78±5.4% and males with 138.69±5.07% NLRP3 KO mice (Figure 19A). The quantification of the last five minutes of LTP between female littermate controls with 144.78±5.41% and male mice with 158.41±6.6% seem to display a higher LTP for male mice (Figure 19A'). Quantification of the last five minutes of LTP at 6 months old mice show a trend of female NLRP3 KO mice to have a higher LTP with 171.43±8.53% compared to males with 145.01±4.92% (Figure 19B), but still no statistics possible due to low N. Bar graph of the last five minutes of LTP between female littermates with 166.02±6.58% and male littermate mice with 149.3±7.3% (Figure 19B') show a slight trend of decreased LTP in male mice. Bar graph of the last five minutes of LTP at the aging time point of 9 months show a trend of male NLRP3 KO mice to have a higher LTP with 136.16± 5.57% compared to females with 127.83±2.02% (Figure 19C). Bar graph of the last five minutes of LTP between female and male littermate and mice show a very slight trend of female LM mice to have a higher LTP 140.11±7.42% compared to male mice with 132.4±4.9% (Figure 19C`). Quantification of the last five minutes of LTP in 12 months old NLRP KO mice show a trend of female NLRP3 KO mice to have a trend towards a lower LTP with 135.79±3.93% compared to males with 160.28±9.24% but still no statistic possible due to low N (Figure 19D). Bar graph of the last five minutes of LTP between LM females with 147.30±7.37% and LM male with 143.1±6.9% show no differences (Figure 19D').

As spine loss and therefore microglia activation increases during age, I also analyzed very old mice with a higher animal number to quantify the results.

3.2.1.2 Morphological analysis of spine density in 3- 12 months old NLRP3 KO mice

Morphological analysis of spine density in apical CA1 region of the hippocampus was performed using the Golgi-Cox method. Spine density of 3 to 12 old months NLRP3 KO mice were analyzed and divided by sex. At the age of 3 months the bar graph of spine density displays no differences between male NLRP3 KO with 1.44±0.02 spines/µm and female NLRP3 KO with 1.42±0.02 spines/µm. Additionally, no sex dependent differences in the group of LM controls (female 1.45±0.02 spines/µm and male 1.49±0.02 spines/µm) were found. Quantification of the spine density in 6 months old mice displays no differences between littermate controls (female 1.55±0.03 spines/µm and male 1.54±0.04 spines/µm) and NLRP3 KO male with 1.47±0.04 spines/µm and female with 1.54±0.03 spines/µm as well. At the time point of 9 months LM female display a slightly higher spine density rate with 1.53±0.05 spines/µm compared to male with 1.42±0.02 spines/µm, but this is only a trend due to low N. NLRP3 KO male with 1.54±0.02 spines/µm and female mice with 1.57±0.03 spines/µm reveals no differences. At the age of 12 months the spine density of NLRP3 KO male mice with 1.72±0.04 spines/µm displays a slightly trend of been enhanced compared to female NLRP3 KO mice with 1.63±0.04 spines/µm. Quantification of spine density of littermate controls shows no differences with female 1.63±0.03 spines/µm and male with 1.60±0.03 spines/µm (Figure 20).

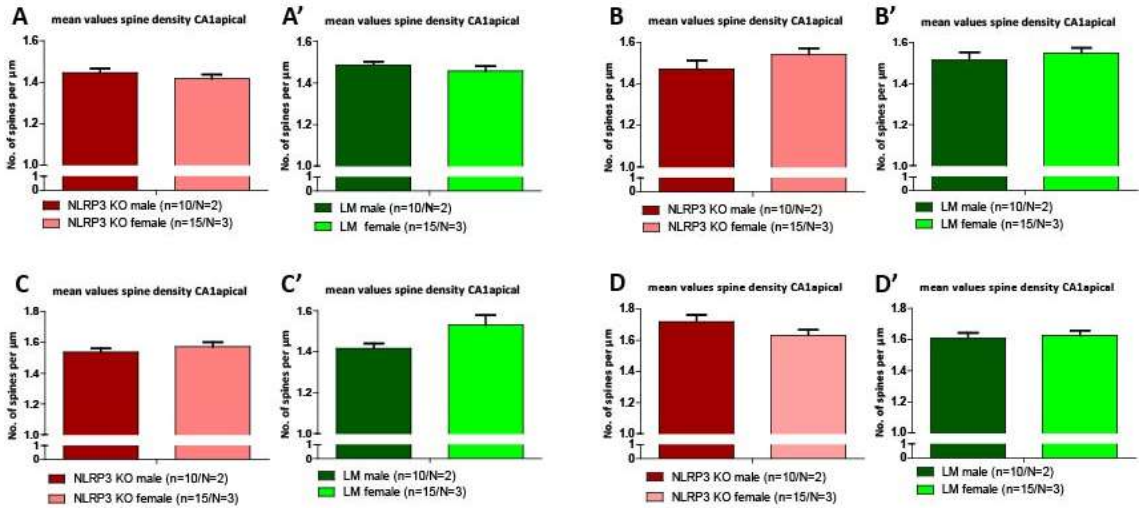

Figure 20 Morphological analysis of spine density in CA1apical hippocampal region of 3-12 months old NLRP3 KO mice. Morphology was investigated on apical dendrites of hippocampal CA1 neurons stained with the Golgi-cox method of 3 to 12 months old littermate control and NLRP3 KO mice. Investigations toward sex dependent differences was done. Number of animals is too low to do statistics. Spines at five apical CA1 dendrites at 2nd or 3rd dendritic branches with a length of 100µm were counted per animal. Spine density is shown as number of spines per µm dendrite. Error bars indicating SEM, n= number of dendrites/N= number of animals.(A) Bar graph of spine density displays no differences between male NLRP3 KO (1.44±0.02) and female NLRP3 KO (1.42±0.02) mice at the age of 3 months.(A') Additionally no sex dependent differences in the group of LM controls (female 1.45±0.02 and male 1.49±0.02) were found. (B' and B) Quantification of the spine density in 6 months old mice display no differences between littermate controls (female 1.55±0.03 and male 1.54±0.04) and NLRP3 KO male (1.47±0.04) and female (1.54±0.03). (C') At the time point of 9 months LM female display a lightly higher spine density rate (1.53±0.05) compared to male (1.42±0.02). This is only a trend due to low N. (C) NLRP3 KO male (1.54±0.02) and female mice

(1.57±0.03) reveals no differences. (D) At the age of 12 months the spine density of NLRP3 KO male mice (1.72±0.04) display a slightly trend of been enhanced compared to female NLRP3 KO mice (1.63±0.04). (D') Quantification of spine density of littermate controls show no differences (female 1.63±0.03 and male 1.60±0.03).

3.2.1.3 Electrophysiological measurements of 24 months old NLRP3 KO mice

At the time point of 24 months the number of animals is high enough to differentiate between sexes. Electrophysiological experiments as well as morphological analysis were performed to investigate whether the KO of the NALP3 inflammasome has a positive effect on spine density during physiological aging. Quantitative analysis of the last five minutes of LTP show a significantly higher LTP rate of female NLRP3 KO mice with 154.23±7.33% compared to males with 127.70±2.98% (p=0.002) (Figure 21A). No differences in the group of littermates were seen (Figure 21B). I wanted to know whether littermate female and NLRP3 KO female also differ in LTP. Bar graph of the last five minutes of LTP between female littermate and NLRP3 KO mice also displays a higher LTP of female NLRP3 KO mice with 154.23±7.33% when compared to LM females with 134.14±5.16% (p=0.035) (Figure 21C). No differences could be seen in the comparison of male mice of both genotypes (Figure 21D). These findings suggest a sex dependent difference with an advantage of knocking out the NALP3 inflammasome in female aged mice.

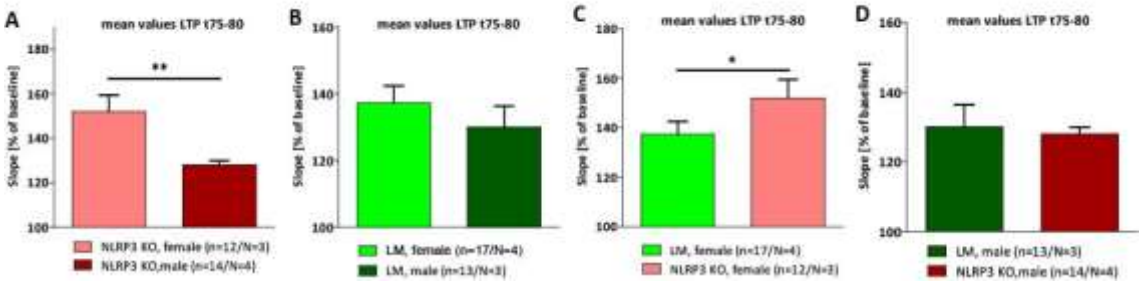

Figure 21 Quantitative analysis of last five minutes of LTP measurements on 24 months old NLRP3 KO mice. Activity-dependent synaptic plasticity was investigated on acute hippocampal slices of 24 months old littermate control female (LM female, light green circles), NLRP3 KO female mice (light red circles) and NLRP3 KO male mice (dark red circles) and quantified via analysis of the last 10 minutes of LTP. Field excitatory postsynaptic potentials (fEPSPs) were recorded in CA1 region by stimulating Schaffer collateral axons of area CA3 at a frequency of 0.1 Hz. The LTP induction rate is shown as percentage % of mean baseline slope. Data points were averaged over 6 time points and error bars indicating SEM, n= number of recorded slices/N= number of animals. Data were analyzed by Student´s t-test. (A) Bar graph of the last five minutes of LTP show a significantly higher LTP of female NLRP3 KO mice (154.23±7.33) compared to males (127.70±2.98) (p=0.002).(B) Bar graph of the LAt five minutes of LTP display no differences between LM male and female mice. (C) Bar graph of the last five minutes of LTP between female littermate and NLRP3 KO mice show a higher LTP of female NLRP3 KO mice (154.23±7.33) compared to LM females (134.14±5.16) (p=0.035). (D) Bar graph of the last five minutes of LTP display no differences between male LM and NLRP3 KO mice.

3.2.1.4 Morphological analysis of spine density in 24 months old NLRP3 KO mice

Morphology was investigated on apical dendrites of hippocampal CA1 neurons stained with the Golgi-cox method of 24 months old littermate control and NLRP3 KO mice. Investigations toward sex dependent differences were done. Bar graph of spine density displays no differences between male NLRP3 KO with 1.38±0.02 spines/µm and female NLRP3 KO mice with 1.34±0.06 spines/µm (Figure 23A). Quantification of spine density displays no sex dependent differences in the group of LM controls. Male have 1.33±0.02 spines/µm and female littermate controls have 1.41±0.02 spines/µm (Figure 23B).

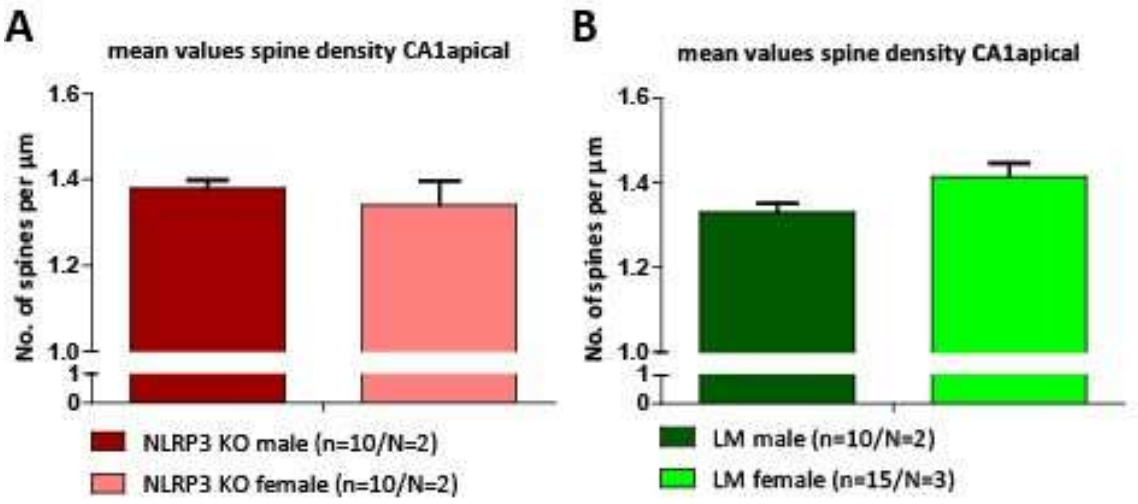

Figure 22 Morphological analysis of spine density in CA1apical hippocampal region of 24 months old NLRP3 KO mice. Morphology was investigated on apical dendrites of hippocampal CA1 neurons stained with the Golgi-cox method of 24 months old littermate control and NLRP3 KO mice. Investigations toward sex dependent differences were done. Spines at five apical CA1 dendrites at 2nd or 3rd dendritic branches with a length of 100 µm were counted per animal. Spine density is shown as number of spines per µm dendrite. Error bars indicating SEM, n= number of dendrites/N= number of animals. Bar graph of spine density displays no differences between male NLRP3 KO (1.38±0.02) and female NLRP3 KO mice (1.34±0.06). Bar graph of spine density displays no sex dependent differences in the group of LM controls (female 1.41±0.03 and male 1.33±0.02).

In summary, age- and sex-dependent analysis of the NLRP3 KO to LM revealed an increased LTP in aged NLRP3 KO female mice compared to age-matched male NLRP3 KO mice as well as littermate controls, leading to the speculation of a positive physiological effect of KO the NALP3 inflammasome within age in a sex dependent manner.

3.3 Inflammation caused by autoimmune antibodies

As Ohkawa et al., could show in 2013 that application of AAB from LGI1 AE patients on hippocampal slices interrupted the LGI1-ADAM22 interaction and lead to a decrease in AMPAR density and therefore to a decreased synaptic transmission level, I wanted to know, whether different AAB samples of patients suffering from AE lead to different electrophysiological and morphological outcomes. Therefore, I first checked whether the AAB samples penetrate deep enough into the hippocampal slice.

3.3.1 Binding of autoimmune antibodies

Acute hippocampal slices of Thy-1 GFP mice also used for electrophysiological experiments were fixed overnight and used for Immunohistochemistry. Neurons are represented via GFP fluorescent signal of the Thy-1 promotor. Blue DAPI signal represents cell bodies by intercalation with the DNA. Red signal represents bound IgG. Higher Cy3 fluorescent signal could be seen after 6 h of AAB incubation only by Patient1 AAB treated slices, therefore more IgG is bound to hippocampus, compared to control Patient AAB treatment and ACSF control (Figure 23).

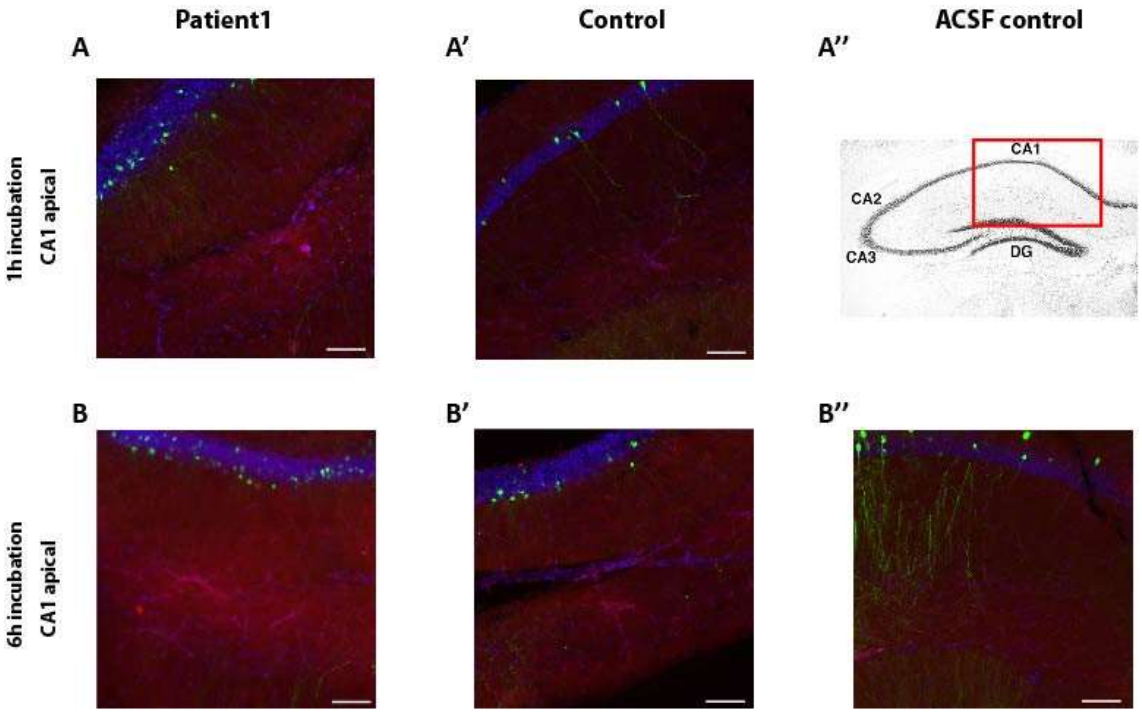

Figure 23 Immunohistochemistry of AAB samples on hippocampal slices. Acute hippocampal slices of Thy-1 GFP mice also used for electrophysiological experiments were fixed overnight in 4% PFA and stored into 30% sucrose for dehydration. 400 µm transversal hippocampal slices were cutted into 30 µm thick sections before Immunohistochemistry. Exposure times of 150 ms for GFP; 4s for human IgG; 3s for GFAP and 50 ms for DAPI. (A) CA1 hippocampal area of slice treated with AAB of Patient1 for 1 h. (B) CA1 area of slice treated for 6 h with Patient1 sample. (A') Serum of healthy control applied on hippocampal slice for 1 h. (B') 6 h treatment of hippocampal slice with serum of control Patient. (A'') schematic view of area imaged. (B'') ACSF control treated slice. Scale bar 200 µm.

3.3.2 LTP deficits are epitope specific

As I could be sure, that the AAB of the patients suffering from AE could penetrate into the hippocampal slice, I started with electrophysiological measurements. First, I wanted to know whether the application of AABs has an effect under basal conditions. Therefore, I started baseline recording and applied AAB 10 minutes afterwards and monitored fEPSP for another 30 minutes of recording. No effects could be seen for AABs from three patients compared to control AAB treated slices (Figure 24), described in more detail below.

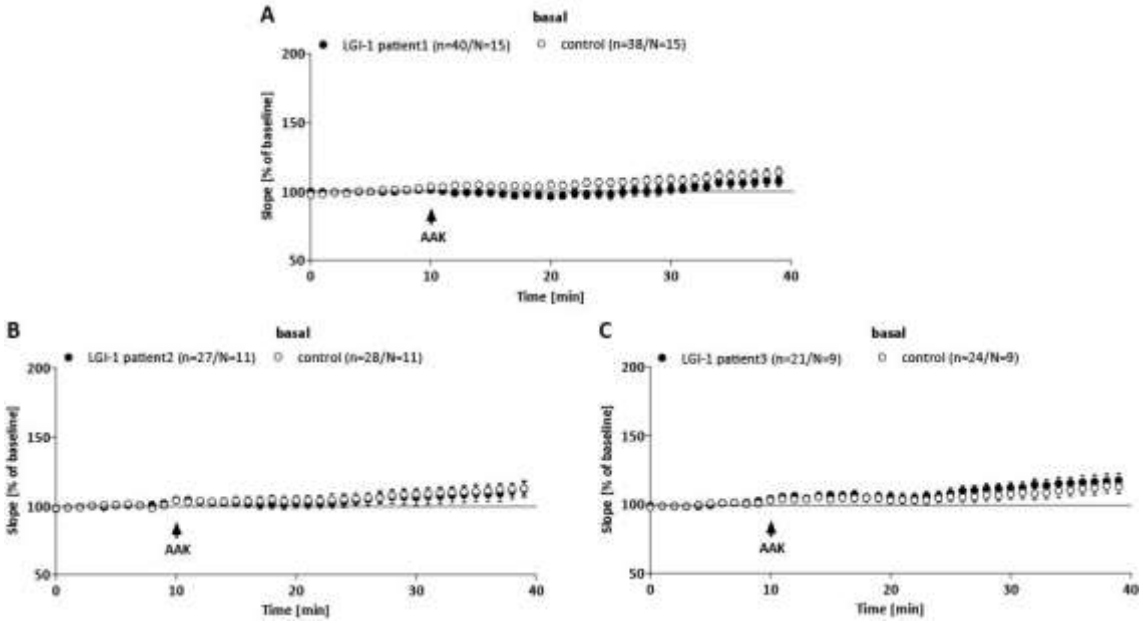

Figure 24 Basal synaptic recording with AAB application. Field excitatory postsynaptic potentials (fEPSPs) of acute hippocampal slices of C57Bl/6-GFP mice treated with control (open circles) or with a-Lgi1-AAB (black circles) of Patient1 (upper middle), Patient2 (lower left) or Patient3 (lower right) were recorded in CA1 region by stimulating Schaffer collateral axons of area CA3 at a frequency of 0.1 Hz. Baseline recording took place for 10 minutes before AAB application and another 30 minutes recording.

Then I started measurements with 1 h incubation time to figure out if differences in synaptic transmission are already visible at that very early time point. Furthermore, I also analyzed long-term application (6 h) as AAB where higher amounts of patient AABs were found compared to control treated slices. At first, I analyzed the LTP and basal synaptic transmission parameters of hippocampal slices treated with AAB of Patient1 suffering of LE.

Field excitatory postsynaptic potentials (fEPSPs) of acute hippocampal slices of C57Bl/6-GFP mice treated with control (open circles) or with a-Lgi1-AAB of Patient1 (black circles) were recorded in CA1 region by stimulating Schaffer collateral axons of area CA3. LTP measurements of acute application of AAB of Patient1 reveal no differences in potentiation levels. Quantification of the last five minutes of LTP supports the findings. The bar graph displays potentiation levels for Patient1 with 134.26±3.92% and for control with 128.06±3.31%. LTP of slices continuously perfused for 6 h with AAB of Patient1 show deficits in LTP with 111.67±4.07%

compared to slices treated with control serum with 126.29±3.94. Quantification of the last ten minutes of long-term application LTP confirms the results (p=0.015) (Figure 25).

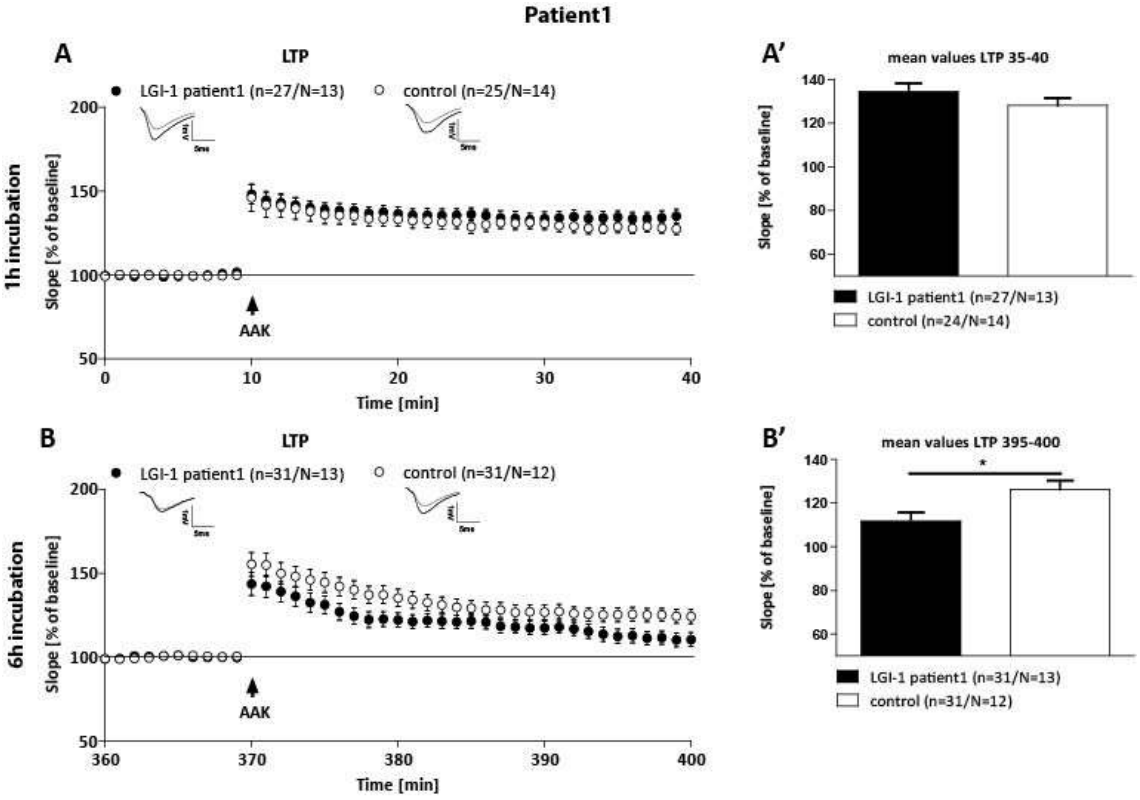

Figure 25 LTP measurements on acute hippocampal slices treated with AAB of Patient1. Field excitatory postsynaptic potentials (fEPSPs) of acute hippocampal slices of C57Bl/6-GFP mice treated with control (open circles) or with a-Lgi1-AAB of Patient1 (black circles) were recorded in CA1 region by stimulating Schaffer collateral axons of area CA3 at a frequency of 0.1 Hz. LTP was induced by application of TBS after 10 min baseline stimulation (arrowhead) in slices treated for 1 hour (A) with control or a-Lgi1-AAB of Patient1 or for 6 hours (B). The LTP induction rate is shown as percentage % of mean baseline slope. (A) During LTP measurement slices were continuously perfused with either control or a-Lgi1-AAB of Patient1 but did not show any differences in potentiation levels for acute measurements. (A') Bar graph of the last five minutes of LTP support the findings (Patient1: 134.32±3.92; Control: 128.06±3.31). (B) LTP of slices continuously perfused for 6 h with AAB show deficits in LTP. (B') Bar graph of the last ten minutes of long-term application LTP confirm the results (Patient1: 111,67±4.07; Control: 126.29±3.94) (p=0.015).

Input/ Output experiments were performed to check if basal synaptic transmission is intact after treatment with AAB of Patient1 for short- and long-term application. Postsynaptic neuronal excitability was comparable at all measured stimulus intensities (25-250 µA). Additionally, PPF paradigm analysis was performed to check for intact presynaptic function. Short-term synaptic plasticity was intact at all ISI (160 -10 ms). Taken together the results indicate intact pre- and postsynaptic function after application of AAB of Patient1 for acute and long-term application of AAB (Figure 26).

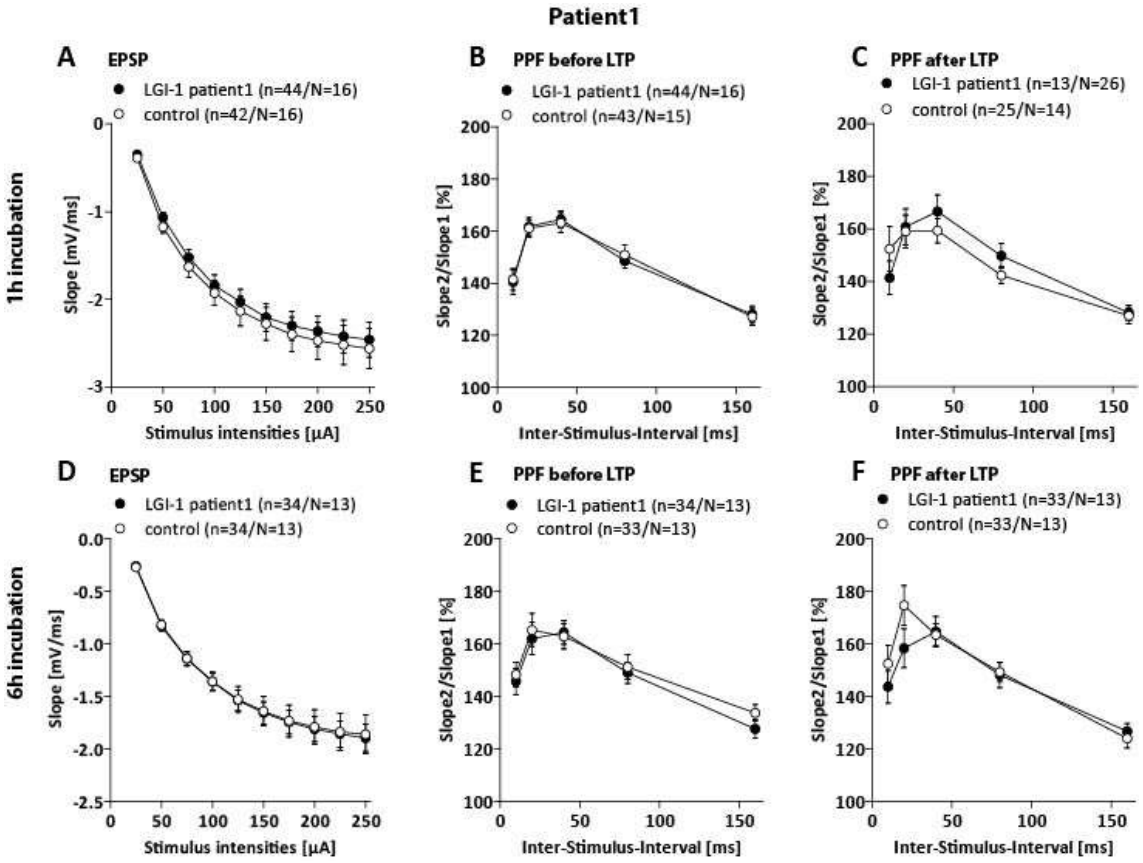

Figure 26 Basal synaptic transmission of Patient1. Field excitatory postsynaptic potentials (fEPSPs) of acute hippocampal slices of C57Bl/6-GFP mice treated either with control (open circles) or with a-Lgi1-AAB of Patient1 (black circles) were recorded in CA1 region by stimulating Schaffer collateral axons of area CA3 at a frequency of 0.1 Hz. Input/ Output curves revealed no differences in postsynaptic function after 1 h (A) or after 6 hours (D) treatment of acute slices with a-Lgi1-AAB of Patient1. PPF paradigm before (B) first LTP recording revealed no differences in presynaptic function after 1 h treatment of acute slices with either control or a-Lgi1-AAB of Patient1. (E) PPF paradigm before second LTP recording after 6 h of AAB treatment revealed also no differences. PPF paradigm after (C) first LTP recording revealed no differences in presynaptic function after 1 h treatment of acute slices with either control or a-Lgi1-AAB of Patient1. PPF paradigm after 6 hours of incubation with Patient1 sample after second LTP (F) revealed no differences at all.

As application of samples of Patient1 on acute hippocampal slices lead to normal pre- and postsynaptic function but alterations in LTP after long application, I also wanted to know whether this is true for samples of other Patients. Therefore, I did the same analysis as before with samples of another Patient. Patient1 is suffering from LE, Patient2 in turn is suffering from FBDS.

LTP measurements with sample of Patient2 did not show any differences in potentiation levels for acute measurements. Bar graph of the last five minutes of LTP supports the findings. Patient2 displays a potentiation level of 118.88±3.35% and control slices show 120.81±3.63%. LTP of slices continuously perfused for 6 h with AAB show also no deficits in LTP. As depicted in the bar graph of the last five minutes with 118.30±3.92% potentiation for Patient2 and 115.34±2.75% for control slices (Figure 27).

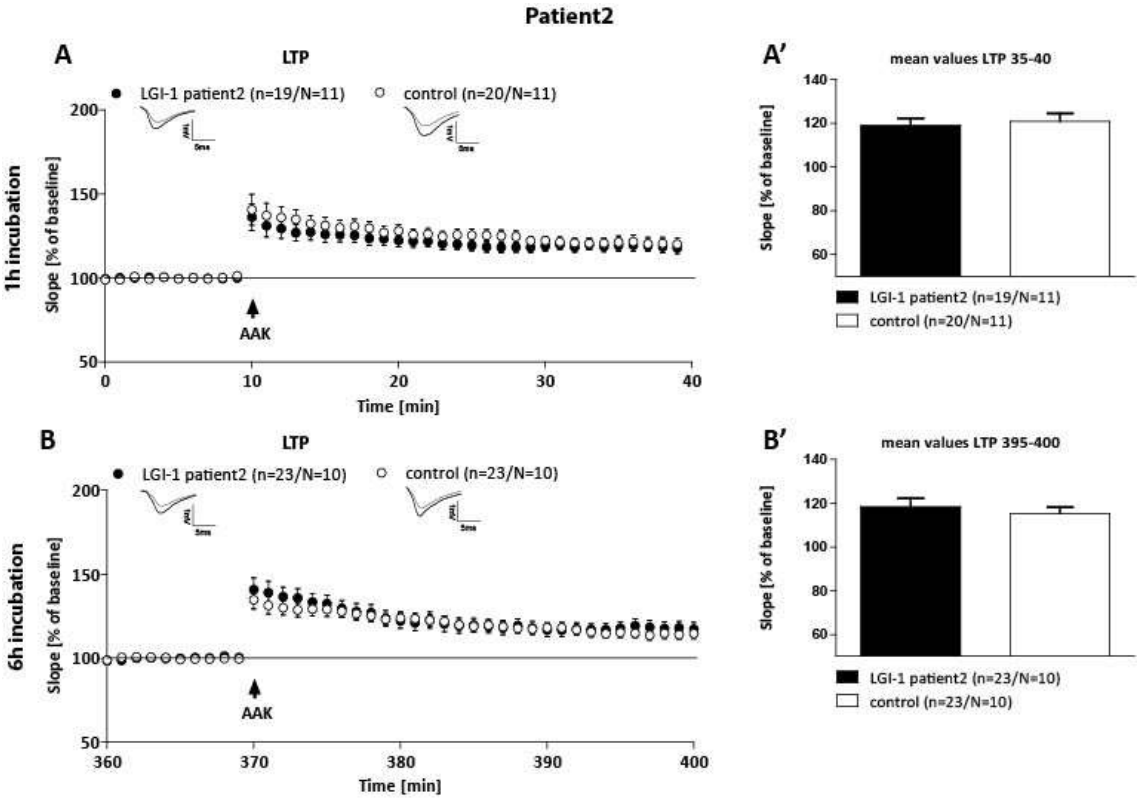

Figure 27 LTP measurements on acute hippocampal slices treated with AAB of Patient2. Field excitatory postsynaptic potentials (fEPSPs) of acute hippocampal slices of C57Bl/6-GFP mice treated with control (open circles) or with a-Lgi1-AAB of Patient2 (black circles) were recorded in CA1 region by stimulating Schaffer collateral axons of area CA3 at a frequency of 0.1 Hz. LTP was induced by application of TBS after 10 min baseline stimulation (arrowhead) in slices treated for 1 hour (A) with control or a-Lgi1-AAB of Patient1 or for 6 hours (B). The LTP induction rate is shown as percentage % of mean baseline slope. (A) During LTP measurement slices were continuously perfused with either control or a-Lgi1-AAB of Patient2 but did not show any differences in potentiation levels for acute measurements. (A') Bar graph of the last five minutes of LTP support the findings (Patient2: 118.88±3.35; Control: 120.81±3.63). (B) LTP of slices continuously perfused for 6 h with AAB show also no deficits in LTP. (B') Bar graph of the last ten minutes of long-term application LTP confirm the results (Patient2: 118.30±3.92; Control: 115.34±2.75).

Additionally, I wanted to check also here for pre- and postsynaptic function. No differences in Input/ Output measurements could be seen for acute as well as long-term application of AAB of Patient2. I analyzed the PPF paradigm for each condition before and after LTP measurements, but I did not record any differences (Figure 28).

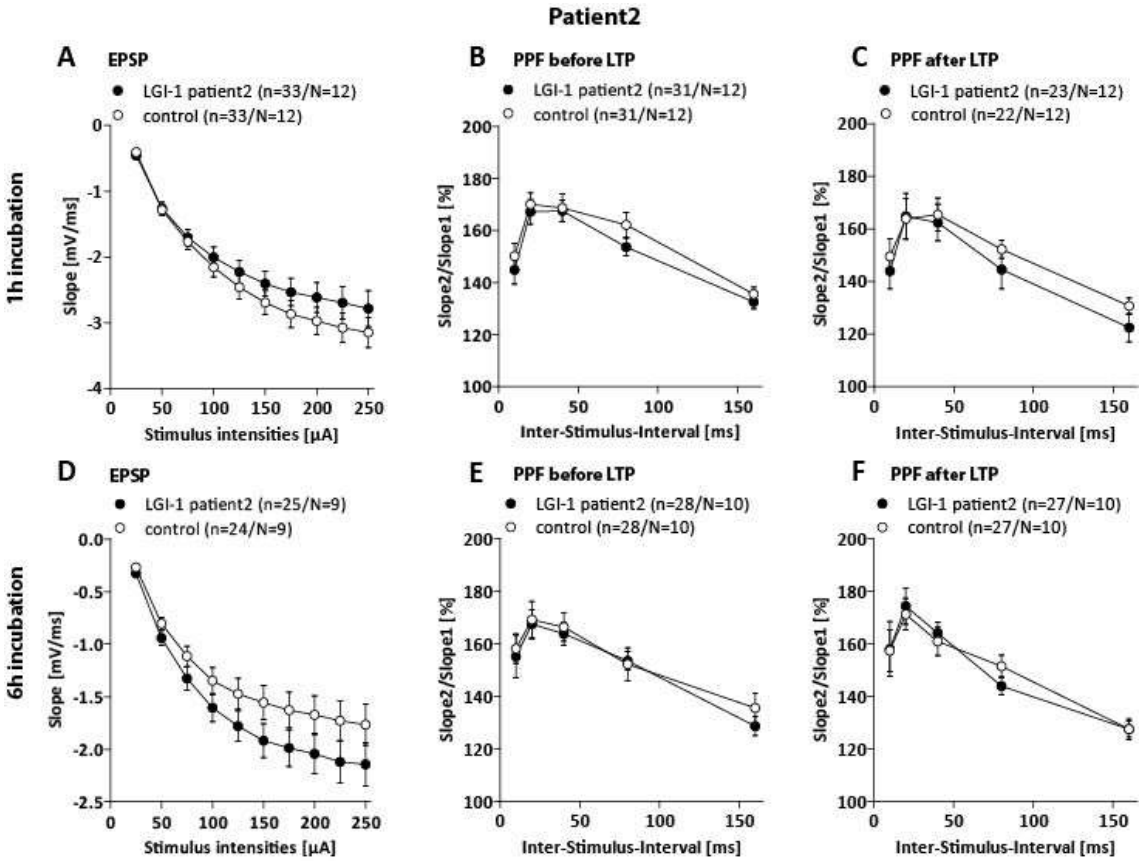

Figure 28 Basal synaptic transmission of Patient2. Field excitatory postsynaptic potentials (fEPSPs) of acute hippocampal slices of C57Bl/6-GFP mice treated either with control (open circles) or with a-Lgi1-AAB of Patient2 (black circles) were recorded in CA1 region by stimulating Schaffer collateral axons of area CA3 at a frequency of 0.1 Hz. Input/ Output curves revealed no differences in postsynaptic function after 1 h (A) or after 6 h (D) treatment of acute slices with a-Lgi1-AAB of Patient2. PPF paradigm before (B) first LTP recording revealed no differences in presynaptic function after 1 h treatment of acute slices with a-Lgi1-AAB of Patient2. (E) PPF paradigm before second LTP recording after 6 h of AAB treatment revealed also no difference at all ISI. PPF paradigm after (C) first LTP recording revealed no differences in presynaptic function after 1 h treatment of acute slices with either control or a-Lgi1-AAB of Patient2. PPF paradigm after 6 h of incubation with Patient2 sample after second LTP (F) revealed no differences at all.

To corroborate the results another Patient was analyzed in terms of LTP and basal synaptic transmission. Patient3 is suffering from FBDS like Patient2. LTP measurements of acute application of Patient3 sample reveal no differences in potential levels compared to control treated slices. Quantification of the last five minutes via bar graph supports the findings (Patient3: 123.36±3.37%; Control: 124.80±4.80%). LTP of slices continuously perfused for 6 h with AAB show also no deficits in LTP. Bar graph of the last five minutes of long-term application LTP confirms the results (Patient3: 115.38±2.33%; Control: 115.48±2.45%) (Figure 29). The results are comparable with the results of Patient2, but not Patient1 suffering from LE instead of FBDS.

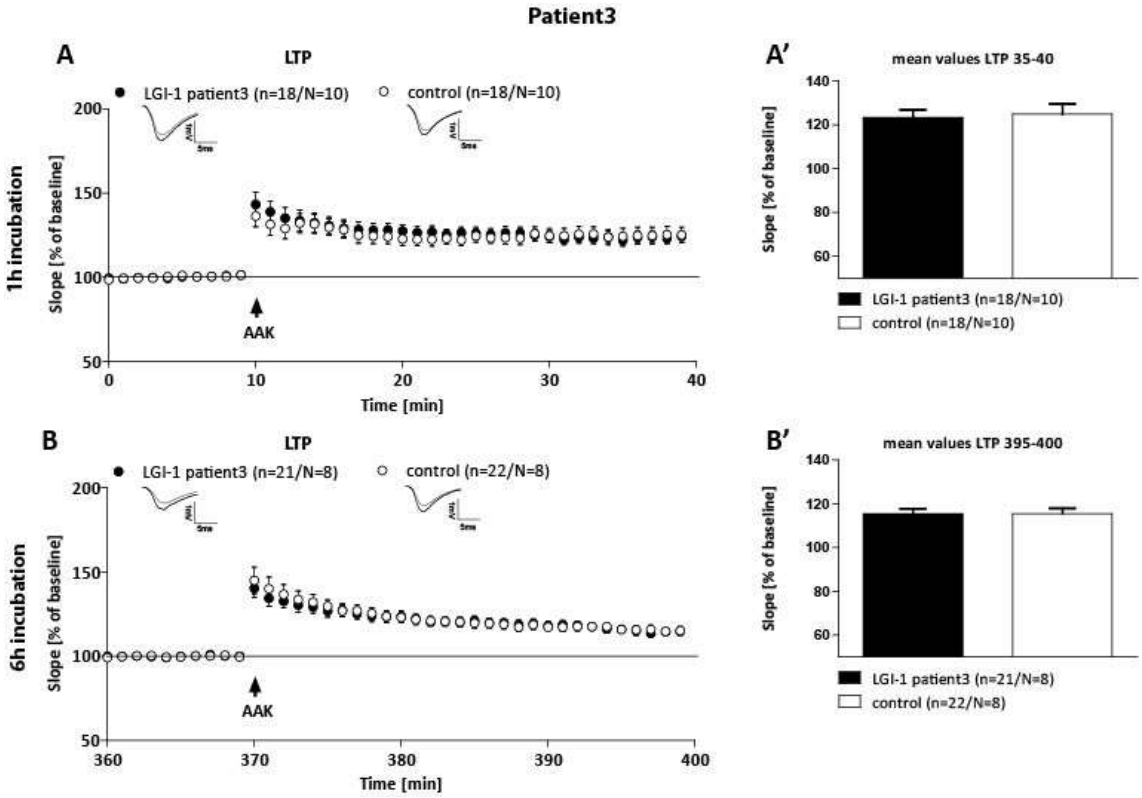

Figure 29 LTP measurements on acute hippocampal slices treated with AAB of Patient3. Field excitatory postsynaptic potentials (fEPSPs) of acute hippocampal slices of C57Bl/6-GFP mice treated with control (open circles) or with a-Lgi1-AAB of Patient3 (black circles) were recorded in CA1 region by stimulating Schaffer collateral axons of area CA3 at a frequency of 0.1 Hz. LTP was induced by application of TBS after 10 min baseline stimulation (arrowhead) in slices treated for 1 h (A) with control or a-Lgi1-AAB of Patient3 or for 6 h (B). The LTP induction rate is shown as percentage % of mean baseline slope. (A) During LTP measurement slices were continuously perfused with either control or a-Lgi1-AAB of Patient3 but did not show any differences in potentiation levels for acute measurements. (A') Bar graph of the last five minutes of LTP support the findings (Patient3: 123.36±3.37; Control: 124.80±4.80). (B) LTP of slices continuously perfused for 6 h with AAB show also no deficits in LTP. (B') Bar graph of the last ten minutes of long-term application LTP confirm the results (Patient3: 115.38±2.33; Control: 115.48±2.45).

Also, in this stack of experiments, I wanted to check for pre- and postsynaptic function. Postsynaptic Input/ Output measurements display no differences for acute as well as long-term application of AAB of Patient3. PPF before first LTP recording revealed no differences in presynaptic function after 1 h treatment of acute slices with either control or a-Lgi1-AAB of Patient3. PPF paradigm before second LTP recording after 6 h of AAB treatment instead reveals differences at an ISI of 10 ms. Slices treated with control AABs reveals a higher ratio of slope1 to slope2 which could be due to a higher vesicle recycling in the presynapse. As control AABs of other patients do not show this shape of curve it maybe an artifact. PPF paradigm after first LTP recording revealed no differences in presynaptic function after 1 h treatment of acute slices with either control or a-Lgi1-AAB of Patient3. PPF paradigm after 6 h of Patient3 sample incubation after second LTP revealed also no differences (Figure 30).

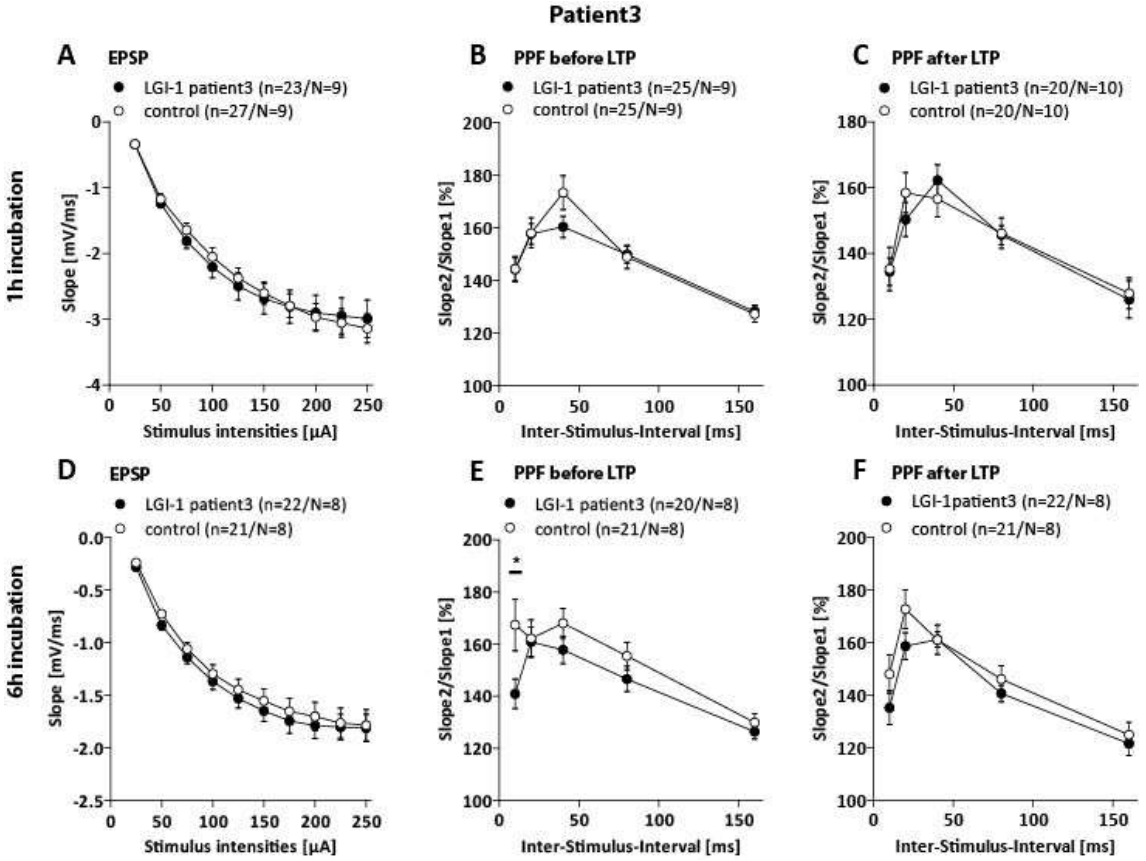

Figure 30 Basal synaptic transmission of Patient3 Field excitatory postsynaptic potentials (fEPSPs) of acute hippocampal slices of C57Bl/6-GFP mice treated either with control (open circles) or with a-Lgi1-AAB of Patient3 (black circles) were recorded in CA1 region by stimulating Schaffer collateral axons of area CA3 at a frequency of 0.1 Hz. Input/ Output curves revealed no differences in postsynaptic function after 1 h (A) or after 6 h (D) treatment of acute slices with a-Lgi1-AAB of Patient3. PPF paradigm before (B) first LTP recording revealed no differences in presynaptic function after 1 h treatment of acute slices with either control or a-Lgi1-AAB of Patient3. (E) PPF paradigm before second LTP recording after 6 h of AAB treatment reveals differences at ISI 10 ms. Slices treated with control reveals a higher ratio of slope1 to slope 2 which could maybe due to a higher vesicle recycling in the presynapse. PPF paradigm after (C) first LTP recording revealed no differences in presynaptic function after 1 h treatment of acute slices with either control or a-Lgi1-AAB of Patient3. PPF paradigm after 6 h of Patient3 sample incubation after second LTP (F) revealed also no differences.

3.3.3 Morphological changes in spine density after AAB application

As electrophysiological recordings reveal changes in LTP after long-term application of AAB of Patient1 but not Patient2 or 3, I wanted to check whether these findings could be substantiated with morphological alterations. Therefore, I analyzed the spine density in pyramidal cells of CA1 apical region as well as dentate gyrus granule cells.

Spine density of apical CA1 pyramidal cell dendrites after acute application of Patient1 on BL6 acute hippocampal slices reveals no differences with 1.91±0.05 spines/µm compared to slices treated with control serum with 1.95±0.05 spines/µm (Figure 31A). Similar results were obtained after long application of AAB of Patient1 with 1.84±0.04 spines/µm compared to control serum treated slices with 1.78±0.04 spines/µm (Figure 31B). Spine density of DG granule cell dendrites after long application of Patient1 on BL6 acute hippocampal slices in turn is decreased with 1.73±0.05 spines/µm compared to slices treated with control serum with 1.89± 0.03 spines/µm (p=0.014) (Figure 31C).

With regard to Patient2, spine density of apical CA1 displays no differences with 2.04±0.06 spines/µm compared to control 1.96±0.06 spines/µm (Figure 31A'). CA1 apical spine density after 6 h application of AAB of Patient2 reveals also no differences with 2.00±0.03 spines/µm compared to slices treated with control serum with 1.96±0.04 spines/µm (Figure 31B'). Dentate gyrus spines density after long application of Patient2 also reveals no differences with 2.23±0.07 spines/µm compared to control slices with 2.19±0.07 spines/µm (Figure 31C').

After acute application of Patient3 AABs on BL6 acute hippocampal slices, spine density of apical CA1 pyramidal cell dendrites reveals no differences with 1.86±0.04 spines/µm compared to slices treated with control serum with 1.87±0.03 spines/µm (Figure 31A''). Same is true for spine density of apical CA1 dendrites after long application of AAB of Patient3 on BL6 acute hippocampal slices with 1.80±0.04 spines/µm compared to control serum treated slices with 1.87±0.03 spines/µm (Figure 31B''). Spine density of DG granule cell dendrites after long application of Patient3 also reveals no differences with 2.00±0.05 spines/µm compared to control with 1.96±0.06 spines/µm (Figure 31C'').

Together these data reflect the electrophysiological measurements, where only long-term application of AAB of Patient1 was leading to alterations in LTP curve.

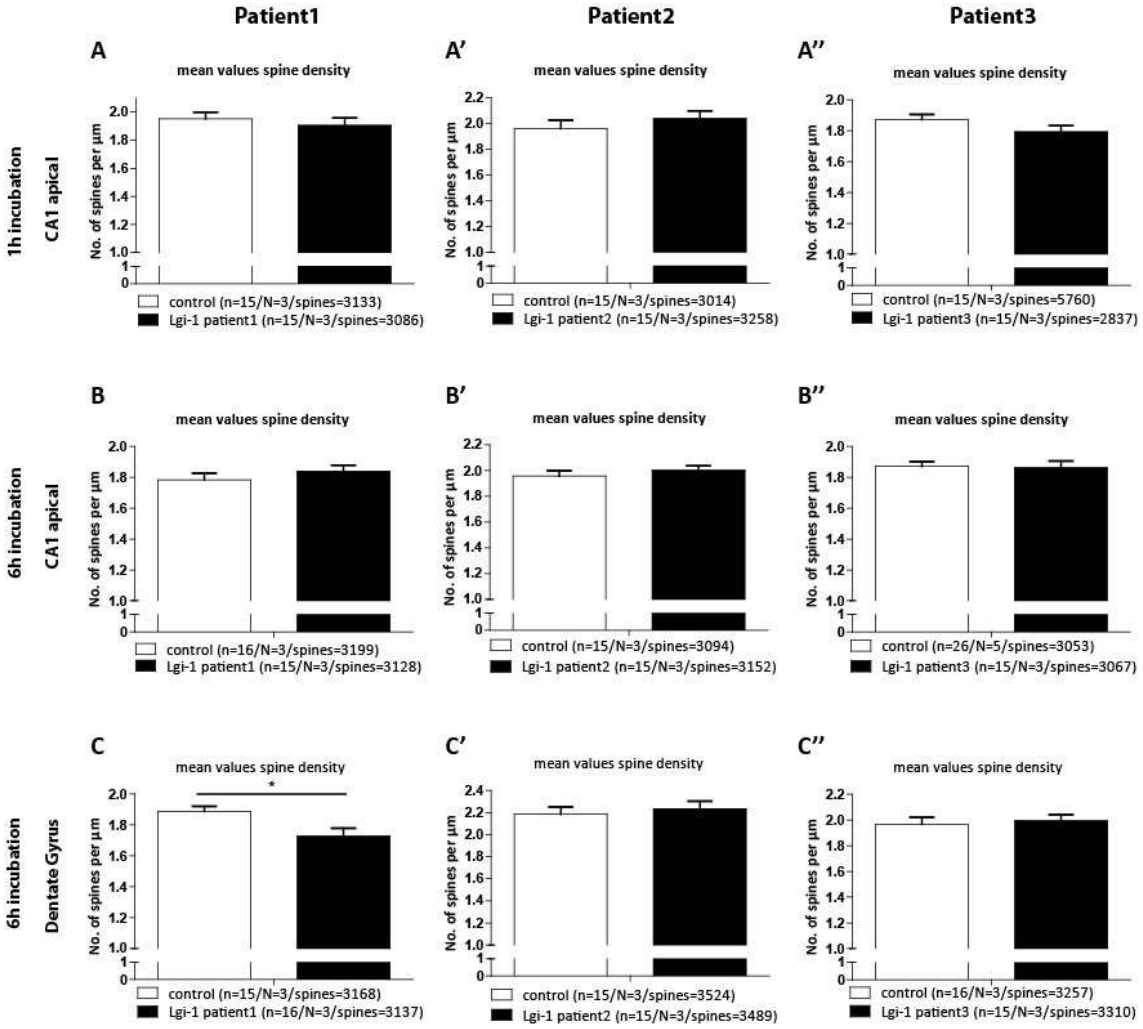

Figure 31 Analysis of spine density in CA1 apical and DG hippocampal region of all 3 Patients after 1 h and 6 h application of AAB. (A) Spine density of apical CA1 pyramidal cell dendrites after acute application of Patient1 on BL6 acute hippocampal slices reveals no differences (1.91±0.05) compared to slices treated with control serum (1.95±0.05). (B) Spine density of apical CA1 dendrites after along application of AAB of Patient1 on BL6 acute hippocampal slices (1.84±0.04) reveals also no differences compared to slices treated with control serum (1.78±0.04). (C) Spine density of DG granule cell dendrites after long application of Patient1 on BL6 acute hippocampal slices (1.73±0.05) is decreased compared to slices treated with control serum (1.89± 0.03) (p=0.014). (A') Spine density of apical CA1 pyramidal cell dendrites after acute application of Patient2 on BL6 acute hippocampal slices (2.04±0.06) reveals no differences compared to slices treated with control serum (1.96±0.06). (B') Spine density of apical CA1 dendrites after along application of AAB of Patient2 on BL6 acute hippocampal slices (2.00±0.03) reveals also no differences compared to slices treated with control serum (1.96±0.04). (C') Spine density of DG granule cell dendrites after long application of Patient2 on BL6 acute hippocampal slices (2.23±0.07) reveals no differences compared to slices treated with control serum (2.19±0.07). (A'') Spine density of apical CA1 pyramidal cell dendrites after acute application of Patient3 on BL6 acute hippocampal slices (1.86±0.04) reveals no differences compared to slices treated with control serum (1.87±0.03). (B'') Spine density of apical CA1 dendrites after along application of AAB of Patient3 on BL6 acute hippocampal slices (1.80±0.04) reveals also no differences compared to slices treated with control serum (1.87±0.03). (C'') Spine density of DG granule cell dendrites after long application of patien3 on BL6 acute hippocampal slices (2.00±0.05) reveals no differences compared to slices treated with control serum (1.96±0.06). Data presented as mean ± SEM, n = number of dendrites, N= number of animals, spines=number of total spines. Scale bar of confocal images 5 µm.

4. Discussion

Synaptic plasticity is one of the most important mechanisms of the brain to build memories. Thereby, strengthening and weakening of a synapse occur upon activity for example in case of LTP or LTD. In many diseases these mechanisms are disrupted but can be rescued via the application of molecules acting positively in physiological situations or via the knockout of special genes. This study can be divided into three parts where I analyzed synaptic plasticity at hippocampal CA1-CA3 synaptic pathway in order to investigate: 1. Alzheimer's disease, normally occurring later in lifespan; 2. Physiological aging with respect to inflammation and 3. An autoimmune disease that is more likely to occur early in life. I also looked for potential rescue molecules or mechanisms in the respective disease. One potential rescue molecule could be APPsα, as previous studies could show a positive effect on synapses (Hick et al., 2015; Ishida et al., 1997; Tyan et al., 2012, Fol et al., 2016). And indeed, I also could find out that recAPPsα is able to stabilize LTP in NexCre cDKO mice and additionally I could show that recAPPsα is acting via the α7-nAChR, which was unclear until then (3.1.1 Inhibition of α7-nAChR by BTX blocks positive effects of recAPPsα on LTP). Furthermore, I determined that recAPPsα is able to stabilize LTP in aged hatu.P301S mice that display a tau-tangle phenotype like in Alzheimer's disease (3.1.2.1 Increased LTP of aged htau mice rescued via application of recAPPsα). But I did not only look for APPsα, a cleavage product of the non-amyloidogenic pathway but also for Aηα, a small peptide from the η-secretase pathway and recorded contrary results compared to APPsα (3.1.3 Injection of Aηα show no effect on hippocampal synaptic plasticity). Another potential rescue mechanism I investigated during my thesis is the KO of the NALP3 inflammasome. The study of Heneka et al. (2013) could show a positive effect of knocking out the NALP3 inflammasome in APP KO mice. Therefore, I wanted to know whether this result is also true for physiological aging. Indeed, I could see positive effects that are additionally sex dependent (3.2.1 Sex dependent differences occur during aging). The last part of my thesis deals with human autoimmune antibodies and its functions on activity dependent synaptic plasticity in the murine hippocampus. In my thesis, I was able to show that long-term application of AAB of different patients leads to epitope dependent changes in LTP and spine density in acute hippocampal slices (3.3 Inflammation caused by autoimmune antibodies).

4.1 APPsα and Aηα as potential rescue molecules in Alzheimer's disease

In the first part of my thesis, I looked for different cleavage products of the APP family to have positive functions on synaptic plasticity. Therefore, I analyzed the effect of APPsα, a cleavage product of the non-amyloidogenic pathway, on the LTP of NexCre cDKO mice ($NexCre^{+/T}APP^{flox/flox}APLP2^{flox/flox}APLP1^{-/-}$). Additionally, I looked for BTX in these experiments acting via the alpha7 nicotinic acetylcholine receptor (α7-nAChR). Furthermore, I checked for APPsα as a potential rescue molecule for altered plasticity in htau.P301S mice, representing tau tangles in the brain like in Alzheimer's disease. Furthermore, I looked for the function with respect to synaptic plasticity of another cleavage product of APP in the η-secretase pathway: Aηα. The main finding regarding the cleavage products of APP showed that there are differences in the effect of APPsα and Aηα on acute hippocampal slices with respect to electrophysiological measurements, described in more detail below.

4.1.1 APPsα in NexCre cDKO mice

As a recent study (Hick et al.,2015) could show a rescued LTP curve in NexCre cDKO mice after the application of recAPPsα, I intend to get information about the referring receptor. Under the control of the NEX promotor the ablation of APP is triggered at embryonic day 11.5 in mice with an APLP2 deficient background. Hick et al., could also show that APPsα is able to rescue LTP deficits in NexCre cDKO by acute application of APPsα on hippocampal slices. Another study of Taylor et al. (2008) pointed out that infusion of recAPPsα into the dentate gyrus (DG) of rats enhances DG-PP LTP *in vivo*. These results were matching to the study of Moreno et al., (2015) reporting that recAPPsα is able to rescue LTP deficits in an age-dependent manner *in vitro*. Regarding the results, I assume that APPsα acts positively on LTP deficits in hippocampal region, but the receptor is still unknown. A previous study could show, that alpha7 nicotinic acetylcholine receptor (α7-nAChR) seems to be a target to rescue deficits in hippocampal LTP in Aβ infused rats (Chen et al., 2006). The α7-nAChR seems to play a big role in AD. As it is mainly located in neurons of the basal forebrain which projects to the hippocampus and cortex, the brain areas exhibiting severe plaque pathology in AD (Wang et al., 2000). In this regard the α7-nAChR might be not only a target for APPsβ but also for APPsα. Acute slices of NexCre cDKO mice treated with 10 nM recAPPsα or 10 nM recAPPsα with wash in of 10 nM BTX, a ligand of the respective receptor, 10 minutes before starting baseline recording display an indistinguishable LTP curve in induction and maintenance whereas the application of BTX together with APPsα on the other hand lead to a reduction of LTP induction and maintenance (3.1.1 Inhibition of α7-nAChR by BTX blocks positive effects of recAPPsα on LTP). This result leads

to the suggestion that on the one hand APPsα is acting via the α7-nAChR because in its presence and the absence of BTX, LTP was enhanced. On the other hand, BTX only binds to the α7-nACh receptor in the absence of APPsα and therefore seems to be its antagonist.

4.1.2 APPsα in htau.P301S mice

APPsα is known to have various positive effects on synaptic plasticity (Corrigan et al., 2012; Ring et al., 2007, Weyer et al., 2011), therefore it was used in this part of my study to rescue the imbalance in LTP in aged hTau.P301S mice. This transgenic mouse model expresses MAPT with a P301S mutation. This tauopathy model is associated with autosomal-dominant disease in humans and shows several molecular, cellular, and behavioral features of human tauopathy, including tau hyperphosphorylation, tau filament formation, neurodegeneration, and motor impairment. The mice exhibit widespread tau pathology, affecting the cerebral cortex, hippocampus, brain stem, and spinal cord. In the spinal cord, tau pathology leads to a progressive loss of motor neurons up to approximately 50 %, and severe motor impairment (Allen et al., 2002). At the age of 10-13 weeks there is an initial phenotype of htau.P301S. A reduced spine density and first effects of cognitive decline are specific markers at this time point. The results of electrophysiological measurements show a significantly lower LTP in induction phase, which is not stable until the maintenance phase of LTP measurements. Also, Boeckhoorn and colleagues could show in 2006 a trend of decreased LTP in CA1 hippocampal region in young transgenic tau P301S mice compared to wildtype mice. Maybe the initial spine loss seen in literature is leading to a decreased induction phase of LTP that can be compensated through existing physiological spines leading to a stable LTP in maintenance. As there was significantly decreased induction phase of LTP in young htau.P301S mice, measurements with older htau.P301S mice were performed to analyze the advanced phenotype.

At the time point of 16-18 weeks, the phenotype of htau.P301S mice is characterized by tangles in the cortex and hippocampus and a progressive spine loss. In the hippocampus, a decrease in spine density and spine length has been observed starting at 2.5 months of age (Xu et al., 2014). At the age of 20 weeks, weight loss and severe motor deficits upon progressive loss of motor neurons up to 50 %, displayed by paralysis of hind feet, are observed. Astro- and microgliosis are one of the main inflammatory processes observed at this stage. The results of LTP measurements in acute hippocampal slices display a significant higher LTP curve in htau.P301S mice. The results of Boeckhoorn and colleagues 2006 also proves an increase of LTP even before onset of hyperphosphorylation and tauopathy in DG granule cells of 8-10 weeks old transgenic tau P301S mice compared to wildtype. This result maybe a hint towards altered LTP also in other

regions in a progressed aging time point due to progressive spine loss from DG towards CA3 and CA3 hippocampal region. Not only a decrease in LTP could be a result of spine loss but also hyperexcitation could be a sign of altered synaptic plasticity. Oligomeric protein assemblies have been shown to bind and activate a variety of pattern recognition receptors (PRRs) (Komic et al., 2018), thus activating microglia cells as well as astrocytes. As brain homeostasis is altered in htau.P301S mice models upon microgliosis and astrogliosis (Allen et al., 2002), remaining spines could be hyperactivated during LTP, resulting in increased vesicle release or increased receptor incorporation into the membrane to compensate progressive spine loss. This hypothesis is in line with the PPF data, representing a higher PPF in htau.P301S mice and an even higher LTP in APPsα treated transgenic mice. The theory of altered presynaptic vesicle release rescued via APPsα application can be based on studies showing that APP is localized at the presynaptic active zone (Lassek et al., 2013, Wilhelm et al., 2014). Also the EPSP data, representing the postsynaptic part, could reflect the assumption of a spine loss in htau.P301S mice. EPSP curve of transgenic mice is significantly decreased reflecting a decreased number or a reduced function of spines. With the application of 10 nM recAPPsα the imbalance in homeostasis is rescued.

4.1.3 Function of Aηα

In my electrophysiological experiments the hypothesis of Willem et al. could not be confirmed. In the study of Willem et al. (2015) they could show, that pharmacological BACE1 inhibition with oral dose of 100 mg/kg SCH1682496 lowers hippocampal LTP. Additionally, Aηα but not Aηβ conditioned media from untransfected cells or artificial cerebrospinal fluid significantly inhibited LTP. In my study a vector was chosen for injection of Aηα into hippocampal region. Therefore, differences in the outcome of my study and the study of Willem et al. could be due to other components of the media, missing in my experiments. Furthermore, the stimulating protocol was different. Willem and colleagues used a high-frequency stimulation protocol with 10 trains of 10 pulses at 100 Hz applied, with 2-s inter-train intervals. I used a TBS stimulating protocol that consist 10 trains of 4 pulses at 100 Hz in a 200 ms interval, repeated 3 times (see Figure 10). Also, the injection of Aηα could lead to inevitable neuronal damage, which putatively influence the experiments. Aηα injection was performed in Heidelberg in the lab of U. Müller. WtR6 littermate controls were injected with an empty vector only containing Venus (pAAVss-Syn-lckVenus(1x10e9)) whereas Aηα injection was performed with two different titer pAAVss-Syn-lckVenus-T2A-Aη-α(1*10e9) and pAAVss-Syn-lckVenus-T2A-Aη-α(1*10e10). They could prove, that 3 weeks after injection pyramidal cell layer of CA1-CA3 hippocampal neurons was intact and as control injection of WT animals with inactivated vector lead to physiological LTP this

theory of neuronal damage due to injection could be disposed. Another theory could be based on the low titer. This theory is supported by the fact that there are no visible differences in electrophysiological measurements for both titers. In Heidelberg they were able to tag the pAAVss-Syn-lckVenus-T2A-Aη-α via human specific antibody (6E10) and it was expressed widely in hippocampal region. Also, the microscopically search for fluorescent light, representing the expression of the vector through the yellow fluorescent protein Venus, in the hippocampal region directly before measurements was positive. The AAV-vectors contained the synapsin promotor, therefore expression of the encoded fluorescent protein Venus was linked to neurons. Therefore, one can be sure that Aηα was expressed in the region of interest but maybe not high enough. The titer of 10^9 and 10^{10} was as high or even higher as the titer used for APPsα experiments, because of the comparability of these experiments the titer was chosen. To manifest this hypothesis, the experiments need to be repeated with a higher, but still physiological titer of Aηα.

4.1.4 APPsα vs other cleavage products

There are various cleavage products from the APP family with various functions. APPsα a cleavage product from the non-amyloidogenic pathway has been proven to act neuroprotective (Turner et al., 2003; Copanaki et al., 2010) whereas peptides from the amyloidogenic pathway have neurodegenerative functions. Amyloid β for example as well as tau protein have well established roles in Alzheimer's disease. In postmortem AD brains they are visible as amyloid plaques and neurofibrillary tangles (NFTs), the two hallmarks of AD (Shipton et al., 2011). First, at picomolar concentrations Aβ was shown to be essential for synaptic plasticity by modulating synaptic vesicle release (Abramov et al., 2009, Wang et al., 2012) leading to enhanced LTP (Puzzo et al., 2008). Second, acute application of natural or synthetic Aβ has been proven to impair hippocampal LTP when used in nanomolar concentrations (Cullen et al., 1997; Lambert et al., 1998) and NFTs are elevated in the hippocampal CA1 area and correlate with memory decline (Markesbery et al., 2006). APPsβ, another fragment from the amyloidogenic pathway that is identical in primary sequence except for the last 16 amino acids compared to APPsα, failed to show any detectable effects on synaptic plasticity and spine density (Richter et al., 2018). One could have thought about a nearly identical or even similar function of APPsβ, but it seems like only the last 16 amino acids (CTα16) have a positive function in the brain. This theory has been proven by Richter and colleagues where they could show that LTP deficits of conditional CNS specific APP/APLP2 double knockout mice (Hick et al., 2015) are rescued by application of CTα16 to the same extend as APPsα (Richter et al., 2018). APPsα seems to be a potential rescue

molecule in terms of Alzheimer's disease with its various positive functions for example neuroprotection or spine formation (Barger and Harmond 1997; Turner et al., 2003; Copanaki et al., 2010; Richter et al., 2018). Furthermore, APPsα is able to act on disease associated alterations like extensive NMDA receptor activation (Ryan et al., 2013) as well as acting positive on Aβ toxicity (Barger and Mattson, 1996). Additionally, reduced levels of sAPPα could contribute to neuronal degeneration in AD as well (Furukawa et al., 1996). As Aηα is a short sequence from APPsα (Figure 2) one could assume, that it has a comparable function. CTFs (carboxy-terminal fragments) produced by η-secretase are enriched in dystrophic neurites in an AD mouse model as well as in human AD brains. Furthermore, they could show that in mice treated with a potent BACE1 inhibitor, the secretase leading to Aηα formation, hippocampal LTP was reduced. Moreover, when recombinant or synthetic Aη-α was applied on hippocampal slices *ex vivo*, LTP was lowered (Willem et al., 2015). This is not adaptable for Aηβ. LTP was unaffected when Aηβ was applied. Nevertheless, in my study Aηα seems to have no influence on acute hippocampal slices when used in the same concentration as APPsα.

4.2 NALP3 in physiological aging

The second part of my study contains the knockout (KO) of the NALP3 inflammasome and its effects on physiological aging. As also inflammatory processes play an important role in the progress of neurodegenerative diseases like AD, special attention was given to this part of my thesis. Aβ activation of the NALP3 inflammasome in microglia is fundamental for interleukin-1β (IL-1ß) maturation, a pro-inflammatory cytokine, promoting inflammatory processes (Halle et al., 2008). IL-1ß is a molecule shown to limit adult neurogenesis and recovery of presynaptic termini (Garber et al., 2018), a mechanism essential for hippocampal recovery in neurodegenerative diseases as well as physiological aging. Also, Heneka et al. (2013) could show that KO of NLRP3 is beneficial regarding impaired spatial memory and reduced brain caspase-1 and IL-1β activation. Additionally, they showed an enhanced Aβ clearance (Heneka et al., 2013). Therefore, a positive effect of the KO of the NALP3 inflammasome is assumed regrading physiological aging.

4.2.1 Sex dependent differences in the brain

The sex dependent analysis showed that in aged NLRP3 KO female mice increased LTP compared to age matched male NLRP3 KO mice as well as littermate controls are detected, leading to the speculation of a positive physiological effect of KO the NALP3 inflammasome within age in a sex

dependent manner. There are various studies dealing with the question about sex dependent differences in the brain that are linked to numerous of diseases (Whitacre 2011; Lenz et al., 2013; Lenz and McCarthy 2014; Schwarz and Bilbo, 2018; Liu et al., 2019). One could assume that males are more likely to be diagnosed with disorders that have distinct developmental origins such as autism or schizophrenia (Werling und Geschwind 2013). Compared to that, females are more likely to be diagnosed with disorders that occur later in life like depression and anxiety disorders (Schwarz and Bilbo, 2018). The study of Lenz and McCarthy (2014) reported a differentially regulated inflammatory system in male and female brain, depending on the number of microglial cells. Another study of Lenz proved that immune cells in the brain interact with the nervous systems during development and that they are crucial for sexual differentiation of brain and behavior (Lenz et al., 2013). Another recent study pointed out that female microglia phagocytize more neural progenitor cells and healthy cells compared to males and that females also have higher expression of several phagocytic pathway genes in the hippocampus compared to males (Nelson et al., 2017). Also, the number and morphology of microglia throughout development is dependent upon the sex and age. Males have more microglia early in postnatal development whereas females have more microglia with an activated morphology later in development (Schwarz et al., 2011). As the number of activated microglia is enhanced with age in female one could claim, that KO of the NALP3 inflammasome located in microglia cells and responsible for cytokine release is leading to an improved phenotype as seen in my study. The study of Liu et al (2019) could show that female mice are more sensitive to chronic unpredictable mild stress and this is leading to the activation of microglia in a sex dependent manner. This discovery suggested that females were inclined to have more pro-inflammatory cytokines after stress. Lenz and McCarthy (2014) cleared out that in the developing rodent brain across during the neonatal period males have more microglia cells than females that releases prostaglandins which are essential contributors to the induction and maintenance of dendritic spine excitatory synapses in the developing male brain. Additionally, they could show, that the expressions of BDNF and its receptor TrkB is decreased in a more pronounced way in the hippocampus in female compared to male mice due to stress. As BDNF is crucial for development of new connections, restoration of failing brain cells and protection of healthy brain cells, this could lead to a disadvantage in the female brain. Furthermore, they could also show a sex-specific relationship between BDNF and hippocampal microglia-related inflammatory biomarkers. The study speculated that the imbalance of microglial pro- and anti-inflammatory states as well as the BDNF-TrkB-dependent pathway in hippocampus is involved in depressive-like behaviors (Liu et al., 2019). Overall, there is evidence for sex dependent differences in the brain.

4.3 Autoimmune antibodies

The last part of my thesis deals with an autoimmune disease triggered by autoimmune antibodies. The clinical significance and spectrum of AE is rapidly expanding after the initial discovery of the two most prevalent types of AE, namely, anti–leucine-rich glioma-inactivated 1 (anti-LGI1) and anti-N-methyl-D-aspartate receptor (anti-NMDAR) encephalitis (Kim et al., 2017; Dalmau et al., 2008; Lai et al., 2010; Irani et al., 2010). A study of Planagumà and colleagues in 2015 could show that autoimmune antibodies could alter the function of NMDAR resulting in memory and behavior alterations. Another study of Hughes et al., 2010 could show that these alterations occur without effecting number of spines, dendritic complexity, localization or expression of other synaptic proteins as well as cell survival. Lalic et al., could show in 2011 that LE IgG increases the release probability on MF-CA3 pyramidal cell synapses compared to the control IgG. In my study I could show a decreased LTP in CA1/CA3 hippocampal area as well as decreased spine density in DG granule cells after long-term application of AAB of Patient1. As only Patient1 is showing an altered LTP and IgG4 subclass was present as in others but IgG1 subclass was absent one could assume, that the binding of LGI-1 AAB is epitope dependent. Therefore, the binding site of LGI-1 needs to be clarified. Lovero et al. (2015) could show that leucine-rich, glioma inactivated protein 1 (LGI1) is a paracrine signal released from pre- and postsynaptic neurons that acts specifically through a disintegrin and metalloproteinase protein 22 (ADAM22) to set postsynaptic strength. If the interaction of ADAM22 and LGI-1 is altered through AAB, postsynaptic strength is decreased; resulting impaired LTP buildup. This result fits with Patient1 as LTP is decreased after long application of AAB on acute hippocampal slices. Other studies additionally showed that IgG4 subclass AAB alters neuronal function through a disruption of LGI-1 and ADAM22 which is leading to a secondary dysregulation of synaptic receptors and therefore altered synaptic transmission (Niks et al., 2008; Arino et al., 2006). Another study that deals with NMDAR-AAB could show that patients AAB increase the rate of internalization in a time and activity dependent manner. After 4 h no significant differences where seen while after 12 h the internalization rate of NMDAR was significantly enhanced in Patient's antibody treated hippocampal neurons (Moskato et al., 2016). Same is true for experiments performed in this study. After short-term application of AAB of Patient1 on acute hippocampal slices no differences in LTP was recorded but after long-term application of 6 h, decreased LTP was seen. As basal synaptic transmission is unaffected, one could assume a NMDAR dependent mechanism. As PPF overall is not altered, the presynaptic part seems to be unaffected.

Nevertheless, Figure 32 shows possible binding sites of autoimmune antibodies on LGI1. In the left upper panel (healthy) the LGI1 protein interacts with its EPTP domain (blue) with the ADAM22 receptor postsynaptically and with the ADAM23 receptor presynaptically (red). LGI1 also interacts with other LGI1 proteins via binding of the LRR domain (green) to the EPTP domain. In Patient1 (upper right panel) the LRR domain interaction is blocked due to AAB binding, only the EPTP domain can interact with ADAM22/23. Therefore, pre- and post-synaptic interaction is disturbed. The binding site of AABs in Patient1 is LGI-1. In the lower left panel, the AAB is binding to the EPTP domain and therefore the binding of LGI1 to its receptors ADAM22/23 is blocked. Autointeraction of LGI1 is still possible and this was seen in Patient2. In Patient3 the AAB bind also on EPTP domain and therefore prevent binding of LGI1 to ADAM22/23 just as with Patient 2. Additionally, the AAB binds to the LRR domain but in a way the LRR/EPTP still remains possible. Taken together, AABs of Patient1 interact with LGI-1 whereas in Patient2 and 3 the interaction takes place with ADAM22. This result is reflected in the LTP data, where only alterations could be seen by Patient1. Therefore, the interaction of the EPTP domain with the LRR domain seems to be crucial for the maintenance of LTP.

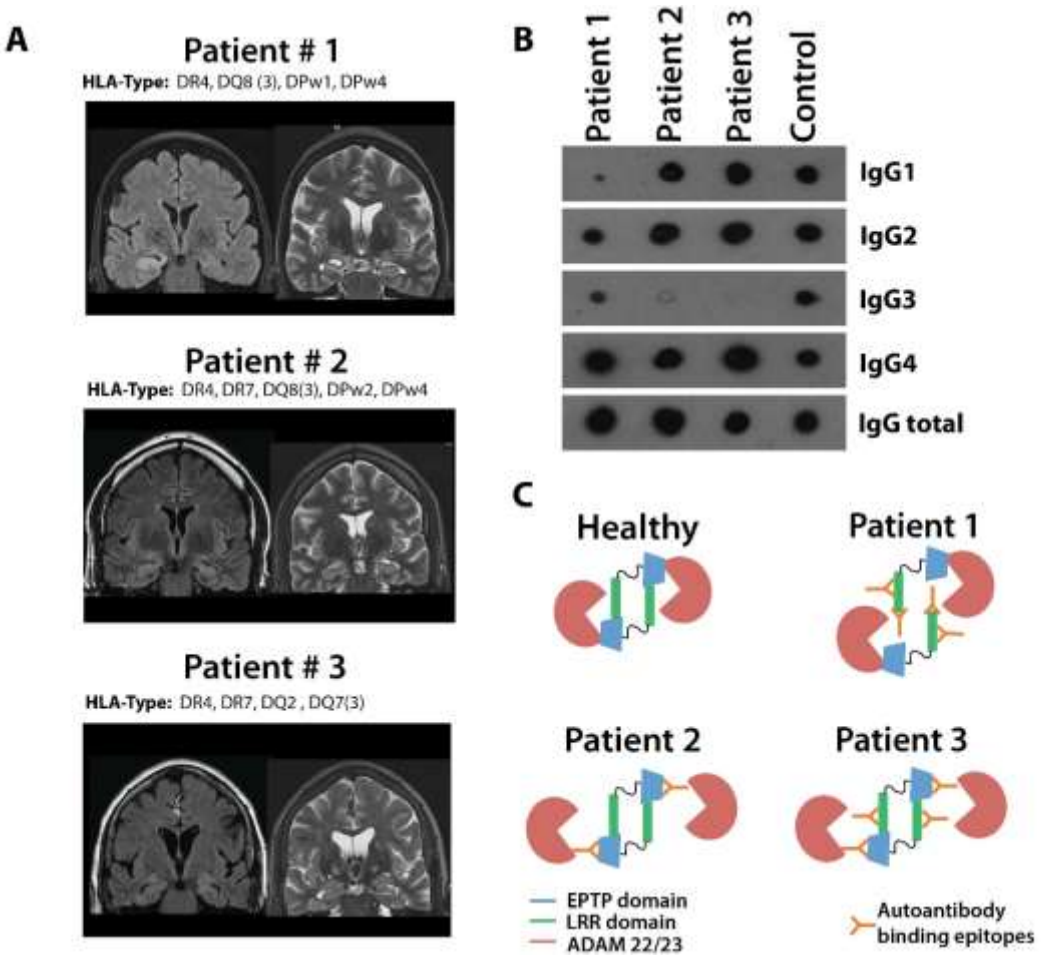

Figure 32 Patients brain and IgG epitopes. (A) Serial MRI sections regarding the hippocampus. Patient1 developed a hippocampal sclerosis. Patient2 and 3 did not. (B) Dot blot analysis splitting up the IgG fraction of the three patients into IgG subclasses; (C) schematic presentation of the data of the epitope mapping which show the binding of the anti-LGI1 abs of the respective patients to the LGI1 molecule according to Yamagata and coworker (Yamagata et al., 2018). Ab binding to epitopes with the highest affinity is marked with a Y, respectively**.** In the healthy control the LGI1 protein interact with its EPTP domain (blue) with the ADAM22 receptor postsynaptically and with the ADAM23 receptor presynaptically (red). It also interacts with other LGI1 proteins via binding of the LRR domain (green) to the EPTP domain. In Patient1 the LRR domain interaction is blocked due to AAB binding, only the EPTP domain can interact with Adam22/23. In the lower left panel (Patient2) the AAB is binding to the EPTP domain and therefore the binding of LGI1 to its receptors ADAM22/23 is blocked. Autointeraction of LGI1 is still possible. In Patient3 the AAB bind also on EPTP domain and therefore prevent binding of LGI1 to ADAM22/23 just as with Patient2. Additionally, the AAB bind to the LRR domain but in a way the LRR/EPTP still remains possible. HLA=human Leukocyte Antigens, HLA-DR/DQ/DP=cell surface receptor proteins on antigen presenting cells (MHC subclass II).

This result suggests that epitope specific binding of AABs lead to different clinical outcomes represented in distinct LTP levels as well as spine density differences in different hippocampal regions.

5. Conclusion and Outlook

In my thesis, I could show various functions of different molecules regarding synaptic plasticity under the aspect of aging and gender. On the one hand APPsα, a cleavage product from the APP family via the non-amyloidogenic pathway has a positive effect on LTP in APP/APLP2 cDKO mice acting via the α7-nAChR. Additionally, in aged, but not young htau.P301S mice representing tau tangles in the hippocampus, like in Alzheimer's disease, application of recAPPsα is leading to a rescued LTP as well as EPSP towards WT level, whereas LTD and presynaptic function seems to be uneffected. One need to have a look into the exact mechanism of the recaps acting on the α7-nAChR. On the other hand, the application of Aηα, another cleavage product from the APP family via the η-secretase, shows no effect on electrophysiological measurements. As other studies reported a negative function of Aηα on LTP one need to administrate the titer of Aηα to ensure using the right concentration.

Another finding indicates a sex dependent positive effect of the KO of the NLRP3-Inflassamome in aged mice. With age the inflammation system in the brain is susceptible for interferences, which in some case is leading to hyperactivation and damage of neurons. Whereas in young mice the KO of the NALP3 inflammasome seems to have no influence on the synaptic plasticity in the murine hippocampus, in aged female mice the KO of the NALP3 inflammasome has an advantage towards an increased LTP compared to male mice as well as age and sex matched littermate controls. To define the exact time point when the positive effect of KO the NALP3 inflammasome occurs, experiments need to be done on more aging time points between 12 and 24 months. One could also have a look for other inflammasomes like the NLRP1 inflammasome mainly found in neurons to have a positive effect on synaptic plasticity during aging processes. Furthermore, there is need for further investigation on the exact mechanism, why females show an enhanced LTP whereas males do not. Therefore, one could have a look for sex dependent function of distinct molecules like IL-1β released via the NLRP3 inflammasome in aged WT animals.

The last part of my thesis deals with autoimmune antibodies, where I confirmed that long-term but not acute application of human AAB on acute hippocampal slices is leading to a reduced LTP, which is additionally epitope dependent. To verify the epitope dependent effect of AAB on long-term application as well as morphological changes, more patients suffering from the same type of autoimmune disease like Patient1 need to be included in the study. Furthermore, the application time of ABB or the concentration need to be changed to have a closer look into incubation time and acute functions of AAB. One also needs to identify the mechanism of spine density alteration in the hippocampus after long-term application of AAB of Patient1.

References

Abderrazak A, Syrovets T, Couchie D, El Hadri K, Friguet B, Simmet T and Rouis M (2015). NLRP3 inflammasome: From a danger signal sensor to a regulatory node of oxidative stress and inflammatory diseases. Redox Biology 4:297-304.

Abramov E, Dolev I, Fogel H, Ciccotosto GD, Ruff E, Slutsky I (2009). Amyloid-beta as a positive endogenous regulator of release probability at hippocampal synapses. Nature neuroscience 12:1567-1576.

Allen B, Ingram E, Takao M, Smith MJ, Jakes R, Virdee K, Yoshida H, Holzer M, Craxton M, Emson PC, Atzori C, Migheli A, Crowther RA, Ghetti B, Spillantini MG, Goedert M (2002). Abundant tau filaments and nonapoptotic neurodegeneration in transgenic mice expressing human P301S tau protein. J Neurosci. 22(21):9340-51.

Alzheimer A (1907). Über eine eigenartige Erkrankung der Hirnrinde. Vortrag in der Versammlung Südwestdeutscher Irrenärzte in Tübingen am 3. November 1906. Allgemeine Zeitschrift für Psychiatrie und psychisch-gerichtliche Medizin 64:146-148.

Andersen P, Morris R, Amaral D, Bliss T, O'Keefe J (2006). The Hippocampus Book. Oxford Neuroscience Series.

Andreasson KI, Bachstetter AD, Colonna M, Ginhoux F, Holmes C, Lamb B, Landreth G, Lee DC, Low D, Lynch MA, Monsonego A, O'Banion MK, Pekny M, Puschmann T, Russek-Blum N, Sandusky LA, Selenica MLB, Takata K, Teeling J, Town T and Van Eldik LJ (2016). Targeting innate immunity for neurodegenerative disorders of the central nervoussystem. Journal of Neurochemistry. 1-70.

Arino H, Armangue T, Petit-Pedrol M, Sabater L, Martinez-Hernandez E, Hara M, Lancaster E, Saiz A, Dalmau J, Graus F (2016). Anti-LGI1 – associated cognitive impairment Presentation and long-term outcome. Neurology. 87:1-8.

Aydin D, Weyer SW, Muller UC (2012). Functions of the APP gene family in the nervous system: insights from mouse models. Exp Brain Res 217:423-434.

Barger SW, Harmon AD (1997). Microglial activation by Alzheimer amyloid precursor protein and modulation by apolipoprotein E. Nature 388:878-881.

Barger SW, Mattson MP (1996) Participation of gene expression in the protection against amyloid betapeptide toxicity by the beta-amyloid precursor protein. Annals of the New York Academy of Sciences 777:303-309.

Barria A, Muller D, Derkach V, Griffith LC, Soderling TR (1997). Regulatory phosphorylation of AMPA-type glutamate receptors by CaM-KII during long-term potentiation. Science (New York, NY) 276:2042-2045.

Bauernfeind FG, Horvath G, Stutz A, Alnemri ES, Macdonald K, Speert D, Fernandes-Alnemri T, Wu J, Monks BG, Fitzgerald KA, Hornung V and Latz E (2009). NF-kappaB activating pattern recognition and cytokine receptors license NLRP3inflammasome activation by regulating NLRP3expression. J. Immunol. 183:787-791.

Biagi E, Candela M, Franceschi C, Brigidi P (2011). The aging gut microbiota: new perspectives. Ageing Res Rev. 10:428–429.

Bliss TV, Collingridge GL (1993). A synaptic model of memory: long-term potentiation in the hippocampus. Nature 361:31-39.

Bliss TV, Lømo T (1973). Long-lasting potentiation of synaptic transmission in the dentate area of the anaesthetized rabbit following stimulation of the perforant path. The Journal of physiology 232:331-356.

Boekhoorn K, Terwel D, Biemans B, Borghgraef P, Wiegert O, Ramakers GJA, de Vos K, Krugers H, Tomiyama T, Mori H, Joels M, van Leuven F and Lucassen PJ (2006). Improved Long-Term Potentiation and Memory in Young Tau-P301L Transgenic Mice before Onset of Hyperphosphorylation and Tauopathy. The Journal of Neuroscience 26(13):3514-3523.

Borg JP, Ooi J, Levy E, Margolis B (1996). The phosphotyrosine interaction domains of X11 and FE65 bind to distinct sites on the YENPTY motif of amyloid precursor protein. Molecular and cellular biology 16:6229-6241.

Brager DH, Cai X, Thompson SM (2003). Activity-dependent activation of presynaptic protein kinase C mediates post-tetanic potentiation. Nature neuroscience 6:551-552.

Cajal SR (1894). The Croonian Lecture: La Fine Structure des Centres Nerveux. Proc Roy Soc London, 55:444-468.

Cao X, Sudhof TC (2001). A transcriptionally [correction of transcriptively] active complex of APP with Fe65 and histone acetyltransferase Tip60. Science (New York, NY) 293:115-120.

Chen L, Yamada K, Nabeshima T, Sokabe M (2006). alpha7 Nicotinic acetylcholine receptor as a target to rescue deficit in hippocampal LTP induction in beta-amyloid infused rats. Neuropharmacology 50:254-268.

Citri A, Malenka RC (2007). Synaptic Plasticity: Multiple Forms, Functions, and Mechanisms. Neuropsychopharmacology 33:18-41.

Coll RC, Robertson AAB, Chae JJ, Higgins SC, Muñoz-Planillo R, Inserra MC, Vetter I, Dungan LS, Monks BG, Stutz A, Croker DE, Butler MS, Haneklaus M, Sutton CE, Núñez G, Latz E, Kastner DL, Mills KHG, Masters SL, Schroder K, Cooper MA and O'Neill LAJ (2015). A small molecule inhibitior of the NLRP3 inflammasome is a potential therapeutic for inflammatory diseases. Nat Med. 21(3):248-255.

Copanaki E, Chang S, Vlachos A, Tschape JA, Muller UC, Kogel D, and Deller T (2010). sAPPalpha antagonizes dendritic degeneration and neuron death triggered by proteasomal stress. Mol Cell Neurosci, 44, 386-393.

Corrigan F, Vink R, Blumbergs PC, Masters CL, Cappai R, van den Heuvel C (2012). sAPPα rescues deficits in amyloid precursor protein knockout mice following focal traumatic brain injury. Journal of neurochemistry 122:208-220.

Cullen WK, Suh YH, Anwyl R, Rowan MJ (1997). Block of LTP in rat hippocampus in vivo by β - amyloid precursor protein fragments. Neuroreport 8:3213-3217.

Cunningham C (2013). Microglia and neurodegeneration: the role of systemic inflammation. Glia. 61(1):71-90.

Dalmau J, Gleichman AJ, Hughes EG, Rossi JE, Peng X, Lai M, Dessain SK, Rosenfeld MR, Balice-Gordon R, Lynch DR. (2008). Anti-NMDA-receptor encephalitis: case series and analysis of the effects of antibodies. Lancet Neurol. 7:1091-1098.

DeBoer SR, Dolios G, Wang R, Sisodia SS (2014). Differential release of beta-amyloid from dendrite- versus axon-targeted APP. The Journal of neuroscience: the official journal of the Society for Neuroscience 34:12313-12327.

Dinarello CA (1998). Interleukin-1 beta, interleukin-18, and the interleukin 1 beta converting enzyme. Ann. NY Acad. Sci. 856:1-11.

Dobrunz LE, Huang EP, Stevens CF (1997). Very short-term plasticity in hippocampal synapses. Proceedings of the National Academy of Sciences of the United States of America 94:14843-14847.

Doss S, Wandinger KP, Hyman BT, Panzer JA, Synofzik M, Dickerson BB, Mollenhauer B, Scherzer CR, Ivinson AJ, Finke C, Schöls L, Müller Vom Hagen J, Trenkwalder C, Jahn H, Höltje M,

Biswal BB, Harms L, Ruprecht K, Buchert R, Höglinger GU, Oertel WH, Unger MM, Körtvélyessy P, Bittner D, Priller J, Spruth EJ, Paul F, Meisel A, Lynch DR, Dirnagl U, Endres M, Teegen B, Probst C, Komorowski L, Stöcker W, Dalmau J, Prüss H (2014). High prevalence of NMDA receptor IgA/IgM antibodies in different dementia types. Ann Clin Transl Neurology 1:822-32.

Dudek SM, Bear MF (1993). Bidirectional long-term modification of synaptic effectiveness in the adult and immature hippocampus. JNeurosci 13:2910-2918.

Fol R, Braudeau J, Ludewig S, Abel T, Weyer SW, Roederer JP, Brod F, Audrain M, Bemelmans AP, Buchholz CJ, Korte M, Cartier N, Muller UC (2016) Viral gene transfer of APPsalpha rescues synaptic failure in an Alzheimer's disease mouse model. Acta neuropathologica 131:247-266.

Franceschi C and Campisi J (2014). Chronic Inflammation (Inflammaging) and Its Potential Contribution to Age-Associated Diseases. The Journals of Gerontology (A)69:4-9.

Franceschi C, Bonafé M, Valensin S, Olivieri F, De Luca M, Ottaviani E and de Benedictis G (2006). Inflamm-aging: An Evolutionary Perspective on Immunosenescence. Annals of the New York Academy of Sciences 908(1)244-254.

Freund TF, Buzsaki G (1996). Interneurons of the hippocampus. Hippocampus 6:347-470.

Fukata Y, Adesnik H, Iwanaga T, Bredt DS, Nicoll RA, Fukata M (2006). Epilepsy-Related Ligand/Receptor Complex LGI1 and ADAM22 Regulate Synpatic Transmission. Science. 313:1792-1795.

Fukata Y, Yokoi N, Miyazaki Y, Fukata M (2017). The LGI1–ADAM22 protein complex in synaptic transmission and synaptic disorders. Neuroscience Research. 116:39-45.

Fukunaga K, Muller D, Miyamoto E (1995). Increased phosphorylation of Ca2+/calmodulin-dependent protein kinase II and its endogenous substrates in the induction of long-term potentiation. The Journal of biological chemistry 270:6119-6124.

Furukawa K, Sopher BL, Rydel RE, Begley JG, Pham DG, Martin GM, Fox M, Mattson MP (1996) Increased activity-regulating and neuroprotective efficacy of alpha-secretase-derived secreted amyloid precursor protein conferred by a C-terminal heparin-binding domain. Journal of neurochemistry 67:1882-1896.

Garber C, Vasek MJ, Vollmer LL, Sun T, Jiang X, Klein RS (2018). Astrocytes decrease adult neurogenesis during virus-induced memory dysfunction via IL-1. Nat Immunol. 19(2):151-161.

Goebbels S, Bormuth I, Bode U, Hermanson O, Schwab MH, Nave KA (2006). Genetic targeting of principal neurons in neocortex and hippocampus of NEX-Cre mice. Genesis 44:611-621.

Goedert M, Wischik CM, Crowther RA, Walker JE, Klug A (1988). Cloning and sequencing of the cDNA encoding a core protein of the paired helical filament of Alzheimer disease: identification as the microtubule-associated protein tau. ProcNatlAcadSciUSA 85:40514055.

Goshen I, Yirmiya R (2009). Interleukin-1 (IL-1): a central regulator of stress responses. Front. Neuroendocrinol. 30:30-45.

Halle A, Hornung V, Petzold GC, Stewart CR, Monks BG, Reinheckel T, Fitzgerald KA, Latz E, Moore KJ, Golenbock DT (2008). The NALP3 inflammasome is involved in the innate immune response to amyloid-β. Nature Immunol. 9, 857-865.

Hebert LE, Weuve J, Scherr PA, Evans DA (2013). Alzheimer disease in the United States (2010-2050) estimated using the 2010 census. Neurology 80:1778-1783.

Heine J, Prüss H, Kopp UA, Wegner F, Then Bergh F, Münte T, Wandinger KP, Paul F, Bartsch T, Finke C (2018). Beyond the limbic system: Disruption and functional compensation of large-scale brain networks in Patients with anti-LGI1 encephalitis. J. Neurol. Neurosurg. Psychiatry. 1191-1199.

Heneka MT, Kummer MP and Latz E (2014). Innate immune activation in neurodegenerative disease. Nature Rewievs. 14:463-477.

Heneka MT, Kummer MP, Stutz A, Delekate A, Schartz S, Saecker AV, Griep A, Axt D, Remus A, Tzeng TC, Gelpi E, Halle A, Korte M, Latz E and Golenbock DT (2013). NLRP3 is activated in Alzheimer's disease and contributes to pathology in APP/PS1 mice. Nature. 493, 674-678.

Henneberger C, Bard L, King C, Jennings A, Rusakov DA (2013). NMDA receptor activation: two targets for two co-agonists. Neurochemical research 38:1156-1162.

Herron CE, Lester RA, Coan EJ, Collingridge GL (1986). Frequency-dependent involvement of NMDA receptors in the hippocampus: a novel synaptic mechanism. Nature 322:265-268.

Hick M, Herrmann U, Weyer SW, Mallm JP, Tschape JA, Borgers M, Mercken M, Roth FC, Draguhn A, Slomianka L, Wolfer DP, Korte M, Muller UC (2015). Acute function of secreted amyloid precursor protein fragment APPsalpha in synaptic plasticity. Acta neuropathologica 129:21-37.

Ho VM, Lee JA, Martin KC (2011). The cell biology of synaptic plasticity. Science (New York, NY) 334:623628.

Holtmaat A, Svoboda K (2009). Experience-dependent structural synaptic plasticity in the mammalian brain. Nature reviews Neuroscience 10:647-658.

Hughes EG, Peng X, Gleichman AJ, Lai M, Zhou L, Tsou R, Parsons TD, Lynch DR, Dalmau J and Balice-Gordon RJ (2010). Cellular and synaptic mechanisms of anti-NMDA receptor encephalitis. Journal of Neuroscience.30:5866-75.

Irani SR, Alexander S, Waters P, Kleopa KA, Pettingill P, Zuliani L, Peles E, Buckley C, Lang B, Vincent A. (2010). Antibodies to Kv1 potassium channel-complex proteins leucine-rich, glioma inactivated 1 protein and contactin-associated protein-2 in limbic encephalitis, Morvan's syndrome and acquired neuromyotonia. Brain. 133:2734-2748.

Irani SR, Pettingill P, Kleopa KA, Schiza N, Waters P, Mazia C, Zuliani L, Watanabe O, Lang B, Buckley C, Vincent A (2012). Morvan syndrome: Clinical and serological observations in 29 cases. Ann. Neurol.72:241-255.

Irani SR, Stagg CJ, Schott JM, Rosenthal CR, Schneider SA, Pettingill P, Waters P, Thomas A, Voets NL, Cardoso MJ,. Cash DM, Manning EN, Lang B, Smith SJM, Vincent A, Johnson MR (2013). Faciobrachial dystonic seizures: The influence of immunotherapy on seizure control and prevention of cognitive impairment in a broadening phenotype. Brain. 136:3151-3162.

Ishida A, Furukawa K, Keller JN, Mattson MP (1997). Secreted form of beta-amyloid precursor protein shifts the frequency dependency for induction of LTD, and enhances LTP in hippocampal slices. Neuroreport 8:2133-2137.

Jin C and Flavell RA (2010). Molecular Mechanism of NLRP3 Inflammasome Activation. J Clin Immunol. 30:628-631.

Jorissen E, Prox J, Bernreuther C, Weber S, Schwanbeck R, Serneels L, Snellinx A, Craessaerts K, Thathiah A, Tesseur I, Bartsch U, Weskamp G, Blobel CP, Glatzel M, De SB, and Saftig P (2010). The disintegrin/metalloproteinase ADAM10 is essential for the establishment of the brain cortex. J Neurosci, 30, 4833-4844.

Katz B and Miledi R (1968). The role of calcium in neuromuscular facilitation. J Physiol, 195:481-492.

Klevanski M, Saar M, Baumkotter F, Weyer SW, Kins S, Muller UC (2014). Differential role of APP and APLPs for neuromuscular synaptic morphology and function. Molecular and cellular neurosciences 61:201-210.

Kohara K, Pignatelli M, Rivest AJ, Jung HY, Kitamura T, Suh J, Frank D, Kajikawa K, Mise N, Obata Y, Wickersham IR, Tonegawa S (2014). Cell type-specific genetic and optogenetic tools reveal hippocampal CA2 circuits. Nature neuroscience 17:269-279.

Komic A, Martinez-Quinones P, McCarthy CG, Webb CR, Wenceslau CF (2018). Increase in soluble protein oligomers triggers the innate immune system promoting inflammation and vascular dysfunction in the pathogenesis of sepsis. Clinical Science 132 (13) 1433-1438.

Korte M, Schmitz D (2016). Cellular and System Biology of Memory: Timing, Molecules, and Beyond. Physiological reviews 96:647-693.

Krishnan V and Nestler EJ (2010). Linking Molecules to Mood. New Insight Into the Biology of Depression. The American Journal of Psychiarty 1305-1320.

Kuhn PH, Wang H, Dislich B, Colombo A, Zeitschel U, Ellwart JW, Kremmer E, Rossner S, Lichtenthaler SF (2010). ADAM10 is the physiologically relevant, constitutive alpha-secretase of the amyloid precursor protein in primary neurons. Embo j 29:3020-3032.

Kummer JA, Broekhuizen R, Everett H, Agostini L, Kuijk L, Martinon F, van Bruggen R und sTschopp J (2007). Inflammasome Components NALP 1 and 3 Show Distinct but Separate Expression Profiles in Human Tissues Suggesting a Site-specific Role in the Inflammatory Response. Journal of Histochemistry & Cytochemistry. 55(5):443-452.

Lai M, Huijbers MG, Lancaster E, Graus F, Bataller L, Balice-Gordon R, Cowell JK, Dalmau J (2010). Investigation of LGI1 as the antigen in limbic encephalitis previously attributed to potassium channels: a case series. Lancet Neurol. 9:776-785.

Lalic T, Pettingill P, Vincent A and Capogna M (2011). Human limbic encephalitis serum enhances hippocampal mossy fiber-CA3 pyramidal cell synaptic transmission. Epilepsia 52(1):121-131.

Lamason R, Zhao P, Rawat R, Davis A, Hall JC, Chae JJ, Agarwal R, Cohen P, Rosen A, Hoffman EP und Nagaraju K (2006). Sexual dimorphism in immune response genes as a function of puberty. BMC Immunology. 7(2), 1-14.

Lambert MP, Barlow AK, Chromy BA, Edwards C, Freed R, Liosatos M, Morgan TE, Rozovsky I, Trommer B, Viola KL, Wals P, Zhang C, Finch CE, Krafft GA, Klein WL (1998). Diffusible, nonfibrillar ligands derived from A β 1–42 are potent central nervous system neurotoxins. Proc Natl Acad Sci U S A 95:6448-6453.

Lassek M, Weingarten J, Einsfelder U, Brendel P, Muller U, Volknandt W (2013). Amyloid precursor proteins are constituents of the presynaptic active zone. Journal of neurochemistry 127:48-56.

Latz E, Xiao TS and Stutz A (2013). Activation and regulation of the inflammasomes. Nature Rev.Immunol. 13:397-411.

Lenz KM and McCarthy MM (2014). A Starring role for Microglia in Brain Sex Differences. Neuroscientist 21(3):306-321.

Lenz KM, Nugent BM, Haliyur R, McCarthy MM (2013) Microglia are essential to masculinization of brain and behavior. J Neurosci 33:2761-2772.

Lin-Lin Liu, Jia-Mei Li, Wen-Jun Su, Bo Wang, Chun-Lei Jiang (2019). Sex differences in depressive-like behaviour may relate to imbalance of microglia activation in the hippocampus. Brain, Behavior, and Immunity.

Lorenzo A, Yuan M, Zhang Z, Paganetti PA, Sturchler-Pierrat C, Staufenbiel M, Mautino J, Vigo FS, Sommer B, and Yankner BA (2000). Amyloid beta interacts with the amyloid precursor protein: a potential toxic mechanism in Alzheimer's disease. Nat Neurosci, 3, 460-464.

Lovero KL, Fukata Y, Adam J. Granger AJ, Fukata M and Nicoll RA (2015). The LGI1–ADAM22 protein complex directs synapse maturation through regulation of PSD-95 function. PNAS 4129-4137.

Lucin KM and Wyss-Coray T (2009). Immune activation in brain aging and neurodegeneration: too much or too little? Neuron. 64:110-122.

Ludewig S, Korte M (2017). Novel Insights into the Physiological Function of the APP (Gene) Family and Its Proteolytic Fragments in Synaptic Plasticity. Frontiers in Molecular Neuroscience 9.

Lynch MA (2004). Long-Term Potentiation and Memory. Physiological reviews 84:87-136.

Mallm JP, Tschape JA, Hick M, Filippov MA, Muller UC (2010). Generation of conditional null alleles for APP and APLP2. Genesis (New York, NY : 2000) 48:200-206.

Manahan-Vaughan D, Kulla A, Frey JU (2000). Requirement of translation but not transcription for the maintenance of long-term depression in the CA1 region of freely moving rats. The Journal of neuroscience: the official journal of the Society for Neuroscience 20:8572-8576.

Markesbery MR, Schmitt FA, Kryscio RJ, Davis DG, Smith CD, Wekstein DR (2006). Neuropathologic substrate of mild cognitive impairment. Arch Neurol 63:38-46.

Martinon F, Burns K and Tschopp J (2002). The Inflammasome: A Molecular Platform Triggering Activation of Inflammatory Caspases and Processing of proIL-β. Molecular Cell. 10:417-426.

Mayer MC, Schauenburg L, Thompson-Steckel G, Dunsing V, Kaden D, Voigt P, Schaefer M, Chiantia S, Kennedy TE, Multhaup G (2016). Amyloid precursor-like protein 1 (APLP1) exhibits stronger zincdependent neuronal adhesion than amyloid precursor protein and APLP2. Journal of neurochemistry 137:266-276.

Miller TD, Chong TTJ, Aimola Davies AM, Ng TWC, Johnson MR, Irani SR, Vincent A, Husain M, Jacob S, Maddison P, Kennard C, Gowland PA, Rosenthal CR (2017). Focal CA3 hippocampal subfield atrophy following LGI1 VGKC-complex antibody limbic encephalitis. Brain. 140:1212-1219.

Moore AH, Wu M, Shaftel SS, Graham KA, O'Banion MK (2009). Sustained expression of interleukin-1beta in mouse hippocampus impairs spatial memory. Neuroscience. 164(4):1484-1495.

Moreno L, Rose C, Mohanraj A, Allinquant B, Billard JM, Dutar P (2015) sAbetaPPalpha Improves Hippocampal NMDA-Dependent Functional Alterations Linked to Healthy Aging. Journal of Alzheimer's disease : JAD 48:927-935.

Moscato EH, Peng X, Jain A, Parsons TD, Dalmau J and Balice-Gordon RJ (2014). Acute Mechanisms Underlying Antibody Effects in Anti–N-Methyl-D-Aspartate Receptor Encephalitis. Ann Neurol. 76:108-119.

Navarro V, Kas A, Apartis E, Chami L, Rogemond V, Levy P, Psimaras D, Habert MO, Baulac M, Delattre JY, Honnorat J (2016). Motor cortex and hippocampus are the two main cortical targets in LGI1-antibody encephalitis. Brain. 139: 1079-1093.

Nelson HL, Warden S, Lenz KM (2017). Sex differences in microglial phagocytosis in the neonatal hippocampus. Brain, Behavior, and Immunity 64:11-22.

Niks EH, van Leeuwen Y, Leite MI, Dekker FW, Wintzen AR, Wirtz PW, Vincent A, van Tol MJD, Jol-van der Zijde CM, Verschuuren JJGM (2008). Clinical fluctuations in MuSK myasthenia gravis are related to antigen-specific IgG4 instead of IgG1. J Neuroimmunol. 195:151-156.

Norden DM, Trojanowski PJ, Walker FR and Godbout JP (2016). Insensitivity of astrocytes to interleukin 10 signaling following peripheral immune challenge results in prolonged microglial activation in the aged brain. Neurobiol Aging. 44:22-41.

O'Keefe J, Nadel L (1978). The Hippocampus as a Cognitive Map. Oxford: Clarendon.

Ohkawa T, Fukata Y, Yamasaki M, Miyazaki T, Yokoi N, Takashima H, Watanabe M, Watanabe O, Fukata M (2013). Autoantibodies to Epilepsy-Related LGI1 in Limbic Encephalitis Neutralize LGI1-ADAM22 Interaction and Reduce Synaptic AMPA Receptors. J. Neuroscience. 33:18161-18174.

Patten AR, Yau SY, Fontaine CJ, Meconi A, Wortman RC, Christie, BR (2015). The Benefits of Exercise on Structural and Functional Plasticity in the Rodent Hippocampus of Different Disease Models. Brain Plasticity 1:97-127.

Petit-pedrol M, Sell J, Planagumà J, Radosevic M, Mannara F, Haselmann H, Ceanga M, Sabater L, Spatola M, Soto D, Gasull X, Dalmau J, Geis C. (2018). LGI1 antibodies alter Kv1.1 and AMPA receptors changing synaptic excitability, plasticity and memory. Brain. 3144-3159.

Planagumà J, Leypoldt F, Mannara F, Gutiérrez-Cuesta, Martin-Garcia E, Aguilar E, Titulaer MJ, Petit-Pedrol M, Jain A, Balice-Gordon R, Lakadamyali M, Graus F, Maldonado R and Dalmau J (2015). Human N-methyl D-aspartate receptor antibodies alter memory and behaviour in mice. BRAIN. 138:94-109.

Polydoro M, Acker CM, Duff K, Castillo PE and Davies P (2009). Age-Dependent Impairment of Cognitive and Synaptic Function in the htau Mouse Model of Tau Pathology. The Journal of Neuroscience 29(34):10741-10749.

Prox J, Bernreuther C, Altmeppen H, Grendel J, Glatzel M, D'Hooge R, Stroobants S, Ahmed T, Balschun D, Willem M, Lammich S, Isbrandt D, Schweizer M, Horre K, De Strooper B, Saftig P (2013) Postnatal disruption of the disintegrin/metalloproteinase ADAM10 in brain causes epileptic seizures, learning deficits, altered spine morphology, and defective synaptic functions. The Journal of neuroscience : the official journal of the Society for Neuroscience 33:12915-12928, 12928a.

Puzzo D, Privitera L, Leznik E, Fà M, Staniszewski A, Palmeri A, Arancio O. (2008). Picomolar amyloid-β positively modulates synaptic plasticity and memory in hippocampus. J Neurosci 28:14537-14545.

Rathinam VAK, Vanaja SK and Fitzgerald KA (2012). Regulation of inflammasome signaling. Nature immunology. 13(4):333-342.

Regehr WG (2012). Short-term presynaptic plasticity. Cold Spring Harbor perspectives in biology 4:a005702.

Reinhard C, Hebert SS, and De SB (2005). The amyloid-beta precursor protein: integrating structure with biological function. EMBO J, 24, 3996-4006.

Richter MC, Ludewig S, Winschel A, Abel T, Bold C, Salzburger LR, Klein S, Han K, Weyer SW, Fritz AK, Laube B, Wolfer DP, Buchholz CJ, Korte M, Müller UC (2018). Distinct in vivo roles of secreted APP ectodomain variants APPsα and APPsβ in regulation of spine density, synaptic plasticity, and cognition. EMBO Journal 37:11.

Ring S, Weyer SW, Kilian SB, Waldron E, Pietrzik CU, Filippov MA, Herms J, Buchholz C, Eckman CB, Korte M, Wolfer DP, Muller UC (2007). The secreted beta-amyloid precursor protein ectodomain APPs alpha is sufficient to rescue the anatomical, behavioral, and electrophysiological abnormalities of APP-deficient mice. The Journal of neuroscience: the official journal of the Society for Neuroscience 27:7817-7826.

Rosahl TW, Geppert M, Spillane D, Herz J, Hammer RE, Malenka RC, and Sudhof TC (1993). Short-term synaptic plasticity is altered in mice lacking synapsin I. Cell, 75:661-670.

Ryan MM, Morris GP, Mockett BG, Bourne K, Abraham WC, Tate WP, Williams JM (2013) Timedependent changes in gene expression induced by secreted amyloid precursor protein-alpha in the rat hippocampus. BMC genomics 14:376.

Saijo K and Glass CK (2011). Microglial cell origin and phenotypes in health and disease. Nature Reviews. 11:775-787.

Saresella M, La Rosa, F, Piancone F, Zoppis M, Marventano I, Calabrese E, Rainone V, Nemni R, Mancuso R and Clerici M (2016). The NLRP3 and NLRP1 inflammasomes are activated in Alzheimer's disease. Molecular Neurodegeneration.11(23):1-14.

Sarubin N, Hilbert S, Naumann F, Zill P, Wimmer AM, Nothdurfter C, Rupprecht R, Baghai TC, Bühner M, Schüle C (2017). The sex-dependent role of the glucocorticoid receptor in depression: variations in the NR3C1 gene are associated with major depressive disorder in women but not in men. European Archives of Psychiatry and Clinical Neuroscience, 267(2):123-133.

Schaeffer EL, Figueiro M, and Gattaz WF (2011). Insights into Alzheimer disease pathogenesis from studies in transgenic animal models. Clinics (Sao Paulo), 66, 45-54.

Schwarz JM and Bilbo SD (2012). Sex, glia, and development: Interactions in health and disease. Hormones and Behavior 62(3):243-253.

Scoville WB, Milner B (1957). Loss of recent memory after bilateral hippocampal lesions. Journal of neurology, neurosurgery, and psychiatry 20:11-21.

Seagar M, Russier M, Caillard O, Maulet Y, Fronzaroli-Molinieres L, De San Feliciano M, Boumedine-Guignon N, Rodriguez L, Zbili M, Usseglio F, Formisano-Tréziny C, Youssouf F, Sangiardi M, Boillot M, Baulac S, Benitez MJ, Garrido JJ, Debanne D, El Far O (2017). LGI1 tunes intrinsic excitability by regulating the density of axonal Kv1 channels. Proc. Natl. Acad. Sci. 114:7719-7724.

Selkoe DJ, Hardy J (2016). The amyloid hypothesis of Alzheimer's disease at 25 years. EMBO Mol Med 8:595-608.

Seshadri S, Beiser A, Kelly-Hayes M, Kase CS, Au R, Kannel WB, Wolf PA (2006) The lifetime risk of stroke: estimates from the Framingham Study. Stroke 37:345-350

Shipton OA, LeitzJR, Dworzak J, Acton CEJ, Tunbridge EM, Denk F, Dawson HN, Vitek MP, Wade-Martins R, Paulsen O, Vargas-Caballero M (2011). Tau Protein Is Required for Amyloid β-Induced Impairment of Hippocampal Long-Term Potentiation. The Journal of Neuroscience 31(5):1688-1692.

Soba P, Eggert S, Wagner K, Zentgraf H, Siehl K, Kreger S, Lower A, Langer A, Merdes G, Paro R, Masters CL, Muller U, Kins S, Beyreuther K (2005). Homo- and heterodimerization of APP family members promotes intercellular adhesion. Embo j 24:3624-3634.

Streit WJ, Xue QS, Tischer J and Bechmann I (2014). "Microglial pathology." Acta Neuropathol Commun. 2:142.

Strowig T, Henao-Mejia J, Elinav E and Flavell R (2012). Inflammasomes in health and disease. Nature. 481:278-286.

Szatmari P, Offord DR, Boyle MH (1989). Ontario Child Health Study: prevalence of attention deficit disorder with hyperactivity. J Child Psychol Psychiatry 30(2):219-30.

Taylor CJ, Ireland DR, Ballagh I, Bourne K, Marechal NM, Turner PR, Bilkey DK, Tate WP, Abraham WC (2008) Endogenous secreted amyloid precursor protein-alpha regulates hippocampal NMDA receptor function, long-term potentiation and spatial memory. Neurobiol Dis 31:250-260.

Thompson J, Bi M, Murchison AG, Makuch M, Bien CG, Chu K, Farooque P, Gelfand JM, Geschwind MD, Hirsch LJ, Somerville E, Lang B, Vincent A, Leite MI, Waters P, Irani SR (2018). The importance of early immunotherapy in Patients with faciobrachial dystonic seizures. Brain. 141: 348-356.

Turner PR, O'Connor K, Tate WP, and Abraham WC (2003). Roles of amyloid precursor protein and its fragments in regulating neural activity, plasticity and memory. Prog Neurobiol, 70: 132.

Tyan SH, Shih AY, Walsh JJ, Maruyama H, Sarsoza F, Ku L, Eggert S, Hof PR, Koo EH, Dickstein DL (2012). Amyloid precursor protein (APP) regulates synaptic structure and function. Molecular and cellular neurosciences 51:43-52.

Van Sonderen A, Coenders EC, Sanchez E, De MAAM, Van MH, Wirtz PW, Schreurs MW, Sillevis Smitt PA, Titulaer MJ (2016). Anti-LGI1 encephalitis. Neurology. 87(14):1449-1456.

Viding E, Spinath FM, Price TS, Bishop DV, Dale PS, Plomin R (2004). Genetic and environmental influence on language impairment in 4-year-old same-sex and opposite-sex twins. J Child Psychol Psychiatry. 45(2):315-25.

von Koch CS, Zheng H, Chen H, Trumbauer M, Thinakaran G, van der Ploeg LH, Price DL, Sisodia SS (1997). Generation of APLP2 KO mice and early postnatal lethality in APLP2/APP double KO mice. Neurobiol Aging 18:661-669.

Walsh DM and Selkoe DJ (2007). A beta oligomers - a decade of discovery. J Neurochem. 101:1172-1184.

Wang H, Megill A, He K, Kirkwood A, Lee HK (2012) Consequences of inhibiting amyloid precursor protein processing enzymes on synaptic function and plasticity. Neural plasticity 2012:272374.

Wang HY, Lee DH, Davis CB, Shank RP (2000) Amyloid peptide Abeta(1-42) binds selectively and with picomolar affinity to alpha7 nicotinic acetylcholine receptors. Journal of neurochemistry 75:1155-1161

Werling DM and Geschwind DH (2013). Sex differences in autism spectrum disorders. Current Opinion Neurology 26(2):146-153.

Weyer SW, Klevanski M, Delekate A, Voikar V, Aydin D, Hick M, Filippov M, Drost N, Schaller KL, Saar M, Vogt MA, Gass P, Samanta A, Jaschke A, Korte M, Wolfer DP, Caldwell JH, Muller UC (2011). APP and APLP2 are essential at PNS and CNS synapses for transmission, spatial learning and LTP. Embo j 30:2266-2280.

Whitacre CC (2011). Sex differences in autoimmune disease. Nat Immunol 2(9):777-780.

Wilhelm BG, Mandad S, Truckenbrodt S, Krohnert K, Schafer C, Rammner B, Koo SJ, Classen GA, Krauss M, Haucke V, Urlaub H, Rizzoli SO (2014). Composition of isolated synaptic boutons reveals the amounts of vesicle trafficking proteins. Science (New York, NY) 344:1023-1028.

Willem M, Tahirovic S, Busche MA, Ovsepian SV, Chafai M, Kootar S, Hornburg D, Evans LD, Moore S, Daria A, Hampel H, Muller V, Giudici C, Nuscher B, Wenninger-Weinzierl A, Kremmer E, Heneka MT, Thal DR, Giedraitis V, Lannfelt L, Muller U, Livesey FJ, Meissner F, Herms J, Konnerth A, Marie H, Haass C (2015). eta-Secretase processing of APP inhibits neuronal activity in the hippocampus. Nature 526:443-447.

Xu H, Rösler TW, Carlsson T, de Andrade A, Bruch J, Höllerhage M, Oertel WH, Höglinger GU (2014). Memory deficits correlate with tau and spine pathology in P301S MAPT transgenic mice. Neuropathol Appl Neurobiol. 40(7):833-43.

Xu Y, Sheng H, Bao Q, Wang Y, Lu J, Ni X. (2015). NLRP3 inflammasome activation mediates estrogen deficiency-induced depression- and anxiety-like behavior and hippocampal inflammation in mice. Brain, Behavior, and Immunity. 56, 175-186.

Yamagata A, Miyazaki Y, Yokoi N, Shigematsu H, Sato Y, Goto-Ito S, Maeda A, Goto T, Sanbo M, Hirabayashi M, Shirouzu M, Fukata Y, Fukata M, Fukai S (2018). Structural basis of epilepsy-related ligand-receptor complex LGI1-ADAM22. Nat. Commun. 9:1-13.

Yoshikai S, Sasaki H, Doh-ura K, Furuya H, Sakaki Y (1990). Genomic organization of the human amyloid beta-protein precursor gene. Gene 87:257-263.

Zengel JE, Magleby KL (1982). Augmentation and facilitation of transmitter release. A quantitative description at the frog neuromuscular junction. The Journal of general physiology 80:583-611.

Zucker RS, Regehr WG (2002). Short-term synaptic plasticity. Annual review of physiology 64:355-405.

Abbreviations

(*f*)EPSP	(field) excitatory postsynaptic potential
EC	enthorinal cortex
(α)BTX	α-Bungerotoxin
°C	grad Celsius
µm	micrometer
AAB	autoimmune antibody
ACSF	artificial cerebrospinal fluid
ADAM	α-disintegrin and metalloproteinase
AE	autoimmune mediated encephalitis
AMPA	α-amino-3-hydroxy-5-methyl-4-isoxazolepropionic acid
APLP1 and 2	amyloid precursor-like protein 1 and 2
APP	amyloid precursor protein
APPsα	secreted Amyloid precursor protein ectodomain after α-secretase cleavage
APPsβ	amyloid precursor protein
ASC	secreted Amyloid precursor protein ectodomain after β-secretase cleavage
Aβ	amyloid-β
BACE-1	β-site APP cleaving enzyme
BDNF	brain derived neurotrophic factor
CA	cornu Ammonis
CARD	caspase recruitment domain
CASP1	caspase-1
CERAD	consortium to establish a registry for Alzheimer's Disease
CTF-η	carboxy terminal fragment η
DAMP	damage associated molecular pattern
DG	dentate gyrus
E-LTP	early LTP
EPTP	epitempin
FAD	familiar form of Alzheimer’s disease
FBDS	fraciobrachial dystonic seizures
FV	fiber Volley

g	gram
GR	glucocorticoid receptor
h	hour
HLA	human leukocyte antigens
HLA-DR/DP/DQ	cell surface receptor proteins on antigen presenting cells (MHC class II)
IL	interleukin
ISI	inter stimulus interval
L	liter
LE	limbic encephalitis
LGI1	leucin rich glioma inactivated protein 1
L-LTP	late LTP
LM	littermate
LRR	leucin rich repeat
LTD	long-term depression
LTP	long-term potentiation
M	mol
min	minute
MRI	magnetic resonance imaging
ms	millisecond
mV	millivolt
NALP3/ NLRP3	NOD („nucleotide-binding oligomerization domain“)-, LRR („leucin rich repeat“- und „pyrin domain-containing 3“) protein
NFT	neurofibrillary tangle
Nfκb	nuclear factor 'kappa-light-chain-enhancer' of activated B-cells
nM	nano molar
NMDA	N-Methyl-D-Aspartat
NOD	nucleotide-binding oligomerization domain
ns	not significant
OHC	organotypic hippocampal cultures
PB	phosphate buffer
PBS	phosphate buffered saline

PKA	cyclic adeonosine 3’,5’-monophosphate (cAMP)–proteinkinase
PKC	proteinkinase C
PPD	paired pulse depression
PPF	paired pulse facilitation
PRR	pattern recognition receptor
PS (1 or2)	presenilin (1 or 2)
PSD	post synaptic Density
PTP	post tetanic potentiation
ROI	region of interest
RRP	ready releasable pool
RT	room temperature
SEM	standard deviation
STP	short-term plasticity
TBS	theta burst stimulation
TLR	toll-like receptor
WT	wildtype
ZNS	central nervous system

List of figures

List of tables

Acknowledgements

An dieser Stelle möchte ich mich bei allen Menschen bedanken, die zum Gelingen dieser Dissertation beigetragen haben und mich stets in meinen Vorhaben unterstützt haben.

Zuerst möchte ich mich bei meinen Doktorvater Prof. Doktor Martin Korte bedanken. Dank seinem vollsten Vertrauen in mich und meine Arbeit ist diese Dissertation, sowie auch schon die Bachelor- Und Masterarbeit in seiner Arbeitsgruppe erst möglich gewesen.

Prof. Dr. Reinhard Köster danke ich für die Übernahme des Koreferates, sowie Prof. Dr. Michael Steinert für die Leitung der Prüfungskommission.

Zudem möchte ich mich bei allen Leuten bedanken, die an den verschiedenen Projekten beteiligt waren. Dazu zählen alle Personen aus dem Labor von Ulrike Müller aus Heidelberg, die mir geholfen haben die Ergebnisse zu den APPsα, Aηα und htau.P301S Versuchen zu erzielen. Ebenso zählen Peter Körtvelyessy und alle Kollegen dazu, die sich am Projekt zu den Autoimmunantikörpern beteiligt haben. Außerdem danke ich dem Team um Michael Heneka, welches mich auch schon in der Masterarbeit in Bezug auf das NALP3 Projekt unterstützt hat.

Ich danke auch Dr. Marta Zagrebelsky, Dr. Kristin Michaelsen-Preusse, Dr. Martin Rothkegel und Dr. Andreas Holz für die wertvollen Ratschläge und Diskussionen.

Ein riesiger Dank geht auch an meine phD-Kollegen: Max Klasmeier, Dr. Shirin Hosseini, Niklas Lonnemann, Steffen Fricke, Jonas Feuge, Abhisarika Patnaik, Charlotte Tacke und speziell Kristin Metzdorf die mich gern auf einen Gang in die Cafeteria vom Laboralltag ablenken durfte.

Ein spezieller Dank geht an Dr. Susann Ludewig, die mich in die Welt der Elektrophysiologie eingeführt hat, während der gesamten Zeit stets unterstützt hat und mir auch schon während der Masterarbeit wertvolle Tipps gegeben hat. Zudem danke ich ihr für das Korrekturlesen meiner Arbeit. In diesem Zuge danke ich auch meiner Freundin Alix Grünhagen.

Reinhard Huwe danke ich für die technische Permisse und Tania Meßerschmidt dafür, immer den vollsten Überblick zu haben und stets für einen Spaß zu haben zu sein.

Der Größte Dank geht an meine ganze Familie. Besonders an meine Mama, die stets vollstes Vertrauen in mich und meine Pläne hat und meinen Papa für seine immerwährende Unterstützung bei all meinen Vorhaben. Ebenso an meine Großeltern Hildegard und Jan und an meinen Bruder Lauritz. Außerdem danke ich meinem Freund Timon Heisig dafür, dass er mir meine wundervolle Tochter Ida geschenkt hat! Ihr baut mich täglich auf. Ich liebe euch!